ELUCIDATING THE ZYG11 PROTEIN INTERACTIONS CONTROLLING MITOTIC SLIPPAGE AND A NOVEL QUIESCENCE PATHWAY

by

JAMES ANDERSON

(Under the Direction of Edward T Kipreos)

ABSTRACT

Cyclin B1 is significant in the progression of the cell cycle because it regulates initiation of mitosis (Knoblich and Lehner, 1993). Cyclin B1 forms a complex with CDK1, then phosphorylates several substrates, leading to mitotic entry (Abe et al., 2011; Knoblich and Lehner, 1993). Cyclin B1 usually is degraded by the anaphase promoting complex/cyclosome (APC/C) during mitosis in order to facilitate mitotic exit (Pines, 2011). $CRL2^{ZYG11A/B}$ is an E3 ubiquitin ligase that contributes to mitotic slippage by targeting cyclin B1 for degradation when APC/C is inactive (Balachandran et al., 2016). We elucidate the interaction between ZYG11B and cyclin B1, and we explore how this interaction is regulated. We show that cyclin B1's CBOX1 and CBOX2 domains interact with ZYG11B, but ZYG11B has a preference for binding to CBOX1. The variant leucine rich repeat (vLRR) regions of ZYG11B interact with cyclin B1. Specifically, vLRR regions 4, 5, and 6 seem to play a significant role in the interaction. We identified four cyclin B1 CBOX1 mutants that have reduced interactions with

ZYG11B. We also show that ZYG11B interacts with cyclin B1 during S phase and mitosis; however, the interaction during S phase is moderately stronger than the interaction in mitosis. Additionally, the interaction between ZYG11B and its E3 scaffold, CUL2, is not cell cycle regulated. Our data so far suggests that the interaction between ZYG11B and cyclin B1 does not depend on post translational modifications (PTMs).

In addition to studying the interaction between ZYG11B and cyclin B1, we also identified a quiescence pathway in H1299 non-small cell lung cancer (NSCLC) cells that ZYG11A and ZYG11B are involved in. We chose to study H1299 cells because ZYG11A is overexpressed in NSCLC tissue, and ZYG11A expression is positively correlated with progression of NSCLC and poor patient prognosis (Wang et al., 2016). We found that ZYG11A and ZYG11B are important to mediate the levels of MCM7, CSE1L/CAS, and CCT as cells enter quiescence. We also present evidence that ZYG11A and ZYGB interact directly with a subset of these proteins, suggesting direct regulation.

INDEX WORDS: ZYG11B; CBOX1; Post translational modifications; Mitotic slippage.

ELUCIDATING THE ZYG11 PROTEIN INTERACTIONS CONTROLLING MITOTIC SLIPPAGE AND A NOVEL QUIESCENCE PATHWAY

by

JAMES ANDERSON

BS, University of Georgia, 2010

MS, University of Alabama, 2012

A Dissertation Submitted to the Graduate Faculty of The University of Georgia in Partial Fulfillment of the Requirements of the Requirements for the Degree

DOCTOR OF PHILOSOPHY

ATHENS, GEORGIA

2020

ELUCIDATING THE ZYG11 PROTEIN INTERACTIONS CONTROLLING MITOTIC SLIPPAGE AND A NOVEL QUIESCENCE PATHWAY

by

JAMES ANDERSON

Major Professor: Edward Kipreos

Committee: Jacek Gaertig

Haini Cai

Karl Lechtreck

Electronic Version Approved:

Ron Walcott

Interim Dean of the Graduate School

The University of Georgia

August 2020

DEDICATION

I dedicate this dissertation to my late grandmother, Julia Anderson-Shell and my late dog, Isis Anderson. Grandma Julia instilled in me to be respectful and selfless. She always was there for anyone in need. Even though she is not here to see me defend my dissertation, I know that she is looking down from above with a smile on her face. Isis Anderson was my first dog. She got me through my PhD. She would greet me with excitement every night I returned home late from lab. She brought joy to my life even during my moments of stress. I miss grandma Julia and Isis. You both forever will be in my heart until we meet again.

ACKNOWLEDGEMENTS

I would like to thank Dr. Edward Kipreos for his knowledge and for guiding me through my dissertation. I also would like to thank my committee members: Dr. Jacek Gaertig, Dr. Haini Cai and Dr. Karl Lechtreck. My committee has been very instrumental to me during my dissertation journey. I want to thank all my labmates past and present. I want to thank my mom, Betty Anderson, my dad, Larry Anderson, and my wife, Dr. Joya Hampton-Anderson for their continuous words of encourage and support throughout my PhD journey. I also want to thank all other family and friends who have played a positive role in my life.

TABLE OF CONTENTS

LIST OF TABLES

Page

LIST OF FIGURES

Page

CHAPTER 1

INTRODUCTION AND LITERATURE REVIEW

Organization of the dissertation

Cullin-RING E3 Ubiquitin ligases (CRLs) have many diverse functions in the cell and are involved in processes such as: DNA replication, apoptosis, signaling, development, and cell cycle control (Chen et al., 2015; Sarikas et al., 2011). CRLs interact with various substrates via different substrate receptors, and CRLs then target these substrates for proteasomal degradation via polyubiquitylation (Cai and Yang, 2016; Chen et al., 2015). $CRL2^{ZYG11A/B}$ is a cullin-2 E3 ubiquitin ligase that has either ZYG11A or ZYG11B as a substrate receptor (Balachandran et al., 2016). $CRL^{ZYG11A/B}$ targets cyclin B1 for degradation, and this cyclin B1 degradation contributes to mitotic slippage after cells are arrested in mitosis by treatment with anti-microtubule drugs (Balachandran et al., 2016). In the first part of Chapter 1, I will review the literature pertaining to what will be covered in Chapter 2. The concepts covered from this literature review are as follows: cullin-RING E3 ubiquitin ligases; cyclin B1; APC/C; the spindle assembly checkpoint; $CRL2^{ZYG11}$;mitotic slippage; cyclin B1 structure; ZYG11B structure; and post translational modifications. In the second part of Chapter 1, I will review the literature

pertaining to what will be covered in Chapter 3. The concepts covered from this literature review are as follows: non-small cell lung cancer; ZYG11A; quiescence; MCM7; CCT3; and CSE1L. Chapter 2 of this dissertation is titled: *Elucidating the protein interactions controlling mitotic slippage*. Chapter 2 maps the binding interface between cyclin B1 and ZYG11B. This chapter also determines whether the interaction between cyclin B1 and ZYG11B is cell cycle regulated and how the interaction is regulated. Chapter 3 of my dissertation is titled: *Identifying a Novel Quiescence Pathway.* In this chapter, we explore the role of $CRL2^{ZYG11A/B}$ in regulating quiescence. In Chapter 4, we discuss the overall implications of my dissertation research and present future directions for the research.

Cullin Ring E3 Ubiquitin Ligases and the Ubiquitin Proteasome System

Cullin-RING E3 ubiquitin ligases (CRLs) are protein complexes that target substrates for destruction by the 26S proteasome via polyubiquitylation (Cai and Yang, 2016; Chen et al., 2015). The components that make up the CRL complexes are: substrate receptors, the RING finger domain protein, cullins, and adaptor proteins (Chen et al., 2015; Zhao and Sun, 2013). CRL complexes vary according to which cullin scaffold is used (Chen et al., 2015; Sarikas et al., 2011). The eight human cullins that have been identified are: cullins 1, 2, 3, 4A, 4B, 5, 7, and 9 (Chen et al., 2015). CRLs are significant to a number of cellular processes such as: cell signaling, cell cycle control, DNA replication, development, and apoptosis (Chen et al., 2015; Sarikas et al., 2011).

Before CRLs can transfer ubiquitin molecules to substrates, the ubiquitin molecule first must be activated on its c-terminus end by the ubiquitin activating enzyme E1 (Lecker et al., 2006). The E1 transfers the activated ubiquitin molecule to the

ubiquitin carrier protein E2 (Lecker et al., 2006). The E2 plus activated ubiquitin then bind to the E3, and the E3 transfers the ubiquitin to the substrate (Lecker et al., 2006). This process is repeated, leading to the polyubiquitylation of the substrate by the E3 followed by proteasomal degradation (Lecker et al., 2006). In mammals there is one known E1 and multiple E2s and hundreds of E3s (Handley et al., 1991; Lecker et al., 2006). The large number of E3s allows the ubiquitin proteasome system to recognize thousands of substrate proteins while maintaining substrate specificity (Lecker et al., 2006).

Cyclin B1 and Mitosis

Mitosis is the division of a cell's genome and cytoplasm and is essential for the proliferation of cells (McIntosh, 2016). Mitosis must be tightly regulated because dysregulation of mitosis can lead to aneuploidies, which in turn can lead to uncontrolled cell division and various cancers (Weaver and Cleveland, 2005). Cyclin B1 is needed for entry into mitosis (Knoblich and Lehner, 1993). Cyclin B1 contains a nuclear export signal and a nuclear import signal, and as a result of these two signals, cyclin B1 normally shuttles back and forth between the nucleus and the cytoplasm when cells are not in mitosis (Takizawa et al., 1999; Toyoshima et al., 1998). However during prophase of mitosis, cyclin B1 tends to move into the nucleus instead of shuttling back and forth between the nucleus and cytoplasm (Lindqvist et al., 2007; Toyoshima-Morimoto et al., 2001). Cyclin B1 switches mainly towards nuclear import during mitosis because Polo-like kinase 1 phosphorylates cyclin B1's nuclear export signal, preventing cyclin B1 from being exported from the nucleus (Toyoshima-Morimoto et al., 2001). Cyclin B1 pairs with CDK1 in order to drive cells into mitosis (Gavet and Pines, 2010).

As is the case for other CDK's, CDK1 without its cyclin partner is not active because its ATP binding site is blocked by the CDK1 T-loop (Li et al., 2015). However, when cyclin B1 binds to CDK1, the T-loop undergoes a confirmation change, allowing for the enzyme's ATP binding site to be accessible (Li et al., 2015). Additionally, Cdk-activating kinase (CAK) phosphorylates the T-loop to activate CDK1 (Li et al., 2015; Wohlbold et al., 2006). CDK1 activity can be suppressed by inhibitory phosphorylation by Wee1 or Myt1; with the inhibitory phosphorylation removed by the phosphatase CDC25, thereby activating CDK1 (Trunnell et al., 2011).

Once the cyclin B1/CDK1 complex is active, it phosphorylates various targets to facilitate mitotic entry (Abe et al., 2011). Cyclin B1/CDK1 phosphorylates condensins to lead to chromosomal condensation (Abe et al., 2011). Cyclin B1/CDK1 phosphorylates various golgi proteins to initiate the fragmentation of the golgi (Preisinger et al., 2005). Cyclin B1/CDK1 phosphorylates components of the nuclear pore complex as well as lamins to facilitate nuclear envelope breakdown (Onischenko et al., 2005; Peter et al., 1990). Cyclin B1/CDK1 also phosphorylates microtubule-associated proteins and centrosomes to aid in mitotic spindle formation (Basu et al., 2020; Vasquez et al., 1999). In order to exit mitosis, cyclin B1 is degraded by the anaphase-promoting complex/cyclosome (APC/C) once the spindle assembly checkpoint is satisfied (Clute and Pines, 1999; Dick and Gerlich, 2013; Hagting et al., 2002). The degradation of cyclin B1 renders the cyclinB1/CDK1 complex inactive, and the complex no longer phosphorylates its substrates that are involved in mitotic entry (Parry and O'Farrell, 2001; Sigrist et al., 1995; Wolf et al., 2006). Protein phosphatase 1 and protein phosphatase 2A become more active during anaphase since cyclin B1 levels are

dropping, and these phosphatases no longer have to compete with cyclin B1/CDK1 (Forester et al., 2007; Ma et al., 2016; Steen et al., 2000; Touati et al., 2019). These phosphatases dephosphorylate the various cyclinB1/CDK1 mitotic substrates, thereby promoting the exit of mitosis and allowing cells to regain an interphase phenotype (Forester et al., 2007; Ma et al., 2016; Steen et al., 2000; Touati et al., 2019).

Anaphase Promoting Complex/Cyclosome and the Spindle Assembly Checkpoint

The anaphase promoting complex/cyclosome (APC/C) is an E3 ubiquitin ligase that plays a major role in degrading cyclin B1, leading to exit from mitosis (Pines, 2011; Watson et al., 2019). APC/C recognizes cyclin B1 via its degron known as the destruction box (Glotzer et al., 1991; van Zon et al., 2010). Even though the destruction box is recognized by APC/C, interaction between APC/C and cyclin B1 is stabilized via Cks (van Zon et al., 2010). Cks serves as a linker protein that links the APC3 subunit of APC with CDK1 of the cyclin B1/CDK1 complex (van Zon et al., 2010).

Before APC/C degrades cyclin B1 at the metaphase-to-anaphase transition of mitosis, APC/C is inhibited by the mitotic checkpoint complex (MCC) (Lara-Gonzalez et al., 2012; Li and Murray, 1991; Rieder et al., 1995). The MCC inhibits APC/C when the spindle assembly checkpoint (SAC) is not satisfied (Hwang et al., 1998; Izawa and Pines, 2015). The SAC is not satisfied when there is either a lack of microtubule attachment to kinetochores or if there is a lack of tension on the kinetochores from the microtubules (Hwang et al., 1998; Li and Nicklas, 1995). The SAC is significant because it prevents APC/C from being prematurely active, and the SAC minimizes the chances of nondisjunction taking place (Hwang et al., 1998; Izawa and Pines, 2015). The way the SAC works is that when mitotic spindles are not attached to kinetochores,

BUB1, BUBR1, BUB3, MAD2, and MAD1 congregate at kinetochores that are not attached to microtubules (De Antoni et al., 2005; Sudakin et al., 2001). These proteins are assembled at kinetochores to generate the MCC (De Antoni et al., 2005; Sudakin et al., 2001). There are two known ways that the MCC inhibits the APC/C (Chao et al., 2012; Izawa and Pines, 2012, 2015). One way the MCC inactivates APC/C is by binding to APC/C's substrate receptor, cdc20, preventing cdc20 from interacting with APC/C (Chao et al., 2012). Another way is that the MCC also can inhibit active APC/C that already is bound to cdc20 (Izawa and Pines, 2015). However, once the mitotic spindles are attached to kinetochores and have tension, the SAC is satisfied, and the MCC is disassembled by the AAA ATPase TRIPP13 and $p31^{comet}$ (Eytan et al., 2014; Teichner et al., 2011; Wang et al., 2019; Westhorpe et al., 2011).

When the SAC is satisfied, activated APC/C targets securin for degradation (Hirano, 2015; Luo and Tong, 2018). Securin is a protein that inhibits separase, and by inhibiting separase, this prevents sister chromatids from separating since the chromatids are joined by cohesion rings (Hornig et al., 2002). However when securin is degraded, this frees the protease separase, and this protease cleaves the cohesion rings that holds together the sister chromatids (Hornig et al., 2002). This in turn allows for anaphase to take place as the sister chromatids separate due to the bipolar tension applied to the sister chromatids from the mitotic spindles (Zhou et al., 2002). APC/C's degradation of securin and cyclin B1 allows the cell to transition into anaphase and telophase respectively (Holloway et al., 1993; Hornig et al., 2002).

APC/C uses cdc20 or cdh1 as substrate receptors when regulating the cell cycle (Kramer et al., 2000). During mitosis, cyclin B/CDK1 and Polo-like kinase 1 (PLK1)

phosphorylate APC/C, allowing APC/C to interact with cdc20 (Kotani et al., 1998; Kramer et al., 2000). This binding of cdc20 contributes to activating APC/C^{cdc20} (Kramer et al., 2000). At the same time, cyclin B1/CDK1 phosphorylates cdh1, which prevents cdh1 from binding to APC1 (Kramer et al., 2000; Qiao et al., 2016). After metaphase when APC/C^{cdc20} is fully active, cyclin B1 levels decrease due to being targeted for degradation by APC/C^{cdc20} (Izawa and Pines, 2011; Kramer et al., 2000). This reduction in cyclin B1 levels decreases CDK1 activity, allowing cdh1 to no longer be inhibited and bind to APC/C (Peters, 1998). Also because cyclin B1/CDK1 promotes the assembly of APC/C^{cdc20}, the reduction in CDK1 activity leads to a decrease in APC/C^{cdc20} (Peters, 1998). Therefore APC/C^{cdc20} is active during mitosis while cyclin B levels are high (after the SAC is satisfied), while APC/C^{cdh1} is active later in mitosis after the reduction in the levels of cyclin B1 (Kramer et al., 2000; Peters, 1998). APC/C^{cdc20} initially degrades cyclin B1 after metaphase, and APC/C^{cdh1} finishes the degradation upon mitotic exit (Afonso et al., 2019; Kramer et al., 2000).

$CRL2^{ZYG11}$

$CRL2^{ZYG11}$ is a cullin-RING E3 ubiquitin ligase complex that is based on cullin-2 (CUL2) as an E3 scaffold (Vasudevan et al., 2007). ZYG-11 is the substrate receptor, and in *C. elegans* there is one version of ZYG-11 (Vasudevan et al., 2007). However, in *Homo sapiens* there are two versions of ZYG-11: ZYG11A and ZYG11B (Vasudevan et al., 2007). ZYG11A or ZYG11B can act as a substrate receptor in mammals (Vasudevan et al., 2007). $CRL2^{ZYG11A/B}$ also consists of the RING finger protein, Rbx1, and the adaptor proteins elongin B and elongin C (Cai and Yang, 2016). Elongin B and C connect ZYG11A or ZYG11B to the CUL2 scaffold (Cai and Yang, 2016; Vasudevan et al.,

2007). In *C. elegans*, ZYG-11 establishes anterior-posterior polarity, and it is involved in separating sister chromatids during anaphase II of meiosis (Liu et al., 2004; Sonneville and Gönczy, 2004). In *C. elegans* and in *Homo sapiens,* ZYG11 and ZYG11A/B, respectively, each target cyclin B1 for proteasomal destruction (Balachandran et al., 2016). Even though APC/C is the main E3 that degrades cyclin B1 under normal circumstances, $CRL2^{ZYG11A/B}$ plays a redundant role with APC/C, targeting cyclin B1 for mitotic degradation under abnormal circumstances (Balachandran et al., 2016; Izawa and Pines, 2011). For example, when APC/C is inhibited, or when there is overproduction of cyclin B1, $CRL2^{ZYG11A/B}$ plays more of a significant role in degrading cyclin B1 during mitosis (Balachandran et al., 2016). Most notably, $CRL2^{ZYG11A/B}$ can contribute to mitotic slippage when the SAC is active and APC/C is inhibited (Balachandran et al., 2016).

Mitotic Slippage

Antimitotic drugs, such as antimicrotubule drugs, constitutively activate the SAC, which in turn causes cells to arrest in mitosis (Gascoigne and Taylor, 2009). Antimicrotubule drugs are able to arrest cells in mitosis because these drugs interfere with microtubule dynamics (Gascoigne and Taylor, 2009). When microtubules are not able to polymerize or depolymerize properly, the failure of microtubules to connect to kinetochores activates the SAC (Balachandran and Kipreos, 2017). Normally, the prolonged mitotic arrest caused by antimicrotubule drugs leads to cells undergoing apoptosis (Matson and Stukenberg, 2011). However, a percentage of cells undergo mitotic slippage instead of apoptosis (Balachandran and Kipreos, 2017). Mitotic slippage occurs when cells exit mitosis without chromosomal division despite the SAC being active (Balachandran and

Kipreos, 2017; Matson and Stukenberg, 2011). $CRL2^{ZYG11A/B}$ leads to mitotic slippage in cells treated with antimicrotubule drugs, and it's believed that the degradation of cyclin B1, despite APC/C inhibition, contributes to mitotic slippage (Balachandran et al., 2016). Mitotic slippage is problematic because it contributes to anticancer drug resistance and leads to aneuploidy (Balachandran and Kipreos, 2017; Gascoigne and Taylor, 2009). Aneuploidy increases the risk of developing cancer (Ganmore et al., 2009; Stopsack et al., 2019).

Cyclin B1 Structure and ZYG11B Structure

Cyclin B1 consists of a flexible N terminal region that contains a destruction box (APC/C-recognized degron), a cyclin box 1 domain (CBOX1), and a cyclin box 2 domain (CBOX2) (Davey and Morgan, 2016; Petri et al., 2007). CBOX1 is located in the N-terminal half of cyclin B1 while CBOX2 is located in the C-terminal half of cyclin B1 (Petri et al., 2007). Each cyclin box is arranged around a central hydrophobic alpha helix (Petri et al., 2007). Four other alpha helices surround the central hydrophobic helix of each cyclin box (Fig. 1.1) (Petri et al., 2007). Thus, CBOX1 and CBOX2 each consists of five alpha helices with the central alpha helix surrounded by four alpha helices (Petri et al., 2007). Cyclin B1 has been shown to interact with CDK through the CBOX1 domain (Morgan, 1997; Petri et al., 2007).

ZYG11B consists of a VHL box, several variant leucine rich repeat (vLRRs) domains, and an armadillo-like (ARM) domain (Fig. 1.2) (Cai and Yang, 2016; Vasudevan et al., 2007). The VHL box interacts with elongin C and CUL2 (Vasudevan et al., 2007). The portion of the VHL box that interacts with CUL2 is known as the CUL2 box (Cai and Yang, 2016; Vasudevan et al., 2007). The vLRRs are similar to leucine

rich repeats (LRRs) (Vasudevan et al., 2007). LRRs consist of several alpha helices connected to beta sheets, and these secondary structures are arranged in a horseshoe-like confirmation (Kobe and Kajava, 2001). LRRs are involved in protein-protein interactions (Kobe and Kajava, 2001). For example, Skp2, which is a substrate receptor of the SCF^{Skp2} complex, has LRR domains (Kobe and Kajava, 2001; Wu et al., 2003). Skp2 regulates entry into S phase and targets substrates such as p27 for degradation (Sabile et al., 2006; Wang et al., 2012). Armadillo domains also are involved in protein-protein interactions (Dokládal et al., 2018). β-catenin is an example of a protein that has an armadillo domain (Huber et al., 1997).

Post Translational Modifications of E3 Ubiquitin Ligase Substrates and Substrate Receptors

Many E3 ubiquitin ligases recognize substrates via post translational modifications (PTMs) (Cai and Yang, 2016). βTrCP is a substrate receptor for the SCF (Skp1–Cullin1–F-box protein) E3 ubiquitin ligase complex, and βTrCP targets phosphorylated Emi1 for degradation during early mitosis (Fuchs et al., 2004; Margottin-Goguet et al., 2003). SCF^{cdc4} also is an E3 ubiquitin ligase that targets phosphorylated Sic1 for destruction in budding yeast, contributing to the G1/S transition (Nasmyth, 1996; Skowyra et al., 1997). $CRL2^{VHL}$ recognizes prolyl-hydroxylated HIFα and targets it for proteasomal degradation (Cai and Yang, 2016).

Substrate receptors of E3 ubiquitin ligases also can be regulated by PTMs (Hein and Nilsson, 2016). For example, cdc20 is phosphorylated by cyclin A2/Cdk2 during interphase, and this phosphorylation prevents cdc20 from interacting with APC/C,

thereby inhibiting activation of APC/C (Hein and Nilsson, 2016). This inactivation of APC/C during interphase allows for proper mitotic entry (Hein and Nilsson, 2016).

Non Small Cell Lung Cancer (NSCLC) and ZYG11A

Cancer is the second leading cause of death In the United States (Siegel et al., 2016). Lung cancer is the leading cause of death from all cancers in the U.S. (Siegel et al., 2016). Most cases of lung cancer are non-small cell lung cancer (NSCLC) (Ettinger et al., 2010). The two main types of NSCLC are nonsquamous cell carcinoma and squamous cell carcinoma (Ettinger et al., 2010).

ZYG11A is over expressed in tissues of non-small cell lung cancer (NSCLC) patients (Wang et al., 2016). Knocking down ZYG11A decreases the migration, proliferation, and invasion of NSCLC cell lines (Wang et al., 2016). This suggests that the overexpression of ZYG11A in NSCLC cells contributes to the progression of NSCLC (Wang et al., 2016). When ZYG11A is knocked down in NSCLC cell lines, cyclin E1 gene expression and protein levels decrease (Wang et al., 2016). However, knocking down ZYG11A followed by cyclin E1 overexpression restores the increased migration and proliferation seen in NSCLC cells when ZYG11A is not knocked down (Wang et al., 2016). Knocking down ZYG11A in NSCLC cells leads to a G0/G1 arrest (Wang et al., 2016). Cells that are arrested in G1 for an extended period of time can exit G1 to enter G0 if they do so before the restriction point in G1 (Cheung and Rando, 2013). Cells exit G1 to enter G0 (quiescence) for numerous reasons such as: serum starvation and high cell confluency (Cheung and Rando, 2013). Since ZYG11A knockdown arrests cells in G0/G1, this implies that ZYG11A overexpression in NSCLC cells normally prevents

cells from arresting in G0, allowing cells to progress through the cell cycle (Wang et al., 2016).

Quiescence

Somatic cells are able to exit the cell cycle into a quiescent state known as G0 when conditions are not optimal for cell cycle progression (Cheung and Rando, 2013). Cells usually enter quiescence due to external stimuli such as serum starvation, mild DNA damage, or crowded conditions (Cheung and Rando, 2013; Heldt et al., 2018). G1 cells can enter quiescence as long as they do so before the restriction point; however G1 cells are committed to progress through the cell cycle after the restriction point is surpassed (Pardee, 1974). A number of genes involved in cell cycle progression are downregulated during quiescence (Cheung and Rando, 2013). Some genes downregulated in quiescence are: *MCM4*, *CCNB1*, and *PCNA* (Cheung and Rando, 2013). MCM4 encodes for minichromosome maintenance complex 4 and is part of the MCM2-7 complex that acts as a helicase and unwinds DNA during DNA replication (Snyder et al., 2009). *CCNB1* encodes for cyclin B1, and, as described above, cyclin B1 forms a complex with CDK1 in order to facilitate entry into mitosis (Gavet and Pines, 2010). *PCNA* encodes for proliferating cell nuclear antigen, and this protein acts as a sliding clamp that increases the processivity of DNA polymerase during DNA replication (Kang et al., 2019). A number of proteins such $p21^{Cip1}$ and $p27^{Kip1}$ are upregulated during quiescence (Cheung and Rando, 2013; Matsumoto et al., 2011). p21 and p27 inhibit cyclin dependent kinases such as CDK2 and CDK4 (Matsumoto et al., 2011).

MCM7, CCT3, and CSE1L

MCM7 is part of the MCM2-7 complex (Snyder et al., 2009). MCM 2-7 is a helicase that is responsible for unwinding DNA during DNA replication (Snyder et al., 2009). During G1, the origin of replication is bound by the origin recognition complex (ORC) (Evrin et al., 2014; Truong and Wu, 2011). The ORC recruits cdt1 and cdc6 (Evrin et al., 2014). Once cdc6 and cdt1 are present on the ORC, MCM2-7 is loaded on the DNA (Evrin et al., 2014). The complex that contains the ORC, cdt1, cdc6, and MCM2-7 is called the pre-replication complex (pre-RC) (Evrin et al., 2014). In S phase, the MCM2-7 is activated and unwinds the origin DNA to initiate DNA replication (Evrin et al., 2014). There are several mechanisms in place to prevent the over-replication of DNA (re-replication) (Truong and Wu, 2011). During S phase, Geminin directly binds to cdt1, inhibiting cdt1's activity (Truong and Wu, 2011). Cdt1 is also targeted for degradation by SCF^{Skp2} and $CRL4^{Cdt2}$ E3 ubiquitin ligases during S phase (Truong and Wu, 2011). Cdc6 is exported out the nucleus during S phase (Truong and Wu, 2011). Since cdt1 and cdc6 no longer interact with the ORC during S phase, this prevents more MCM2-7 from being recruited to the ORC, which in turn prevents re-replication (Truong and Wu, 2011). In NIH/3T3 cells, MCM2, MCM3, MCM5, and MCM7 are removed from chromatin by day 5 of quiescence (Kingsbury et al., 2005). Also in quiescent NIH/3T3 cells, these same MCM2-7 components significantly decrease in the nucleosolic and cytosolic fractions in comparison to their levels in asynchronous and semi-confluent cells (Kingsbury et al., 2005). Even though the levels of MCM proteins decrease in the nucleosolic fractions of quiescent cells, the decreased levels remain relatively stable overtime for MCM3, MCM5, and MCM7, but MCM2 levels significantly decline as

quiescence increases in duration (Kingsbury et al., 2005). Geminin, cdc6, and cdt1 are downregulated during quiescence (Kingsbury et al., 2005; Xouri et al., 2004). MCM7 has increased expression in NSCLC tissues, and increased MCM7 expression is correlated with cancer progression in NSCLC patients (Toyokawa et al., 2011).

CSE1/CAS (CAS) is a nuclear export receptor that exports importin α out of the nucleus (Kutay et al., 1997). Importin α imports various cargoes in the nucleus (Kutay et al., 1997). Upon release of its cargo, importin α must be recycled back to the cytoplasm to allow for subsequent rounds of efficient nuclear import (Kutay et al., 1997). Importin α, CAS, and Ran-GTP form a complex inside the nucleus (Kutay et al., 1997). This Importin α/CAS/Ran-GTP complex leaves the nucleus through the nuclear pore complex (Kutay et al., 1997). RanGAP then hydrolyzes Ran-GTP, in turn disassembling the complex in the cytosol (Kutay et al., 1997). Importin α can then be used for another round of importing cargo into the nucleus (Kutay et al., 1997). Overexpressing CAS inhibits growth and migration of HT-29 colon cancer cells (Jiang and Liao, 2004).

Chaperonin-containing TCP-1 subunit 3 (CCT3) is part of the chaperonin-containing TCP-1 complex (CCT) (Xu et al., 2020). The CCT is a cytoplasmic chaperone, and it forms a barrel-like structure for folding proteins (Vallin and Grantham, 2019). CCT folds numerous proteins such as α-tubulin, β-tubulin, and actin (Llorca et al., 2000; Vallin and Grantham, 2019). CCT3 is overexpressed in hepatocellular carcinoma cells, and high levels correlate with poor prognosis of cancer patients (Zhang et al., 2016).

References

Abe, S., Nagasaka, K., Hirayama, Y., Kozuka-Hata, H., Oyama, M., Aoyagi, Y., Obuse, C., and Hirota, T. (2011). The initial phase of chromosome condensation requires Cdk1-mediated phosphorylation of the CAP-D3 subunit of condensin II. Genes Dev *25*, 863-874.

Afonso, O., Castellani, C.M., Cheeseman, L.P., Ferreira, J.G., Orr, B., Ferreira, L.T., Chambers, J.J., Morais-de-Sá, E., Maresca, T.J., and Maiato, H. (2019). Spatiotemporal control of mitotic exit during anaphase by an aurora B-Cdk1 crosstalk. eLife *8*.

Balachandran, R.S., Heighington, C.S., Starostina, N.G., Anderson, J.W., Owen, D.L., Vasudevan, S., and Kipreos, E.T. (2016). The ubiquitin ligase CRL2ZYG11 targets cyclin B1 for degradation in a conserved pathway that facilitates mitotic slippage. J Cell Biol *215*, 151-166.

Balachandran, R.S., and Kipreos, E.T. (2017). Addressing a weakness of anticancer therapy with mitosis inhibitors: Mitotic slippage. Mol Cell Oncol *4*, e1277293-e1277293.

Basu, S., Roberts, E.L., Jones, A.W., Swaffer, M.P., Snijders, A.P., and Nurse, P. (2020). The Hydrophobic Patch Directs Cyclin B to Centrosomes to Promote Global CDK Phosphorylation at Mitosis. Curr Biol *30*, 883-892.e884.

Cai, W., and Yang, H. (2016). The structure and regulation of Cullin 2 based E3 ubiquitin ligases and their biological functions. Cell Division *11*, 7.

Chao, W.C.H., Kulkarni, K., Zhang, Z., Kong, E.H., and Barford, D. (2012). Structure of the mitotic checkpoint complex. Nature *484*, 208-213.

Chen, Z., Sui, J., Zhang, F., and Zhang, C. (2015). Cullin family proteins and tumorigenesis: genetic association and molecular mechanisms. Journal of Cancer *6*, 233-242.

Cheung, T.H., and Rando, T.A. (2013). Molecular regulation of stem cell quiescence. Nature reviews Molecular cell biology *14*, 329-340.

Clute, P., and Pines, J. (1999). Temporal and spatial control of cyclin B1 destruction in metaphase. Nature Cell Biology *1*, 82-87.

Davey, N.E., and Morgan, D.O. (2016). Building a Regulatory Network with Short Linear Sequence Motifs: Lessons from the Degrons of the Anaphase-Promoting Complex. Mol Cell *64*, 12-23.

De Antoni, A., Pearson, C.G., Cimini, D., Canman, J.C., Sala, V., Nezi, L., Mapelli, M., Sironi, L., Faretta, M., Salmon, E.D.*, et al.* (2005). The Mad1/Mad2 complex as a template for Mad2 activation in the spindle assembly checkpoint. Curr Biol *15*, 214-225.

Dick, A.E., and Gerlich, D.W. (2013). Kinetic framework of spindle assembly checkpoint signalling. Nature Cell Biology *15*, 1370-1377.

Dokládal, L., Benková, E., Honys, D., Dupľáková, N., Lee, L.Y., Gelvin, S.B., and Sýkorová, E. (2018). An armadillo-domain protein participates in a telomerase interaction network. Plant molecular biology *97*, 407-420.

Ettinger, D.S., Akerley, W., Bepler, G., Blum, M.G., Chang, A., Cheney, R.T., Chirieac, L.R., D'Amico, T.A., Demmy, T.L., Ganti, A.K.*, et al.* (2010). Non-small cell lung

cancer. Journal of the National Comprehensive Cancer Network : JNCCN *8*, 740-801.

Evrin, C., Fernández-Cid, A., Riera, A., Zech, J., Clarke, P., Herrera, M.C., Tognetti, S., Lurz, R., and Speck, C. (2014). The ORC/Cdc6/MCM2-7 complex facilitates MCM2-7 dimerization during prereplicative complex formation. Nucleic acids research *42*, 2257-2269.

Eytan, E., Wang, K., Miniowitz-Shemtov, S., Sitry-Shevah, D., Kaisari, S., Yen, T.J., Liu, S.T., and Hershko, A. (2014). Disassembly of mitotic checkpoint complexes by the joint action of the AAA-ATPase TRIP13 and p31(comet). Proceedings of the National Academy of Sciences of the United States of America *111*, 12019-12024.

Forester, C.M., Maddox, J., Louis, J.V., Goris, J., and Virshup, D.M. (2007). Control of mitotic exit by PP2A regulation of Cdc25C and Cdk1. Proceedings of the National Academy of Sciences of the United States of America *104*, 19867-19872.

Fuchs, S.Y., Spiegelman, V.S., and Kumar, K.G. (2004). The many faces of beta-TrCP E3 ubiquitin ligases: reflections in the magic mirror of cancer. Oncogene *23*, 2028-2036.

Ganmore, I., Smooha, G., and Izraeli, S. (2009). Constitutional aneuploidy and cancer predisposition. Hum Mol Genet *18*, R84-R93.

Gascoigne, K.E., and Taylor, S.S. (2009). How do anti-mitotic drugs kill cancer cells? Journal of cell science *122*, 2579-2585.

Gavet, O., and Pines, J. (2010). Progressive activation of CyclinB1-Cdk1 coordinates entry to mitosis. Dev Cell *18*, 533-543.

Glotzer, M., Murray, A.W., and Kirschner, M.W. (1991). Cyclin is degraded by the ubiquitin pathway. Nature *349*, 132-138.

Hagting, A., den Elzen, N., Vodermaier, H.C., Waizenegger, I.C., Peters, J.-M., and Pines, J. (2002). Human securin proteolysis is controlled by the spindle checkpoint and reveals when the APC/C switches from activation by Cdc20 to Cdh1. Journal of Cell Biology *157*, 1125-1137.

Handley, P.M., Mueckler, M., Siegel, N.R., Ciechanover, A., and Schwartz, A.L. (1991). Molecular cloning, sequence, and tissue distribution of the human ubiquitin-activating enzyme E1. Proceedings of the National Academy of Sciences of the United States of America *88*, 258-262.

Hein, J.B., and Nilsson, J. (2016). Interphase APC/C-Cdc20 inhibition by cyclin A2-Cdk2 ensures efficient mitotic entry. Nature communications *7*, 10975.

Heldt, F.S., Barr, A.R., Cooper, S., Bakal, C., and Novák, B. (2018). A comprehensive model for the proliferation–quiescence decision in response to endogenous DNA damage in human cells. Proceedings of the National Academy of Sciences *115*, 2532.

Hirano, T. (2015). Chromosome Dynamics during Mitosis. Cold Spring Harbor perspectives in biology *7*.

Holloway, S.L., Glotzer, M., King, R.W., and Murray, A.W. (1993). Anaphase is initiated by proteolysis rather than by the inactivation of maturation-promoting factor. Cell *73*, 1393-1402.

Hornig, N.C., Knowles, P.P., McDonald, N.Q., and Uhlmann, F. (2002). The dual mechanism of separase regulation by securin. Curr Biol *12*, 973-982.

Huber, A.H., Nelson, W.J., and Weis, W.I. (1997). Three-dimensional structure of the armadillo repeat region of beta-catenin. Cell *90*, 871-882.

Hwang, L.H., Lau, L.F., Smith, D.L., Mistrot, C.A., Hardwick, K.G., Hwang, E.S., Amon, A., and Murray, A.W. (1998). Budding yeast Cdc20: a target of the spindle checkpoint. Science *279*, 1041-1044.

Izawa, D., and Pines, J. (2011). How APC/C-Cdc20 changes its substrate specificity in mitosis. Nature cell biology *13*, 223-233.

Izawa, D., and Pines, J. (2012). Mad2 and the APC/C compete for the same site on Cdc20 to ensure proper chromosome segregation. J Cell Biol *199*, 27-37.

Izawa, D., and Pines, J. (2015). The mitotic checkpoint complex binds a second CDC20 to inhibit active APC/C. Nature *517*, 631-634.

Jiang, M.C., and Liao, C.F. (2004). CSE1/CAS overexpression inhibits the tumorigenicity of HT-29 colon cancer cells. Journal of experimental & clinical cancer research : CR *23*, 325-332.

Kang, M.S., Kim, J., Ryu, E., Ha, N.Y., Hwang, S., Kim, B.G., Ra, J.S., Kim, Y.J., Hwang, J.M., Myung, K.*, et al.* (2019). PCNA Unloading Is Negatively Regulated by BET Proteins. Cell reports *29*, 4632-4645.e4635.

Kingsbury, S.R., Loddo, M., Fanshawe, T., Obermann, E.C., Prevost, A.T., Stoeber, K., and Williams, G.H. (2005). Repression of DNA replication licensing in quiescence is independent of geminin and may define the cell cycle state of progenitor cells. Experimental cell research *309*, 56-67.

Knoblich, J.A., and Lehner, C.F. (1993). Synergistic action of Drosophila cyclins A and B during the G2-M transition. Embo j *12*, 65-74.

Kobe, B., and Kajava, A.V. (2001). The leucine-rich repeat as a protein recognition motif. Curr Opin Struct Biol *11*, 725-732.

Kotani, S., Tugendreich, S., Fujii, M., Jorgensen, P.M., Watanabe, N., Hoog, C., Hieter, P., and Todokoro, K. (1998). PKA and MPF-activated polo-like kinase regulate anaphase-promoting complex activity and mitosis progression. Mol Cell *1*, 371-380.

Kramer, E.R., Scheuringer, N., Podtelejnikov, A.V., Mann, M., and Peters, J.M. (2000). Mitotic regulation of the APC activator proteins CDC20 and CDH1. Molecular biology of the cell *11*, 1555-1569.

Kutay, U., Bischoff, F.R., Kostka, S., Kraft, R., and Görlich, D. (1997). Export of importin alpha from the nucleus is mediated by a specific nuclear transport factor. Cell *90*, 1061-1071.

Lara-Gonzalez, P., Westhorpe, F.G., and Taylor, S.S. (2012). The spindle assembly checkpoint. Curr Biol *22*, R966-980.

Lecker, S.H., Goldberg, A.L., and Mitch, W.E. (2006). Protein degradation by the ubiquitin-proteasome pathway in normal and disease states. Journal of the American Society of Nephrology : JASN *17*, 1807-1819.

Li, R., and Murray, A.W. (1991). Feedback control of mitosis in budding yeast. Cell *66*, 519-531.

Li, X., and Nicklas, R.B. (1995). Mitotic forces control a cell-cycle checkpoint. Nature *373*, 630-632.

Li, Y., Zhang, J., Gao, W., Zhang, L., Pan, Y., Zhang, S., and Wang, Y. (2015). Insights on Structural Characteristics and Ligand Binding Mechanisms of CDK2. International journal of molecular sciences *16*, 9314-9340.

Lindqvist, A., van Zon, W., Karlsson Rosenthal, C., and Wolthuis, R.M. (2007). Cyclin B1-Cdk1 activation continues after centrosome separation to control mitotic progression. PLoS biology *5*, e123.

Liu, J., Vasudevan, S., and Kipreos, E.T. (2004). CUL-2 and ZYG-11 promote meiotic anaphase II and the proper placement of the anterior-posterior axis in C. elegans. Development *131*, 3513-3525.

Llorca, O., Martín-Benito, J., Ritco-Vonsovici, M., Grantham, J., Hynes, G.M., Willison, K.R., Carrascosa, J.L., and Valpuesta, J.M. (2000). Eukaryotic chaperonin CCT stabilizes actin and tubulin folding intermediates in open quasi-native conformations. The EMBO journal *19*, 5971-5979.

Luo, S., and Tong, L. (2018). Structural biology of the separase-securin complex with crucial roles in chromosome segregation. Curr Opin Struct Biol *49*, 114-122.

Ma, S., Vigneron, S., Robert, P., Strub, J.M., Cianferani, S., Castro, A., and Lorca, T. (2016). Greatwall dephosphorylation and inactivation upon mitotic exit is triggered by PP1. Journal of cell science *129*, 1329-1339.

Margottin-Goguet, F., Hsu, J.Y., Loktev, A., Hsieh, H.M., Reimann, J.D., and Jackson, P.K. (2003). Prophase destruction of Emi1 by the SCF(betaTrCP/Slimb) ubiquitin ligase activates the anaphase promoting complex to allow progression beyond prometaphase. Dev Cell *4*, 813-826.

Matson, D.R., and Stukenberg, P.T. (2011). Spindle poisons and cell fate: a tale of two pathways. Mol Interv *11*, 141-150.

Matsumoto, A., Takeishi, S., Kanie, T., Susaki, E., Onoyama, I., Tateishi, Y., Nakayama, K., and Nakayama, K.I. (2011). p57 is required for quiescence and maintenance of adult hematopoietic stem cells. Cell stem cell *9*, 262-271.

McIntosh, J.R. (2016). Mitosis. Cold Spring Harbor perspectives in biology *8*, a023218.

Morgan, D.O. (1997). Cyclin-dependent kinases: engines, clocks, and microprocessors. Annual review of cell and developmental biology *13*, 261-291.

Nasmyth, K. (1996). At the heart of the budding yeast cell cycle. Trends in genetics : TIG *12*, 405-412.

Onischenko, E.A., Gubanova, N.V., Kiseleva, E.V., and Hallberg, E. (2005). Cdk1 and okadaic acid-sensitive phosphatases control assembly of nuclear pore complexes in Drosophila embryos. Mol Biol Cell *16*, 5152-5162.

Pardee, A.B. (1974). A restriction point for control of normal animal cell proliferation. Proceedings of the National Academy of Sciences of the United States of America *71*, 1286-1290.

Parry, D.H., and O'Farrell, P.H. (2001). The schedule of destruction of three mitotic cyclins can dictate the timing of events during exit from mitosis. Current biology : CB *11*, 671-683.

Peter, M., Nakagawa, J., Dorée, M., Labbé, J.C., and Nigg, E.A. (1990). In vitro disassembly of the nuclear lamina and M phase-specific phosphorylation of lamins by cdc2 kinase. Cell *61*, 591-602.

Peters, J.M. (1998). SCF and APC: the Yin and Yang of cell cycle regulated proteolysis. Current opinion in cell biology *10*, 759-768.

Petri, E.T., Errico, A., Escobedo, L., Hunt, T., and Basavappa, R. (2007). The crystal structure of human cyclin B. Cell Cycle *6*, 1342-1349.

Pines, J. (2011). Cubism and the cell cycle: the many faces of the APC/C. Nat Rev Mol Cell Biol *12*, 427-438.

Preisinger, C., Körner, R., Wind, M., Lehmann, W.D., Kopajtich, R., and Barr, F.A. (2005). Plk1 docking to GRASP65 phosphorylated by Cdk1 suggests a mechanism for Golgi checkpoint signalling. Embo j *24*, 753-765.

Qiao, R., Weissmann, F., Yamaguchi, M., Brown, N.G., VanderLinden, R., Imre, R., Jarvis, M.A., Brunner, M.R., Davidson, I.F., Litos, G.*, et al.* (2016). Mechanism of APC/CCDC20 activation by mitotic phosphorylation. Proceedings of the National Academy of Sciences of the United States of America *113*, E2570-2578.

Rieder, C.L., Cole, R.W., Khodjakov, A., and Sluder, G. (1995). The checkpoint delaying anaphase in response to chromosome monoorientation is mediated by an inhibitory signal produced by unattached kinetochores. J Cell Biol *130*, 941-948.

Sabile, A., Meyer, A.M., Wirbelauer, C., Hess, D., Kogel, U., Scheffner, M., and Krek, W. (2006). Regulation of p27 degradation and S-phase progression by Ro52 RING finger protein. Molecular and cellular biology *26*, 5994-6004.

Sarikas, A., Hartmann, T., and Pan, Z.-Q. (2011). The cullin protein family. Genome Biology *12*, 220.

Siegel, R.L., Miller, K.D., and Jemal, A. (2016). Cancer statistics, 2016. CA: a cancer journal for clinicians *66*, 7-30.

Sigrist, S., Jacobs, H., Stratmann, R., and Lehner, C.F. (1995). Exit from mitosis is regulated by Drosophila fizzy and the sequential destruction of cyclins A, B and B3. Embo j *14*, 4827-4838.

Skowyra, D., Craig, K.L., Tyers, M., Elledge, S.J., and Harper, J.W. (1997). F-box proteins are receptors that recruit phosphorylated substrates to the SCF ubiquitin-ligase complex. Cell *91*, 209-219.

Snyder, M., Huang, X.-Y., and Zhang, J.J. (2009). The minichromosome maintenance proteins 2-7 (MCM2-7) are necessary for RNA polymerase II (Pol II)-mediated transcription. The Journal of biological chemistry *284*, 13466-13472.

Sonneville, R., and Gönczy, P. (2004). Zyg-11 and cul-2 regulate progression through meiosis II and polarity establishment in C. elegans. Development *131*, 3527-3543.

Steen, R.L., Martins, S.B., Taskén, K., and Collas, P. (2000). Recruitment of protein phosphatase 1 to the nuclear envelope by A-kinase anchoring protein AKAP149 is a prerequisite for nuclear lamina assembly. The Journal of cell biology *150*, 1251-1262.

Stopsack, K.H., Whittaker, C.A., Gerke, T.A., Loda, M., Kantoff, P.W., Mucci, L.A., and Amon, A. (2019). Aneuploidy drives lethal progression in prostate cancer. Proceedings of the National Academy of Sciences of the United States of America *116*, 11390-11395.

Sudakin, V., Chan, G.K., and Yen, T.J. (2001). Checkpoint inhibition of the APC/C in HeLa cells is mediated by a complex of BUBR1, BUB3, CDC20, and MAD2. J Cell Biol *154*, 925-936.

Takizawa, C.G., Weis, K., and Morgan, D.O. (1999). Ran-independent nuclear import of cyclin B1-Cdc2 by importin beta. Proceedings of the National Academy of Sciences of the United States of America *96*, 7938-7943.

Teichner, A., Eytan, E., Sitry-Shevah, D., Miniowitz-Shemtov, S., Dumin, E., Gromis, J., and Hershko, A. (2011). p31comet Promotes disassembly of the mitotic checkpoint complex in an ATP-dependent process. Proceedings of the National Academy of Sciences of the United States of America *108*, 3187-3192.

Touati, S.A., Hofbauer, L., Jones, A.W., Snijders, A.P., Kelly, G., and Uhlmann, F. (2019). Cdc14 and PP2A Phosphatases Cooperate to Shape Phosphoproteome Dynamics during Mitotic Exit. Cell reports *29*, 2105-2119.e2104.

Toyokawa, G., Masuda, K., Daigo, Y., Cho, H.S., Yoshimatsu, M., Takawa, M., Hayami, S., Maejima, K., Chino, M., Field, H.I.*, et al.* (2011). Minichromosome Maintenance Protein 7 is a potential therapeutic target in human cancer and a novel prognostic marker of non-small cell lung cancer. Mol Cancer *10*, 65.

Toyoshima, F., Moriguchi, T., Wada, A., Fukuda, M., and Nishida, E. (1998). Nuclear export of cyclin B1 and its possible role in the DNA damage-induced G2 checkpoint. Embo j *17*, 2728-2735.

Toyoshima-Morimoto, F., Taniguchi, E., Shinya, N., Iwamatsu, A., and Nishida, E. (2001). Polo-like kinase 1 phosphorylates cyclin B1 and targets it to the nucleus during prophase. Nature *410*, 215-220.

Trunnell, N.B., Poon, A.C., Kim, S.Y., and Ferrell, J.E., Jr. (2011). Ultrasensitivity in the Regulation of Cdc25C by Cdk1. Mol Cell *41*, 263-274.

Truong, L.N., and Wu, X. (2011). Prevention of DNA re-replication in eukaryotic cells. J Mol Cell Biol *3*, 13-22.

Vallin, J., and Grantham, J. (2019). The role of the molecular chaperone CCT in protein folding and mediation of cytoskeleton-associated processes: implications for cancer cell biology. Cell Stress and Chaperones *24*, 17-27.

van Zon, W., Ogink, J., ter Riet, B., Medema, R.H., te Riele, H., and Wolthuis, R.M. (2010). The APC/C recruits cyclin B1-Cdk1-Cks in prometaphase before D box recognition to control mitotic exit. J Cell Biol *190*, 587-602.

Vasquez, R.J., Gard, D.L., and Cassimeris, L. (1999). Phosphorylation by CDK1 regulates XMAP215 function in vitro. Cell motility and the cytoskeleton *43*, 310-321.

Vasudevan, S., Starostina, N.G., and Kipreos, E.T. (2007). The Caenorhabditis elegans cell-cycle regulator ZYG-11 defines a conserved family of CUL-2 complex components. EMBO Rep *8*, 279-286.

Wang, K., Sturt-Gillespie, B., Hittle, J.C., Macdonald, D., Chan, G.K., Yen, T.J., and Liu, S.T. (2019). Correction: Thyroid hormone receptor interacting protein 13 (TRIP13) AAA-ATPase is a novel mitotic checkpoint-silencing protein. J Biol Chem *294*, 10019.

Wang, X., Sun, Q., Chen, C., Yin, R., Huang, X., Wang, X., Shi, R., Xu, L., and Ren, B. (2016). ZYG11A serves as an oncogene in non-small cell lung cancer and influences CCNE1 expression. Oncotarget *7*, 8029-8042.

Wang, Z., Fukushima, H., Inuzuka, H., Wan, L., Liu, P., Gao, D., Sarkar, F.H., and Wei, W. (2012). Skp2 is a promising therapeutic target in breast cancer. Front Oncol *1*.

Watson, E.R., Brown, N.G., Peters, J.M., Stark, H., and Schulman, B.A. (2019). Posing the APC/C E3 Ubiquitin Ligase to Orchestrate Cell Division. Trends in cell biology *29*, 117-134.

Weaver, B.A., and Cleveland, D.W. (2005). Decoding the links between mitosis, cancer, and chemotherapy: The mitotic checkpoint, adaptation, and cell death. Cancer cell *8*, 7-12.

Westhorpe, F.G., Tighe, A., Lara-Gonzalez, P., and Taylor, S.S. (2011). p31comet-mediated extraction of Mad2 from the MCC promotes efficient mitotic exit. Journal of cell science *124*, 3905-3916.

Wohlbold, L., Larochelle, S., Liao, J.C., Livshits, G., Singer, J., Shokat, K.M., and Fisher, R.P. (2006). The cyclin-dependent kinase (CDK) family member PNQALRE/CCRK supports cell proliferation but has no intrinsic CDK-activating kinase (CAK) activity. Cell Cycle *5*, 546-554.

Wolf, F., Wandke, C., Isenberg, N., and Geley, S. (2006). Dose-dependent effects of stable cyclin B1 on progression through mitosis in human cells. Embo j *25*, 2802-2813.

Wu, G., Xu, G., Schulman, B.A., Jeffrey, P.D., Harper, J.W., and Pavletich, N.P. (2003). Structure of a beta-TrCP1-Skp1-beta-catenin complex: destruction motif binding and lysine specificity of the SCF(beta-TrCP1) ubiquitin ligase. Mol Cell *11*, 1445-1456.

Xouri, G., Lygerou, Z., Nishitani, H., Pachnis, V., Nurse, P., and Taraviras, S. (2004). Cdt1 and geminin are down-regulated upon cell cycle exit and are over-expressed in cancer-derived cell lines. European journal of biochemistry *271*, 3368-3378.

Xu, G., Bu, S., Wang, X., Zhang, H., and Ge, H. (2020). Suppression of CCT3 inhibits the proliferation and migration in breast cancer cells. Cancer Cell Int *20*, 218-218.

Zhang, Y., Wang, Y., Wei, Y., Wu, J., Zhang, P., Shen, S., Saiyin, H., Wumaier, R., Yang, X., Wang, C.*, et al.* (2016). Molecular chaperone CCT3 supports proper mitotic progression and cell proliferation in hepatocellular carcinoma cells. Cancer Lett *372*, 101-109.

Zhao, Y., and Sun, Y. (2013). Cullin-RING Ligases as attractive anti-cancer targets. Curr Pharm Des *19*, 3215-3225.

Zhou, J., Yao, J., and Joshi, H.C. (2002). Attachment and tension in the spindle assembly checkpoint. Journal of cell science *115*, 3547-3555.

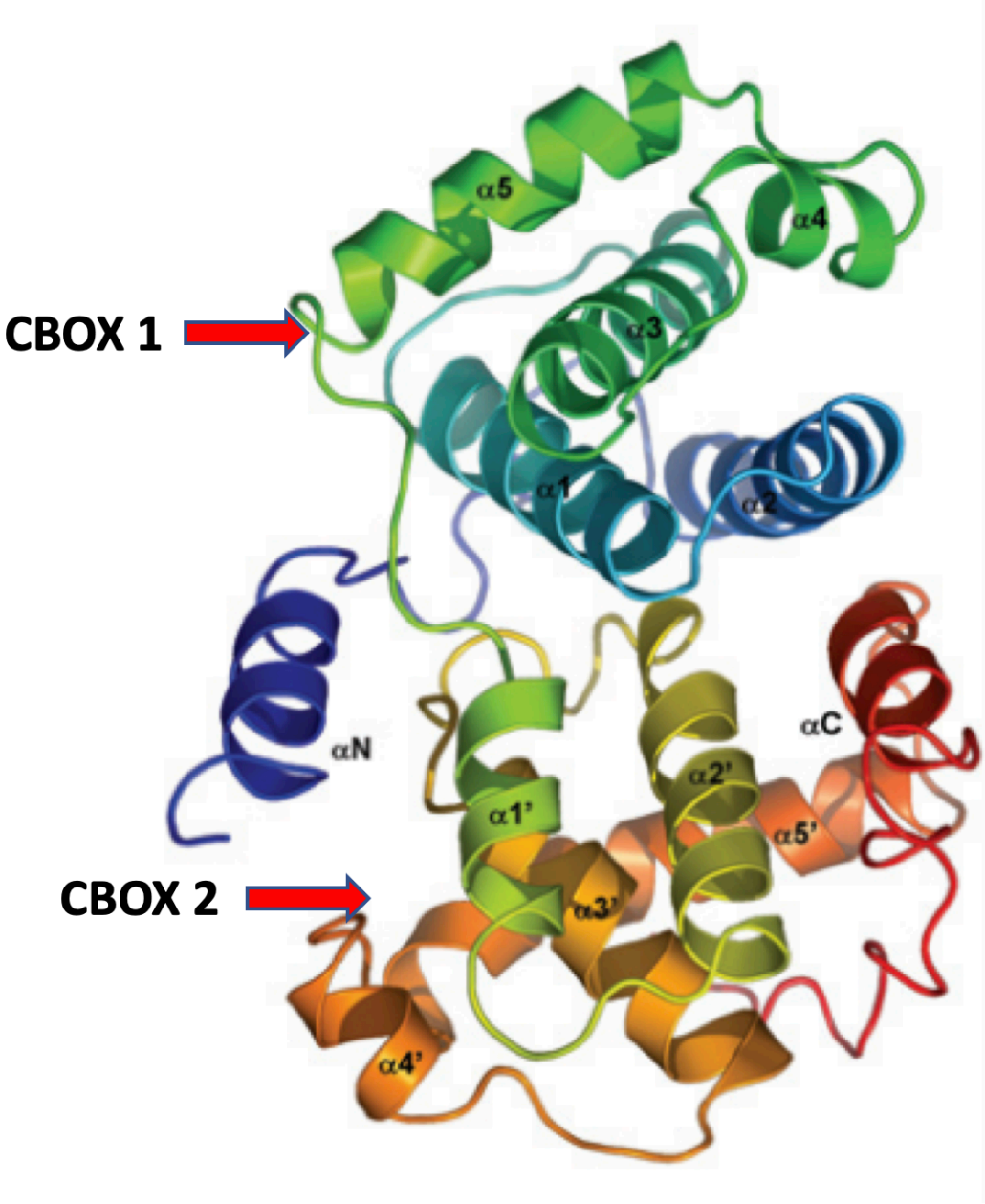

Figure 1.1 Structure of cyclin B1. Cyclin B1 consists of CBOX1 and CBOX2. Each CBOX domain contains a central alpha helix surrounded by four alpha helices. CBOX1 alpha helices in the image above are labeled α1–α5, and CBOX2 alpha helices are labelled α1'–α5' (modified from Petri et al., 2007).

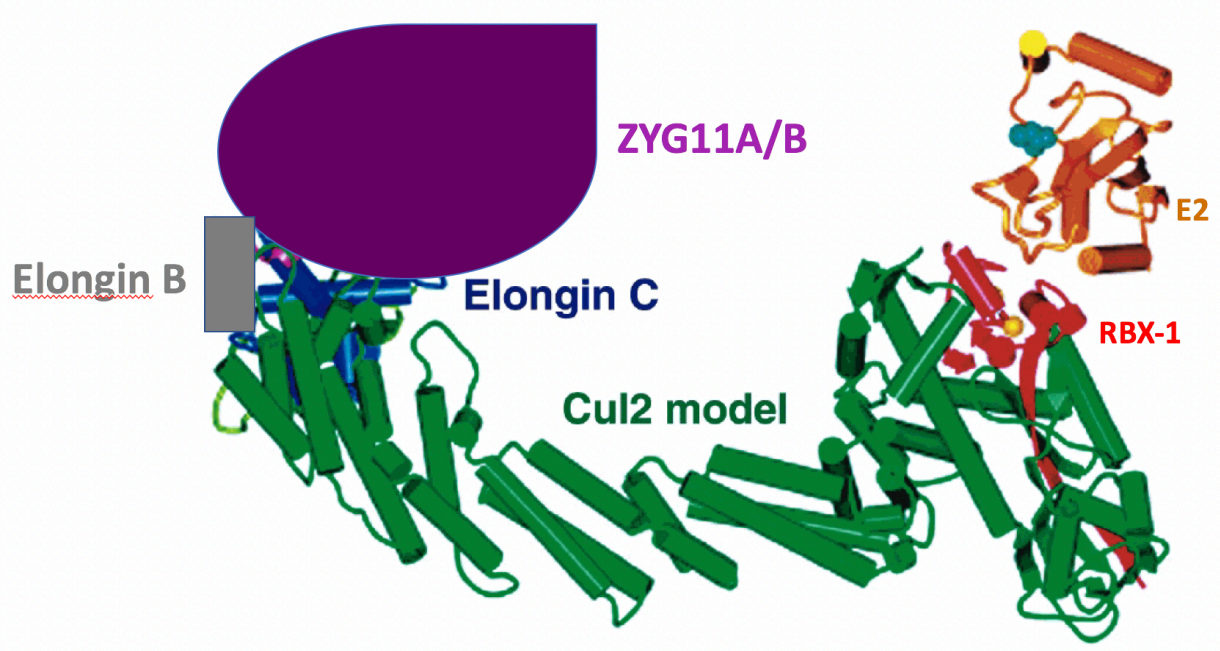

Figure 1.2 Modified Crystal Structure of CRL2$^{ZYG11A/B}$. CRL2$^{ZYG11A/B}$ consists of ZYG11A or ZYG11B as a substrate receptor. CRL2$^{ZYG11A/B}$ also contains elongin B, elongin C, Rbx1, and CUL2. The E2 brings the activated ubiquitin molecule to the complex. The ubiquitin molecule is then transferred from the E2 to the substrate that is attached to the substrate receptor. After the substrate is polyubiquitylated, it is transported to the proteasome for destruction (modified from Wu et al.,2003).

CHAPTER II

ELUCIDATING THE PROTEIN INTERACTIONS CONTROLLING MITOTIC SLIPPAGE

Anderson J.W. and Kipreos E.T. to be submitted to *BMC Molecular and Cell Biology*

Abstract

Cyclin B1 is significant in the progression of the cell cycle because it regulates initiation of mitosis (Knoblich and Lehner, 1993). Cyclin B1 forms a complex with CDK1, then phosphorylates several substrates, leading to mitotic entry (Abe et al., 2011; Knoblich and Lehner, 1993). Cyclin B1 usually is degraded by the anaphase promoting complex/cyclosome (APC/C) during mitosis in order to facilitate mitotic exit (Pines, 2011). $CRL2^{ZYG11A/B}$ is an E3 ubiquitin ligase that contributes to mitotic slippage by targeting cyclin B1 for degradation when APC/C is inactive (Balachandran et al., 2016). This chapter of the dissertation elucidates the interaction between ZYG11B and cyclin B1, and this chapter explores how this interaction is regulated. We show that cyclin B1's CBOX1 and CBOX2 domains interact with ZYG11B, but ZYG11B has a preference for binding to CBOX1. The variant leucine rich repeat (vLRR) regions of ZYG11B interact with cyclin B1. Specifically, vLRR regions 4, 5, and 6 seem to play a significant role in ZYG11B interacting with cyclin B1. We identified four cyclin B1 CBOX1 mutants that have reduced interactions with ZYG11B. We also show that ZYG11B interacts with cyclin B1 during S phase and mitosis; however, the interaction during S phase is moderately stronger than the interaction in mitosis. Additionally, the interaction between ZYG11B and its E3 scaffold, CUL2, is not cell cycle regulated. Our data so far suggests that the interaction between ZYG11B and cyclin B1 does not depend on post translational modification (PTMs), however we will need to perform follow up experiments to conclude this with more certainty. We propose that ZYG11B plays a redundant role with APC/C in the cell cycle, and ZYG11B's role becomes more

significant during abnormal circumstances such as APC/C being inhibited or too much cyclin B1 being present in the cell (Balachandran et al., 2016).

Introduction

Cyclin B1 plays a significant role in regulating entry into Mitosis (Knoblich and Lehner, 1993). Cyclin B1 forms an active complex with CDK1, and this complex phosphorylates various substrates such as lamins, condensins, microtubule associated proteins, centrosomes, and golgi proteins (Abe et al., 2011; Basu et al., 2020; Onischenko et al., 2005; Preisinger et al., 2005). Phosphorylating these substrates allows the cell to transition from interphase to mitosis (Abe et al., 2011). In order for cells to exit mitosis, cyclin B1 must be degraded (Clute and Pines, 1999; Dick and Gerlich, 2013). The anaphase promoting complex/cyclosome (APC/C) is the major E3 ubiquitin ligase that targets cyclin B1 for destruction during mitosis (Pines, 2011). Before APC/C is able to interact with cyclin B1, APC/C is initially inhibited by the spindle assembly checkpoint (SAC) (Izawa and Pines, 2015). The SAC is active when there is a lack of bipolar attachment of mitotic spindles to kinetochores or if the attached mitotic spindles lack tension (Hwang et al., 1998; Li and Nicklas, 1995). When the SAC is not satisfied, the mitotic checkpoint complex (MCC) inhibits APC/C (Izawa and Pines, 2015). This inhibition occurs via two mechanisms (Chao et al., 2012; Izawa and Pines, 2015). One method of inhibition is that the MCC physically interacts with APC/C's substrate receptor, cdc20, preventing cdc20 from interacting with APC/C (Chao et al., 2012). The other method of inhibition is that the MCC inhibits active APC/C that already is bound cdc20 (Izawa and Pines, 2015). In some instances, cells can exit out of mitosis despite the spindle assembly checkpoint not being satisfied (Balachandran and Kipreos, 2017).

This process is called mitotic slippage, and it leads to aneuploidies (Balachandran and Kipreos, 2017). We previously showed that $CRL2^{ZYG11A/B}$ contributes to mitotic slippage by degrading cyclin B1 despite APC/C being inhibited upon treatment of cells with anti-microtubule drugs (Balachandran et al., 2016).

$CRL2^{ZYG11A/B}$ is an E3 ubiquitin ligase that contains cullin-2 as a scaffold and either ZYG11A or ZYG11B as a substrate receptor (Cai and Yang, 2016; Vasudevan et al., 2007). $CRL2^{ZYG11A/B}$ interacts with cyclin B1, polyubiquitylates it, and targets the substrate for proteasomal degradation (Balachandran et al., 2016). $CRL2^{ZYG11A/B}$ has a redundant function with APC/C and plays a more central role in degrading cyclin B1 either when APC/C is inactive or when cyclin B1 is overexpressed (Balachandran et al., 2016).

Since $CRL2^{ZYG11A/B}$ is involved in facilitating mitotic slippage, it is important that we understand what regions on ZYG11B and cyclin B1 are involved in their interaction, as this could allow us to understand how the interaction is regulated (Balachandran et al., 2016). Since $CRL2^{ZYG11A/B}$ is a potential anti-cancer drug target, understanding its interaction with cyclin B1 could also help in the design of novel anti-cancer drugs (Balachandran et al., 2016). We would like to understand how the interaction between $CRL2^{ZYG11A/B}$ and cyclin B1 is regulated because this is a relatively novel pathway that regulates mitosis (Balachandran et al., 2016). Many proteins involved in regulating the cell cycle interact with their substrates in a cell cycle specific manner and depend on post translational modifications for the interactions (Cai and Yang, 2016; Fuchs et al., 2004). For example, the E3 ubiquitin ligase, $SCF^{\beta TrCP}$ targets phosphorylated Emi1 for proteasomal destruction during mitosis (Fuchs et al., 2004; Margottin-Goguet et al.,

2003). This dissertation chapter elucidates the interaction between ZYG11B and cyclin B1 and also investigates how their interaction is regulated.

Results

ZYG11B interacts with CBOX1 and CBOX2 of cyclin B1

We previously showed that ZYG11B interacts with cyclin B1 and targets cyclin B1 for proteasomal degradation (Balachandran et al., 2016). Since ZYG11B physically interacts with cyclin B1, we wanted to determine which domains of cyclin B1 are recognized by ZYG11B. Cyclin B1 contains an N-terminal destruction box followed by a CBOX1 domain and a CBOX2 domain (Brown et al., 2007; Petri et al., 2007). CBOX1 is known to interact with CDK (Morgan, 1997; Petri et al., 2007). Additionally, *C. elegans* ZYG-11 expressed in human cells interacts with CBOX1 of *C. elegans* cyclin B (Balachandran et al., 2016). Based on this information, we sought to determine whether human ZYG11B recognized cyclin B1 via CBOX1 as well.

We generated HA-ZYG11B and truncated cyclin B1-Venus expression constructs. The Venus-tagged cyclin B1 constructs consisted of the following: cyclin B1-Venus, N terminus cyclin B1-Venus, cyclin B1 CBOX1-Venus, and cyclin B1 CBOX2-Venus (Fig. 2.1). The cyclin B1-Venus construct encodes the full-length version of cyclin B1. The N-terminus cyclin B1-Venus construct encodes the N-terminal portion of cyclin B1. This is the same region that contains the destruction box that is recognized by APC/C (Brown et al., 2007). The CBOX1-Venus construct encodes the CBOX1 region plus the five amino acid flexible linker sequence that links CBOX1 to CBOX2 in the full-length cyclin B1. The amino acids of this flexible linker are FGLGR.

The CBOX2-Venus construct encodes the CBOX2 region plus the FGLGR linker. These Venus-tagged constructs were co-expressed with HA-ZYG11B in HEK 293T human embryonic kidney cells. An empty EGFP vector was also co-transfected with HA-ZYG11B as a negative control. Venus-tagged proteins as well as EGFP were immunoprecipitated with GFP-Nano antibodies agarose beads (Allele Biotechnology). The pulled-down samples were run on a western blot and probed for HA-ZYG11B. The results suggest that ZYG11B recognizes cyclin B1 via CBOX1 and CBOX2; however ZYG11B interacts with CBOX1 significantly more than with CBOX2 (Fig 2.2). The N-terminus of cyclin B1 does not interact with ZYG11B, suggesting that human ZYG11B does not recognize cyclin B1 via its destruction box like APC/C does (Balachandran et al., 2016; van Zon et al., 2010).

The result that ZYG11B interacts with CBOX1 and CBOX2 of cyclin B1 was unexpected since previous results show that *C. elegans* ZYG11B only interacts with CBOX1 (Balachandran et al., 2016; Brown et al., 2015; Petri et al., 2007). One possibility for the discrepancy in results was that the FGLGR linker sequence is in both the CBOX1 and CBOX2 Venus-tagged proteins. It was thus possible that the FGLGR sequence is part of the degron recognized by ZYG11B, and as a result CBOX1 and CBOX2 are pulled down with ZYG11B since both cyclin B1 truncations contain the FGLGR sequence. According to the cyclin B1 crystal structure, FGLGR consists of amino acid residues that are accessible on the surface of cyclinB1, and as result this sequence could be a potential degron (Fig. 2.3) (Petri et al., 2007). To test whether FGLGR is involved in the interaction with ZYG11B, we generated additional Venus-tagged cyclin B1 truncations, except this time CBOX1 and CBOX2 were devoid of the

FGLGR sequence. These proteins are called CBOX1 no linker-Venus (CBOX1nl-Venus) and CBOX2 no linker-Venus (CBOX2nl-Venus). A follow up experiment was performed with these new constructs by co-transfecting HEK 293T cells with HA-ZYG11B and the Venus-tagged CBOXnl proteins (Fig. 2.4). In this experiment, after cells were lysed, Venus immunoprecipitations were performed, and we subsequently probed for HA ZYG11B via western blot. ZYG11B interacts with CBOX1nl and CBOX2nl, but ZYG11B interacts stronger with CBOX1nl than with CBOX2nl **(**Fig. 2.5) (Balachandran et al., 2016). This result suggests that the FGLGR linker is not involved in binding to ZYG11B and is not part of the cyclin B1 degron. Therefore, the degron(s) on cyclin B1 that ZYG11B recognizes is located in CBOX1 and CBOX2.

The vLRR domain of ZYG11B interacts with cyclin B1

Since we determined the domains of cyclin B1 that are recognized by ZYG11B, we wanted to determine what region of ZYG11B is responsible for interacting with cyclin B1. ZYG11B contains a VHL box, variant leucine rich repeat (vLRR) regions, and an armadillo-like (ARM) domain (Cai and Yang, 2016; Vasudevan et al., 2007). Leucine rich repeats and armadillo domains have been shown to be involved in protein-protein interactions in other proteins (Dokládal et al., 2018; Kobe and Kajava, 2001). To determine which ZYG11B regions are involved in cyclin B1 binding, we generated several HA-tagged truncations of ZYG11B (Fig. 2.6). The following ZYG11B constructs were created: HA-VHL box, HA-ΔVHL box, HA-vLRR(long), HA-vLRR (short), HA-ARM like domain (long), and ARM like domain (short) (Fig. 2.6). The HA-VHL box + AAs between VHL & LRR protein consists of all the amino acids from the first amino acid in

ZYG11B to the last amino acid right before the start of the first vLRR region. The HA-ΔVHL box protein includes all of ZYG11B minus the N terminal VHL box. The HA-vLRR (long) protein contains all of the vLRR regions plus a few amino acids beyond the vLRR boundaries in both directions. The HA-vLRR (short) protein contains all of the vLRR regions but stops immediately at the vLRR boundaries. The HA-ARM-like domain (long) protein consists of the ARM-like domain plus a few amino acids beyond the ARM-like domain. The HA-ARM like domain (short) protein contains the ARM-like domain but stops immediately at the ARM-like domain boundaries. We generated "long" versions of HA-tagged vLRR and ARM proteins to minimize the chances of disrupting secondary structures that could occur from cutting exactly at the beginning and end of domains when generating the ZYG11B truncations. Figure 2.6 illustrates the various HA-tagged ZYG11B truncations.

To map the interaction between cyclin B1 and the ZYG11B domains, we co-transfected each HA-tagged ZYG11B truncation construct with cyclin B1-Venus in HEK 293T cells. We used HA-ZYG11B as a positive control, and we co-transfected numerous HA-tagged negative control proteins: HA-EB1, HA-MBP, and HA-LRR-1. After transfected cells were lysed, cyclin B1-Venus was immunoprecipitated, and each HA-tagged protein was probed by western blot. The vLRR regions of ZYG11B interact strongly with cyclin B1 (Fig 2.7). Both vLRR proteins interact with cyclin B1, however vLRR(long) interacts stronger with cyclin B1 than does HA-vLRR(short). The likely reason for this significant difference in interaction is probably that the vLRR(long) is more structurally intact than the vLRR(short) due to the additional amino acids flanking the upstream and downstream vLRR boundaries in vLRR(long) (Dao et al., 2014). It is

also possible that the difference in interaction could be due to the extra amino acids found in vLRR(long) actually being involved in the binding with cyclin B1. In this experiment, HA-EB1, HA-MBP, and HA-LRR-1 were tested as negative controls. We used HA-MBP as the negative control comparison in this experiment and in future experiments.

Since we determined that the vLRR region of ZYG11B interacts with cyclin B1, we wanted to determine which vLRR repeats are involved in the interaction. ZYG11B has several vLRR repeats. In the previous experiment, vLRR(long) and vLRR(short) each contain all of the vLRR repeats. Since we are interested in determining which of these specific vLRR repeats are important in the interaction with cyclin B1, I generated three EGFP-tagged truncations of the vLRR repeats. The truncations were made by progressively cleaving ZYG11B from the N terminal side (Fig. 2.8). EGFP-ZYG11B 98-323 contains all 8 vLRR repeats. EGFP-ZYG11B 186-323 contains vLRR repeats 4-8. Lastly, EGFP-ZYG11B 266-323 contains vLRR repeats 7 and 8. The numbers indicated in the name of each EGFP-tagged vLRR truncation is the range of ZYG11B amino acids that are present. We co-transfected each EGFP-tagged vLRR truncation with HA-cyclin B1 and pulled down HA-cyclin B1 in the lysates. Each IP was probed for EGFP via western blot. EGFP empty vector was used as a negative control, and we tested different negative control transfection conditions to optimize expression (as negative control proteins are usually overexpressed relative to the test proteins). We picked the 0.1μg DNA transfection condition for EGFP as the negative control condition for the experiment. EGFP-ZYG11B 186-323 (vLRR repeats 4-8) interacts the strongest with HA-cyclin B1 (Fig. 2.9). However, EGFP-ZYG11B 266-323 (vLRR repeats 7-8) has

a decline in interaction with HA-cyclin B. These two results suggest that the vLRR binding site includes repeats 4, 5, and/or 6 as well as repeats 7 and/or 8, with repeats 4, 5, and/or 6 contributing significantly to the interaction with cyclin B1. EGFP-ZYG11B 98-323 contains vLRR repeats 1-8, but it does not interact with HA-cyclin B1 as strongly as EGFP-ZYG11B 186-323 (repeats 4-8). Also EGFP-ZYG11B 98-323 (repeats 1-8) only interacts moderately more with HA-cyclin B1 than does EGFP-ZYG11B 266-323 (repeats 7-8). EGFP-ZYG11B 186-323 interacts stronger with HA-cyclin B1 than does the longer EGFP-ZYG11B 98-323 probably because EGFP-ZYG11B 186-323 is smaller and contains the binding amino acids. We have seen in previous experiments that smaller truncations with a degron tend to interact stronger with the substrate receptor than larger pieces with the degron. For example, CBOX1 of cyclin B1 interacts significantly stronger with ZYG11B than does full-length cyclin B1 (Figs. 2.2 and 2.5). This stronger interaction could be because it's easier for a substrate receptor to stabilize a bond with a smaller substrate containing the degron than with a larger substrate containing the degron. The same reasoning could apply when a smaller substrate receptor region potentially binds better to a full-length substrate than does a larger substrate receptor region.

Identified CBOX1nl mutants with mild reduction in interaction with ZYG11B

Since we have a better understanding of the general domains in cyclin B1 and ZYG11B that are involved in binding, we wanted to determine specific amino acid residues in cyclin B1 that are recognized by ZYG11B. Mapping these cyclin B1 residues can provide information on the specific degron amino acids that ZYG11B recognizes. We

generated a number of Venus-tagged cyclin B1 mutants. All mutant residues were changed to serine. We generated these mutations based on several parameters. We mutated cyclin B1 amino acids residues that are conserved in cyclin B3 (*C. elegans*), cyclin B1 (*C. elegans*), and cyclin B (*H. sapiens*). We used the alignment of these proteins because they are ZYG11 substrates in humans or *C. elegans*. Also the residues had to be on the surface of cyclin B1 so that they are accessible for binding to ZYG11B. We were able to tell which amino acids are on the surface by looking at 3D representations of human cyclin B1's crystal structure using the Cn3D software (Petri et al., 2007).

For our initial cyclin B1-Venus mutations, we used the above criteria for selecting candidate mutant residues, plus we only picked residues that are on the opposite side of the cyclin B1/CDK interface (Brown et al., 2015). ZYG11B can interact with cyclin B1 that is bound to CDK as well as cyclin B1 that is not bound to CDK (Balachandran et al., 2016). Therefore, we decided to start our screen by mutating residues that are opposite the cyclin B1/CDK binding interface since we knew that those are the only residues accessible when ZYG11B interacts with cyclin B1 that is bound to CDK (Fig. 2.10). Our first cyclin B1-Venus mutant is cyclin B1 6-O mutant-Venus. This mutant contains 6 mutations that are opposite of the cyclin B1/CDK binding interface, are conserved, and are accessible. In figure 2.10, the mutated residues are indicated by the green highlighted "6's". We co-transfected HEK 293T cells with cyclin B1 6-O mutant-Venus and HA ZYG11B. Lysates were subjected to Venus immunoprecipitations (IPs), and HA-ZYG11B was probed in all the samples via western blot. HA-ZYG11B interacts with Cyclin B1 6-O mutant-Venus (Figure 2.11). This result suggests that the six mutated

amino acid residues are not essential components of the cyclin B1 degron recognized by ZYG11B.

Since the cyclin B1 6-O mutant still interacted with ZYG11B, we expanded the number of residues mutated in cyclin B1 6-O to 10 mutations, and we generated another cyclin B1 mutant that has 10 mutations that are on the same side as the cyclin B1/CDK binding interface. These new mutants are called cyclin B1 10-O mutation-Venus and cyclin B1 10-CDK mutation-Venus respectively (Fig. 2.10). In Figure 2.10, the amino acid residues mutated in cyclin B1 10-O mutation-Venus all have the magenta highlighted “O’s” above them. The amino acid residues mutated in cyclin B1 10-CDK have the red highlighted “C’s” above them in the same figure. These Venus-tagged cyclin B1 mutants were co-transfected with HA-ZYG11B. We immunoprecipitated the Venus-tagged proteins in the lysates and probed for HA via western blot. Surprisingly, ZYG11B interacted with both cyclin B1 10-O mutant and cyclin B1 10-CDK mutant (data not shown).

None of the full-length cyclin B1 mutants tested so far led to a reduction in interaction with ZYG11B. Most of the residues mutated are in CBOX1, however we previously showed that ZYG11B interacts with CBOX1 and CBOX2 (Figs. 2.2 and 2.5). Therefore, it is possible that the amino acids mutated in full-length cyclin B1 actually are part of the degron, but ZYG11B still Interacts with the full-length cyclin B1 mutants because CBOX2 is available to bind to (Fig. 2.10). Also, CBOX1 has several mutated residues in the cyclin B1 mutants while CBOX2 has only a few mutated residues in the cyclin B1 mutants. The cyclin B1 10-O mutant has no mutated residues in CBOX2, while the cyclin B1 10-CDK mutant only has two mutant residues in CBOX2 (Fig 2.10).

To address this potential issue, we generated the same combinations of 10 mutations in CBOX1nl-Venus rather than the full-length cyclin B1-Venus. Placing these mutations into a CBOX1nl construct eliminates the issue of ZYG11B interacting with the CBOX2 domain of the full-length cyclin B1. We generated the following fusion proteins: CBOX1nl 6-O mutation-Venus, CBOX1nl 10-O mutation-Venus, and CBOX1nl 10-CDK mutation-Venus. HEK 293T cells were co-transfected with HA-ZYG11B and each of these Venus-tagged CBOX1nl mutant constructs. After cell lysis, Venus pull downs were performed on the lysates, and HA was probed via western blot. ZYG11B has a moderate reduction in interaction with CBOX1nl 6-O and CBOX1nl 10-CDK (Fig. 2.12). This result suggests that the CBOX2 in the full-length cyclin B1 mutant may have caused false-positive interactions in our previous mutagenic screens. However, it is peculiar that the CBOX1nl 10-O mutant does not have a reduction in interaction with ZYG11B despite the CBOX1nl 6-O mutant having a reduction in interaction with ZYG11B. This suggests that the additional three amino acids that are mutated in the CBOX1nl 10-O mutant may be involved in negatively regulating the interaction between cyclin B1 and ZYG11B. Another possibility is that these three mutated residues may unnaturally alter the confirmation of CBOX1nl in such a way that it non-specifically interacts with ZYG11B.

Because we only obtained a modest reduction in interaction of the CBOX1nl mutations with ZYG11B, we sought to test new mutant residue combinations in order to attempt to further disrupt the interaction of CBOX1nl with ZYG11B. We mutated amino acids EMYPPEI in CBOX1nl. Refer to the sequence alignment in figure 2.13 to see the positioning of this mutated region relative to the other mutations. In figure 2.13, the

mutated EMYPPEI sequence is marked by seven subsequent X's highlighted in dark green. We mutated these amino acids because they are clustered together in the cyclin B1 crystal structure, are on the surface, and are highly conserved (Petri et al., 2007). The residues being clustered together suggested to us that they could be a potential binding site for ZYG11B. We produced two Venus-tagged CBOX1nl PEI mutants. One mutant just has mutations of the EMYPPEI residues with the remainder of the cyclin B1 residues being wildtype. This mutant is called CBOX1nl PEI WT-WT. The second mutant has mutations of the EMYPPEI residues as well as the downstream two "O" residues highlighted in magenta in figure 2.13. This mutant is call CBOX1nl PEI WT-O. Once these two PEI constructs were generated, we co-transfected HEK 293T cells with HA-ZYG11B and each of Venus-tagged CBOX1nl PEI mutants. A Venus IP was performed of the lysates, and we probed for HA via western blot. According to the results ZYG11B has a moderate reduction in interaction with the CBOX1nl PEI WT-WT mutant and the CBOX1nl PEI WT-O mutant (data not shown). The result suggests that EMYPPEI on cyclin B1 plays a role in interacting with ZYG11B.

As of now we have four CBOX1nl mutants that have a moderate reduction in interaction with ZYG11B. These mutants are: CBOX1nl 6-O, CBOX1nl 10-CDK, CBOX1nl PEI WT-WT, and CBOX1nl PEI WT-O. Therefore, we combined a number of these mild interacting mutants to determine whether we could get a more significant reduction in interaction with ZYG11B. We also tested a new mutant in which residues TKQE are mutated. Refer to figure 2.14 to see the Venus-tagged CBOX1nl combined mutants that were generated. We co-transfected HEK 293T cells with HA-ZYG11B and each of these Venus-tagged CBOX1nl combined mutants. Venus IPs were performed

and HA-ZYG11B was probed for via western blot. All of the Venus-tagged CBOX1nl combined mutants interact with ZYG11B (Fig. 2.15). Based on these results, we presumably did not mutate all the cyclin B1 residues that are involved in binding with ZYG11B. However, we may have identified some of the residues involved in the interaction due to the partial reduction of binding of certain cyclin B1 mutants with ZYG11B. Additional mutagenic screens will need to be done in the future to further define the degron on cyclin B1.

The interaction between ZYG11B and cyclin B1 is moderately cell cycle regulated, while the interaction between ZYG11B and CUL2 is not cell cycle regulated

E3 ubiquitin ligases tend to recognize their substrates via post translational modifications (PTMs) in a cell cycle-dependent manner (Cai and Yang, 2016). For example, SCF^{cdc4} is an E3 ubiquitin ligase in budding yeast that interacts with phosphorylated Sic1, targeting this substrate for proteasomal degradation (Nasmyth, 1996; Skowyra et al., 1997). Degradation of Sic1 in turn leads to the G1/S transition (Nasmyth, 1996; Skowyra et al., 1997). We want to determine whether the interaction between ZYG11B and cyclin B1 is cell cycle regulated and how the interaction is controlled.

To test for cell cycle specific interactions, we co-transfected HEK 293T cells with HA-ZYG11B and cyclin B1-Venus. We then arrested the cells in either S phase or mitosis. Cells were arrested in S phase via thymidine treatment while cells were arrested in mitosis via nocodazole treatment. Cells were subsequently lysed, and Venus-cyclin B1 was immunoprecipitated. IP samples were then probed for HA-

ZYG11B via western blot. ZYG11B interacts with cyclin B1 slightly more in S phase than in M phase (Fig. 2.16). The amount of HA-ZYG11B expressed in the S phase whole cell lysate is significantly less than the amount of HA-ZYG11B expressed in the M phase whole cell lysate. Despite this significant difference, the HA-ZYG11B signal in the Venus IP is roughly equal for S phase and M phase samples. This suggests that ZYG11B interacts with cyclin B1 to a greater extent during S phase than during mitosis. This is an unexpected result because ZYG11B would be expected to interact with cyclin B1 more in mitosis since ZYG11B is known to contribute to mitotic slippage (Balachandran et al., 2016). The fact that ZYG11B does interact with cyclin B1 during mitosis would allow still ZYG11B to contribute to mitotic slippage despite a lower level of interaction of ZYG11B during M phase compared to S phase.

We also tested whether our truncated version of ZYG1B that binds cyclin B1, ZYG11B 186-323, has cell cycle-regulated binding to cyclin B1. ZYG11B 186-323 contains vLRR regions 4 to 8, and interacts strongly with cyclin B1 (Fig. 2.9). Since the interaction between ZYG11B 186-323 and cyclin B1 is strong, we thought that we might be able to see a greater difference in binding between S phase and M phase samples than we saw in the full-length cell cycle stages experiment. We co-transfected HEK 293T cells with EGFP-ZYG11B 186-323 and HA-cyclin B1. Cells were arrested in S phase or M phase, and the HA-cyclin B1 was pulled down from the lysates, followed by probing for EGFP-ZYG11B 186-323 via western blot (Fig. 2.17). The interaction between ZYG11B 186-323 and cyclin B1 is not cell cycle regulated. There is no significant difference in interaction between ZYG11B 186-323 and cyclin B1 in S phase or M phase.

The interaction between substrate receptors and their E3 scaffolds can be cell cycle regulated (Kotani et al., 1998; Kramer et al., 2000). For example, the interaction between APC/C and its substrate receptor, cdc20, occurs during mitosis (Kotani et al., 1998; Kramer et al., 2000). We wanted to determine whether the interaction between ZYG11B and its CUL2 scaffold is cell cycle regulated. We transfected HEK 293T cells with HA-ZYG11B or with HA-MBP. HA-MBP is a negative control. Cells were arrested in S phase or M phase. HA IPs were performed, and we probed for endogenous CUL2 in the western blot. There was no significant difference in the interaction between ZYG11B and CUL2 in S phase vs. M phase (Figure 2.18). Therefore, the interaction between ZYG11B and CUL2 does not appear to be cell cycle regulated.

Analysis of whether post-translational modifications correlate with the interaction of ZYG11B and cyclin B1 during M phase

We know that ZYG11B contributes to mitotic slippage by targeting cyclin B1 for degradation when APC/C is inhibited, and we determined that ZYG11B physically interacts with cyclin B1 during mitosis (Fig. 2.16) (Balachandran et al., 2016). In light of these observations, we wanted to determine whether the interaction between ZYG11B and cyclin B1 during mitosis depends on post translational modifications (PTMs). We transfected HEK 293T cells with HA-ZYG11B and cyclin B1-Venus. Cells were arrested in mitosis by treating them with nocodazole. Once cells were lysed, lysates were split into two samples. An IP for HA was performed on one sample, and an IP for Venus was performed on the other sample. The HA IP will show us PTMs on the sub-pool of cyclin B1-Venus that interacts with HA-ZYG11B, as well as all PTMs on HA-ZYG11B.

The Venus IP will show us PTMs on the sub-pool of HA-ZYG11B when it interacts with cyclin B1-Venus, as well as all PTMs on cyclin B1-Venus. Both samples were run on an SDS-PAGE gel, stained with Coomassie G250, and the two gel pieces were cut and sent for mass spectrometry analysis. Because HA-ZYG11B and cyclin B1-Venus are similar sizes, we were able to include both proteins in the gel slice for each sample. The gel slices were sent to Emory University's Integrated Proteomics Core where tandem mass spectrometry was used to identify PTMs on HA-ZYG11B and cyclin B1-Venus tryptic peptides. Cyclin B1-Venus that was pulled down in the HA-ZYG11B IP did not identify any *in vivo*-derived PTMs (Table 2.1). We identified phosphorylations and acetylations on cyclin B1 that was pulled down in the cyclin B1-Venus IP. HA-ZYG11B that was pulled down in the cyclin B1-Venus IP did not identify in vivo-derived PTMs (Table 2.2). We also identified acetylations on the ZYG11B that was pulled down in the HA-ZYG11B IP. These results suggest that either the interaction between ZYG11B and cyclin B1 during mitosis does not depend on PTMs, or we missed detecting PTMs that were present. There also is the possibility that PTMs could exist that negatively regulate the interaction between ZYG11B and cyclin B1, however our peptide numbers for the interacting proteins were too low to make a conclusion about negative PTMs (Tables 2.1 and 2.2) We did not get complete peptide coverage from this mass spectrometry analysis (Fig. 2.20). There was 48.49% protein coverage for the sub-pool of cyclin B1 that was pulled down with ZYG11B (Fig. 2.20). Also there was 49.86 % protein coverage for the sub-pool of ZYG11B that interacted with cyclin B1-Venus (Fig. 2.20). Therefore, it's possible that we may have missed PTMs due to our low coverage. We will need to use a different peptidase other than trypsin during our

next mass spectrometry experiment in order to cut our sequences in a manner that will get us better protein coverage. Trypsin tends to cut cyclin B1 and ZYG11B in such a way that the peptide sequences are too large or too small to be analyzed by mass spectrometry.

Discussion

$CRL2^{ZYG11A/B}$ contributes to mitotic slippage by targeting cyclin B1 for degradation while the SAC is active (Balachandran et al., 2016). Mitotic slippage, in turn results in aneuploidies that promote cancer (Balachandran and Kipreos, 2017; Gascoigne and Taylor, 2009). The results obtained in this chapter help us better understand the interaction between ZYG11A/B and cyclin B1 that leads to the mitotic slippage and how this interaction is regulated.

ZYG11B recognizes cyclin B1 via CBOX1 and CBOX2, but ZYG11B has a preference for binding to CBOX1. We were surprised that CBOX2 interacts with ZXYG11B because the CBOX1 domain of cyclin B1 interacts with CDK1, and only the CBOX1 domain of *C. elegans* cyclin B appears to interact with *C. elegans* ZYG-11 (Balachandran et al., 2016; Morgan, 1997; Petri et al., 2007). It is possible that ZYG11B recognizes CBOX1 and CBOX2 to allow ZYG11B to interact with cyclin B1 that is bound to CDK and to interact with cyclin B1 that is not bound to CDK (Balachandran et al., 2016). Since CDK1 interacts with CBOX1, then when cyclin B1 is bound to CDK1, cyclin B1 potentially may only be able to interact with ZYG11B through CBOX2 (Brown et al., 2015; Morgan, 1997; Petri et al., 2007). For example, our CBOX1nl mutants that have reduced interactions with ZYG11B have a number of mutant residues

that are inaccessible while CDK1 is bound, and the mutants have a number of mutant residues that are accessible when CDK1 is bound (Fig 2.21.) (Wood et al., 2019). If the cyclin B1 degron consists mainly of the residues that are inaccessible when CDK1 is bound, then ZYG11B could only interact with cyclin B1 when CDK1 is not bound. However, if the cyclin B1 degron consists mainly of the residues that are accessible when bound to CDK1, then ZYG11B could interact with CBOX1 when CDK1 is bound. Regardless, when CDK1 is not bound to cyclin B1, both CBOX1 and CBOX2 are accessible for ZYG11B binding. Having both CBOX1 and CBOX2 binding domains potentially makes ZYG11B more versatile when interacting with cyclin B1. The vLRR region of ZYG11B interacts with cyclin B1, and vLRR repeats 4, 5, and 6 are particularly significant in the interaction. The fact that there is one interacting domain on ZYG11B is in stark contrast to the two interacting domains that are on cyclin B1. We generated sequential N terminal truncations of the vLRR domains of ZYG11B to determine which vLRR domains interact with cyclin B1. We could also create sequential C terminal truncations of the vLRR domains to get further insight into the interacting region on ZYG11B. Additionally, we could mutate amino acid residues in vLRR repeats 4, 5, and 6 in order to determine which residues on ZYG11B are involved in the interaction. Since vLRR domains 1 to 3 appear to not be significant in binding to cyclin B1, we could investigate what other roles those three domains play. Potentially, those domains are important in interacting with other ZYG11B substrates.

As mentioned earlier in this discussion section, our mutagenic screen of cyclin B1 interacting residues generated four CBOX1 mutants that each have a moderate decrease in interaction with ZYG11B. These mutants are: CBOX1nl 6-O, CBOX1nl 10-

CDK, CBOX1nl PEI WT-WT, and CBOX1nl PEI WT-O. Because we were not able to generate cyclin B1 mutants with significant reductions in interaction with ZYG11B, this suggests that we did not mutate all or most of the residues in the cyclin B1 degron that ZYG11B recognizes. We could test whether a CBOX1 PEI 10-O mutant would lead to a further reduction in interaction with ZYG11B since we did not test this mutant. When we designed these cyclin B1 mutants, we only mutated residues that are conserved, based on the conserved binding of ZYG11 and cyclin B1 in *C. elegans* and humans. It is possible that a number of non-conserved cyclin B1 residues are involved in the interaction with ZYG11B. If that were the case, then that would explain why we only get moderate reductions in interactions with our CBOX1 mutants. Mutating amino acid residues is not the most efficient manner of mapping the binding interface between ZYG11B and cyclin B1 because the binding interface appears to be wide. Generating crystal structures or NMR structures of cyclin B1 bound to ZYG11B would the best way of studying this interaction. We attempted to generate purified ZYG11B proteins for crystal structure and NMR analysis, but this effort was thwarted due to low protein expression of full-length ZYG11B and due to ZYG11B truncations being insoluble. Despite these challenges, in the future we should re-explore resolving the structure of ZYG11B alone as well as ZYG11B bound to cyclin B1. Generating these structures will allow us to thoroughly understand the interaction between ZYG11B and cyclin B1.

The results suggest that ZYG11B interacts with cyclin B1 during S phase and M phase, however ZYG11B interacts with cyclin B1 moderately more in S phase than in M phase. Even though ZYG11B does not interact with cyclin B1 to a greater extent in mitosis, ZYG11B nevertheless still interacts with cyclin B1 during mitosis. Because

ZYG11B interacts with cyclin B1 during mitosis, this supports our previous finding that ZYG11B contributes to mitotic slippage by degrading cyclin B1 when ACP/C is inhibited in mitosis (Balachandran et al., 2016). Cyclin B1 levels begin to rise during S phase, and cyclin B1 reaches its highest level at G2/M (Minshull et al., 1990; Pines and Hunter, 1991). Since ZYG11B slightly interacts with cyclin B1 more during S phase than during M phase, this suggests that ZYG11B may be regulating cyclin B1 levels during S phase to prevent premature entry into mitosis. We also show that ZYG11B interacts with the CRL2 scaffold CUL2 independently of the cell cycle.

We have not identified PTMs that regulate the interaction between ZYG11B and cyclin B1. Our mass spectrometry results of cells arrested in mitosis did not identify relevant PTMs on cyclin B1 sub-pools that interacted with ZYG11B or on ZYG11B sub-pools that interacted with cyclin B1. There are a number of possibilities for this negative result. Since we did not have adequate protein coverage, we may have missed being able to screen residues that had the modifications. Another possibility is that we did not have enough protein in our mass spectrometry samples to determine whether PTMs negatively regulated the interaction between ZYG11B and cyclin B1. We tested mitotic samples, and maybe regulatory PTMs are present in S phase cells, since ZYG11B interacts with cyclin B1 moderately more in S phase than in M phase. It is also possible that we did not identify PTMs because PTMs do not regulate the interaction. We believe that the purpose of ZYG11B in the cell is to play a redundant role with APC/C in order to keep cyclin B1 levels properly regulated. Potentially, a low-level, constitutive (i.e., non-regulated) degradation of cyclin B1 could nevertheless play an important role

under abnormal circumstances such as when cyclin B1 is overexpressed or APC/C is inactive (Balachandran et al., 2016).

Materials and Methods

Expression Constructs

Venus-tagged cyclin B1 truncations were subcloned into the pVenus-N1 cyclin B1 plasmid after cyclin B1 was digested out of the plasmid. The Pines laboratory originally created pVenus-N1 cyclin B1 (addgene plasmid # 26062). All HA-tagged constructs were subcloned into an HA-tagged pEGFP-N1 ΔEGFP plasmid. The pEGFP plasmid was used, but we cleaved out the EGFP tag and placed an HA tag at the N terminus. We then subcloned our insert into this plasmid at the position where the EGFP was once at. We used the pEGFP-N1 ΔEGFP plasmid because this plasmid expresses proteins relatively equally with the Venus-tagged plasmid when co-expressed in HEK 293T cells. Therefore, the co-expressed plasmids can be expressed to similar levels assuming that protein sizes are the same. EGFP-tagged ZYG11B plasmids were subcloned into the pEGFP plasmid (Clontech).

Cell Culture, DNA transfections, and Synchronization

HEK 293T cells were maintained in DMEM (HyClone) with 10% FBS (Sigma-Aldrich) and 100 μg/ml Penicillin/Streptomycin (HyClone). HEK 293T cells were transfected with plasmids expressing human proteins. Polyethylenimine (PEI) was used as the transfection reagent for all transfections. Cells were harvested around 48 hours post transfection. In order to synchronize cells in S phase, cells were treated with 2.5 mM of

thymidine for 24 hours. The first 12 hours of treatment was with thymidine alone, while the second 12 hours of treatment included 50 μM N-acetyl leucy-leucy (ALLnL) added to the media with thymidine. Cells were harvested after the 24-hour thymidine treatment. In order to synchronize cells in M phase, cells were treated with 100 ng/ml nocodazole (Sigma-Aldrich) for 24 hours. The first 12 hours of treatment were with nocodazole alone, while the next 12 hours of treatment included 50 μM of ALLnL added to the media with nocodazole. Cells were harvested after the 24-hour nocodazole treatment. If any experiment did not require cells to be arrested in a certain stage of the cell cycle, then those cells were allowed to grow to confluency. Cells in these circumstances would be treated with 50 μM of ALLnL for 12-20 hours before they were collected. These confluent cells were collected 48 hours post transfection.

Immunoprecipitations

Before IPs, cells were lysed with NP-40 lysis buffer plus additives. The NP-40 lysis buffer consists of the following: 150 mM NaCl, 1mM EDTA, Tris (pH 7.4), 0.5% NP-40, 1mM DTT, 15 μM MG132, and 1x protease inhibitor cocktail (Roche). Lysates were spun at 13,000 rpm for 25 min at 4°C. The supernatants of the lysates were precleared with sepharose 4B beads (Sigma-Aldrich) for one hour. The precleared lysates were used for the IPs. Venus IPs used GFP-Nano antibody agarose beads (Allele Biotechnology), which were incubated with the lysate at 4°C for 1 hour and 45 minutes. HA IPs used protein G Sepharose beads. Before HA IPs were performed, protein G Sepharose beads were blocked with 1% BSA for at least 1 hour at 4°C. After blocking,

lysates were incubated with mouse HA antibodies for at least 1 hour at 4°C. After this incubation, the lysates/HA antibodies were added to the blocked protein G Sepharose beads, and the HA IP was performed overnight at 4°C. Beads were washed four to five times with NP-40 wash buffer for all IPs.

Antibodies and Western blots

We followed the western blot protocol outlined in (Gavini and Parameshwaran, 2020) except we used NuPAGE 4-12% Bis Tris protein gels (Thermo Fisher Scientific) for SDS PAGE, and we used NuPAGE transfer buffer for the wet transfer. We used the following mouse primary antibodies: anti-GFP (GF28R; Thermo Fisher Scientific), anti-HA (Thermo Fisher Scientific), and anti-alpha tubulin (Proteintech). We used the following rabbit primary antibodies: anti-HA (Thermo Fisher Scientific) and anti-cullin-2. Secondary antibodies used were: goat anti-mouse HRP (Proteintech) and goat anti-rabbit HRP (Proteintech).

Acknowledgements

I would like to thank the University of Georgia Department of Cellular Biology for providing me with a teaching assistantship during my graduate school career. This research was supported by grant R01 GM074212 from the National Institute of General Medical Sciences.

References

Abe, S., Nagasaka, K., Hirayama, Y., Kozuka-Hata, H., Oyama, M., Aoyagi, Y., Obuse, C., and Hirota, T. (2011). The initial phase of chromosome condensation requires Cdk1-mediated phosphorylation of the CAP-D3 subunit of condensin II. Genes Dev *25*, 863-874.

Balachandran, R.S., Heighington, C.S., Starostina, N.G., Anderson, J.W., Owen, D.L., Vasudevan, S., and Kipreos, E.T. (2016). The ubiquitin ligase CRL2ZYG11 targets cyclin B1 for degradation in a conserved pathway that facilitates mitotic slippage. J Cell Biol *215*, 151-166.

Balachandran, R.S., and Kipreos, E.T. (2017). Addressing a weakness of anticancer therapy with mitosis inhibitors: Mitotic slippage. Mol Cell Oncol *4*, e1277293-e1277293.

Basu, S., Roberts, E.L., Jones, A.W., Swaffer, M.P., Snijders, A.P., and Nurse, P. (2020). The Hydrophobic Patch Directs Cyclin B to Centrosomes to Promote Global CDK Phosphorylation at Mitosis. Curr Biol *30*, 883-892.e884.

Brown, N.R., Korolchuk, S., Martin, M.P., Stanley, W.A., Moukhametzianov, R., Noble, M.E.M., and Endicott, J.A. (2015). CDK1 structures reveal conserved and unique features of the essential cell cycle CDK. Nature communications *6*, 6769.

Brown, N.R., Lowe, E.D., Petri, E., Skamnaki, V., Antrobus, R., and Johnson, L.N. (2007). Cyclin B and cyclin A confer different substrate recognition properties on CDK2. Cell Cycle *6*, 1350-1359.

Cai, W., and Yang, H. (2016). The structure and regulation of Cullin 2 based E3 ubiquitin ligases and their biological functions. Cell Division *11*, 7.

Chao, W.C.H., Kulkarni, K., Zhang, Z., Kong, E.H., and Barford, D. (2012). Structure of the mitotic checkpoint complex. Nature *484*, 208-213.

Clute, P., and Pines, J. (1999). Temporal and spatial control of cyclin B1 destruction in metaphase. Nature Cell Biology *1*, 82-87.

Dao, T.P., Majumdar, A., and Barrick, D. (2014). Capping motifs stabilize the leucine-rich repeat protein PP32 and rigidify adjacent repeats. Protein science : a publication of the Protein Society *23*, 801-811.

Dick, A.E., and Gerlich, D.W. (2013). Kinetic framework of spindle assembly checkpoint signalling. Nature Cell Biology *15*, 1370-1377.

Dokládal, L., Benková, E., Honys, D., Dupľáková, N., Lee, L.Y., Gelvin, S.B., and Sýkorová, E. (2018). An armadillo-domain protein participates in a telomerase interaction network. Plant molecular biology *97*, 407-420.

Fuchs, S.Y., Spiegelman, V.S., and Kumar, K.G. (2004). The many faces of beta-TrCP E3 ubiquitin ligases: reflections in the magic mirror of cancer. Oncogene *23*, 2028-2036.

Gascoigne, K.E., and Taylor, S.S. (2009). How do anti-mitotic drugs kill cancer cells? Journal of cell science *122*, 2579-2585.

Gavini, K., and Parameshwaran, K. (2020). Western Blot (Protein Immunoblot). In StatPearls (Treasure Island (FL): StatPearls Publishing

Copyright © 2020, StatPearls Publishing LLC.).

Hwang, L.H., Lau, L.F., Smith, D.L., Mistrot, C.A., Hardwick, K.G., Hwang, E.S., Amon, A., and Murray, A.W. (1998). Budding yeast Cdc20: a target of the spindle checkpoint. Science *279*, 1041-1044.

Izawa, D., and Pines, J. (2015). The mitotic checkpoint complex binds a second CDC20 to inhibit active APC/C. Nature *517*, 631-634.

Knoblich, J.A., and Lehner, C.F. (1993). Synergistic action of Drosophila cyclins A and B during the G2-M transition. Embo j *12*, 65-74.

Kobe, B., and Kajava, A.V. (2001). The leucine-rich repeat as a protein recognition motif. Curr Opin Struct Biol *11*, 725-732.

Kotani, S., Tugendreich, S., Fujii, M., Jorgensen, P.M., Watanabe, N., Hoog, C., Hieter, P., and Todokoro, K. (1998). PKA and MPF-activated polo-like kinase regulate anaphase-promoting complex activity and mitosis progression. Mol Cell *1*, 371-380.

Kramer, E.R., Scheuringer, N., Podtelejnikov, A.V., Mann, M., and Peters, J.M. (2000). Mitotic regulation of the APC activator proteins CDC20 and CDH1. Mol Biol Cell *11*, 1555-1569.

Li, X., and Nicklas, R.B. (1995). Mitotic forces control a cell-cycle checkpoint. Nature *373*, 630-632.

Margottin-Goguet, F., Hsu, J.Y., Loktev, A., Hsieh, H.M., Reimann, J.D., and Jackson, P.K. (2003). Prophase destruction of Emi1 by the SCF(betaTrCP/Slimb) ubiquitin ligase activates the

anaphase promoting complex to allow progression beyond prometaphase. Dev Cell *4*, 813-826.

Minshull, J., Golsteyn, R., Hill, C.S., and Hunt, T. (1990). The A- and B-type cyclin associated cdc2 kinases in Xenopus turn on and off at different times in the cell cycle. The EMBO journal *9*, 2865-2875.

Morgan, D.O. (1997). Cyclin-dependent kinases: engines, clocks, and microprocessors. Annual review of cell and developmental biology *13*, 261-291.

Nasmyth, K. (1996). At the heart of the budding yeast cell cycle. Trends in genetics : TIG *12*, 405-412.

Onischenko, E.A., Gubanova, N.V., Kiseleva, E.V., and Hallberg, E. (2005). Cdk1 and okadaic acid-sensitive phosphatases control assembly of nuclear pore complexes in Drosophila embryos. Mol Biol Cell *16*, 5152-5162.

Petri, E.T., Errico, A., Escobedo, L., Hunt, T., and Basavappa, R. (2007). The crystal structure of human cyclin B. Cell Cycle *6*, 1342-1349.

Pines, J. (2011). Cubism and the cell cycle: the many faces of the APC/C. Nat Rev Mol Cell Biol *12*, 427-438.

Pines, J., and Hunter, T. (1991). Human cyclins A and B1 are differentially located in the cell and undergo cell cycle-dependent nuclear transport. The Journal of cell biology *115*, 1-17.

Preisinger, C., Körner, R., Wind, M., Lehmann, W.D., Kopajtich, R., and Barr, F.A. (2005). Plk1 docking to GRASP65 phosphorylated by Cdk1 suggests a mechanism for Golgi checkpoint signalling. Embo j *24*, 753-765.

Skowyra, D., Craig, K.L., Tyers, M., Elledge, S.J., and Harper, J.W. (1997). F-box proteins are receptors that recruit phosphorylated substrates to the SCF ubiquitin-ligase complex. Cell *91*, 209-219.

van Zon, W., Ogink, J., ter Riet, B., Medema, R.H., te Riele, H., and Wolthuis, R.M. (2010). The APC/C recruits cyclin B1-Cdk1-Cks in prometaphase before D box recognition to control mitotic exit. J Cell Biol *190*, 587-602.

Vasudevan, S., Starostina, N.G., and Kipreos, E.T. (2007). The Caenorhabditis elegans cell-cycle regulator ZYG-11 defines a conserved family of CUL-2 complex components. EMBO Rep *8*, 279-286.

Wood, D.J., Korolchuk, S., Tatum, N.J., Wang, L.Z., Endicott, J.A., Noble, M.E.M., and Martin, M.P. (2019). Differences in the Conformational Energy Landscape of CDK1 and CDK2 Suggest a Mechanism for Achieving Selective CDK Inhibition. Cell chemical biology *26*, 121-130.e125.

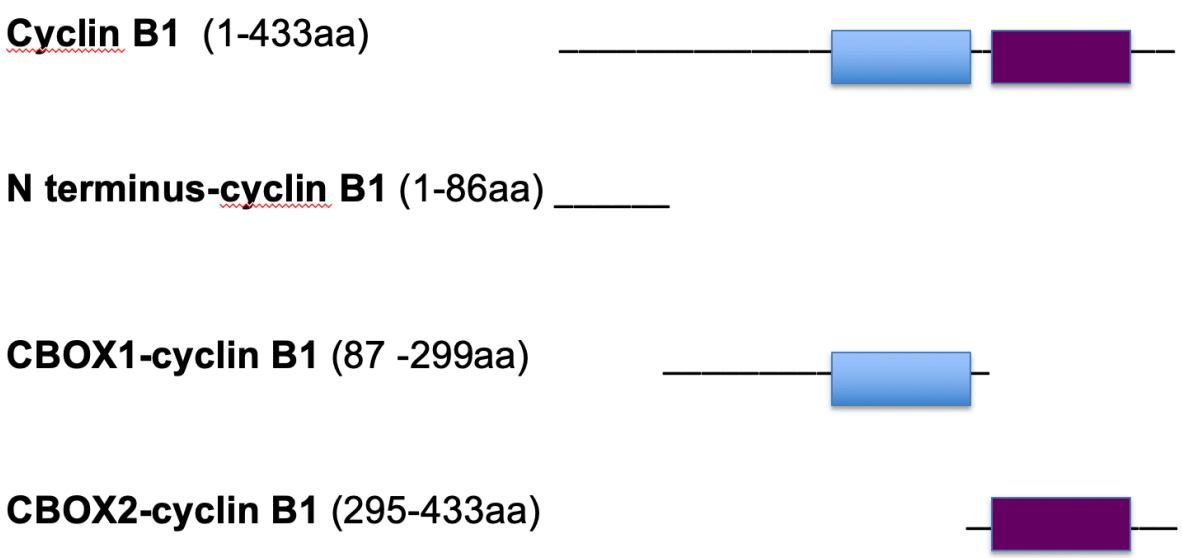

Figure 2.1. Venus-tagged cyclin B1 proteins generated. Expression constructs were made for cyclin B1-Venus, N terminus cyclin B1-Venus, CBOX1-Venus, and CBOX2-Venus. CBOX1 and CBOX2 each contain the five amino acid linker sequence that connects both cyclin boxes together in the full-length cyclin B1 protein. These Venus-tagged constructs were co expressed with HA-ZYG11B in HEK 293T cells in order to map the ZYG11B binding domains on cyclin B1. CBOX1 is depicted by the blue rectangle, and CBOX2 is depicted by the purple rectangle.

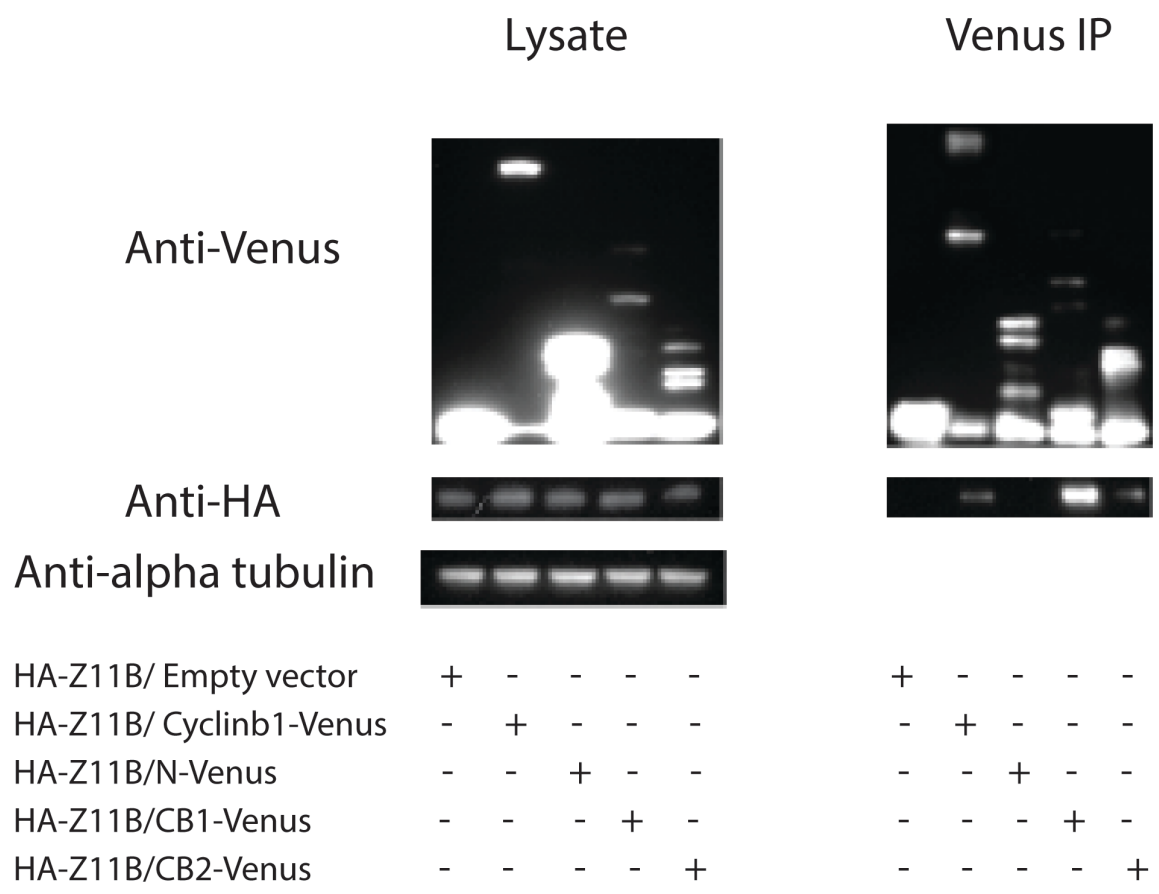

Figure 2.2. ZYG11B interacts with CBOX1 and CBOX2 of cyclin B1, with more interaction with CBOX1. HEK 293T cells were co-transfected with HA-ZYG11B and Venus-tagged cyclin B1 truncations. The Venus-tagged proteins and the EGFP empty vector control were pulled down and probe for interaction with HA-ZYG11B. ZYG11B interacts with CBOX1 (CB1) and CBOX2 (CB2) of cyclin B1, but ZYG11B interacts with CBOX1 significantly more. Note the increase in HA-ZYG11B co-precipitated with CB1-Venus (lane 4 of Venus IP, anti-HA blot). Modified from Balachandran et al., 2016.

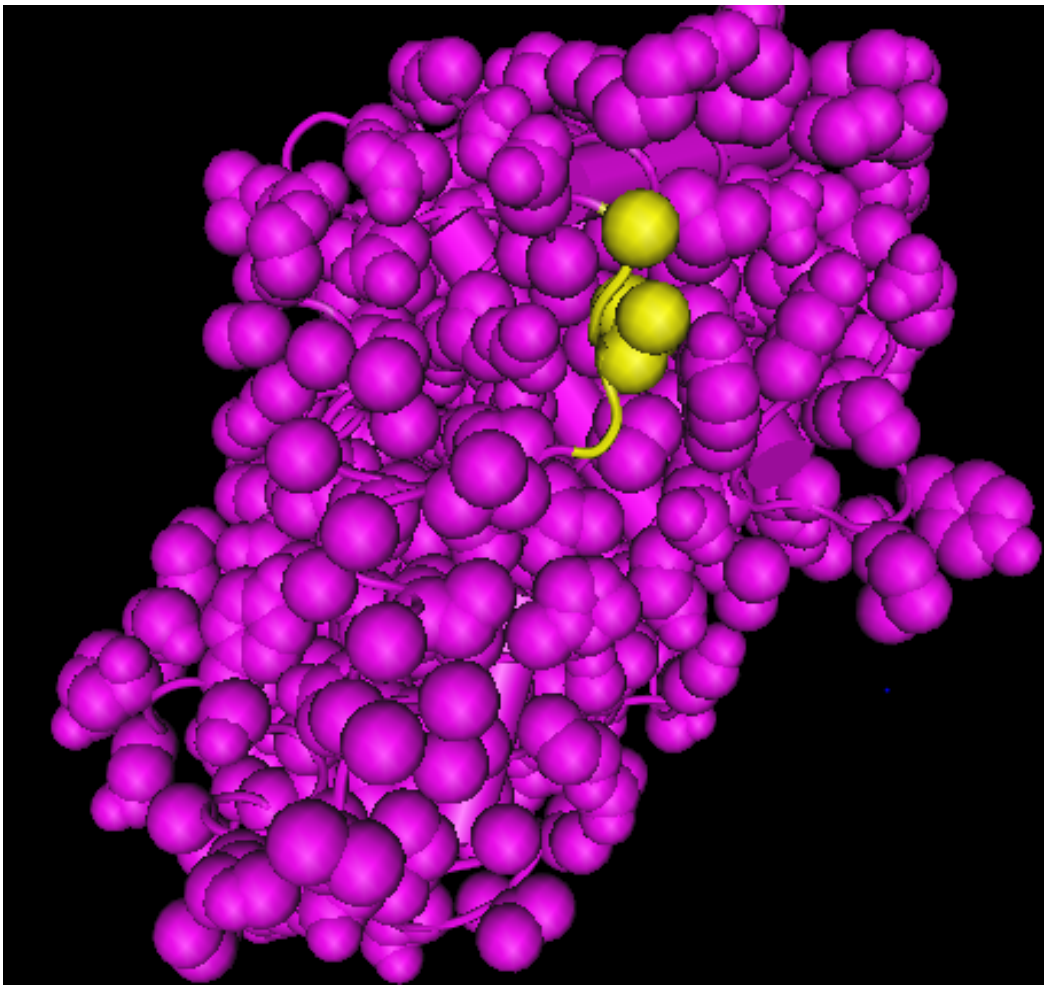

Figure 2.3. The FGLGR amino acid sequence links CBOX1 to CBOX2. A program known as Cn3D was used to visualize the crystal structure of cyclin B1 as obtained in (Petri et al., 2007). The FGLGR amino acid sequence is highlighted in yellow, and the image demonstrates that this sequence is accessible on the surface of cyclin B1.

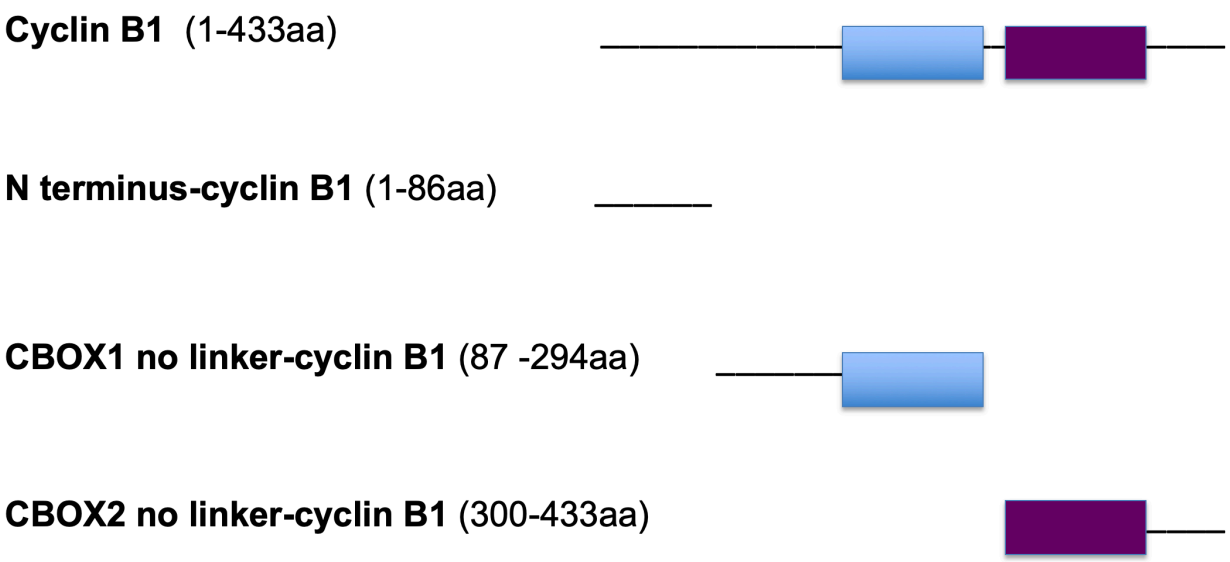

Figure 2.4. Venus-tagged CBOX1 no linker and CBOX2 no linker. CBOX1 cyclin B1 no linker-Venus (CBOX1nl-Venus) and CBOX2 cyclin B1 no linker-Venus (CBOX2nl-Venus) constructs were generated. CBOX1 is depicted by the blue rectangle, and CBOX2 is depicted by the purple rectangle.

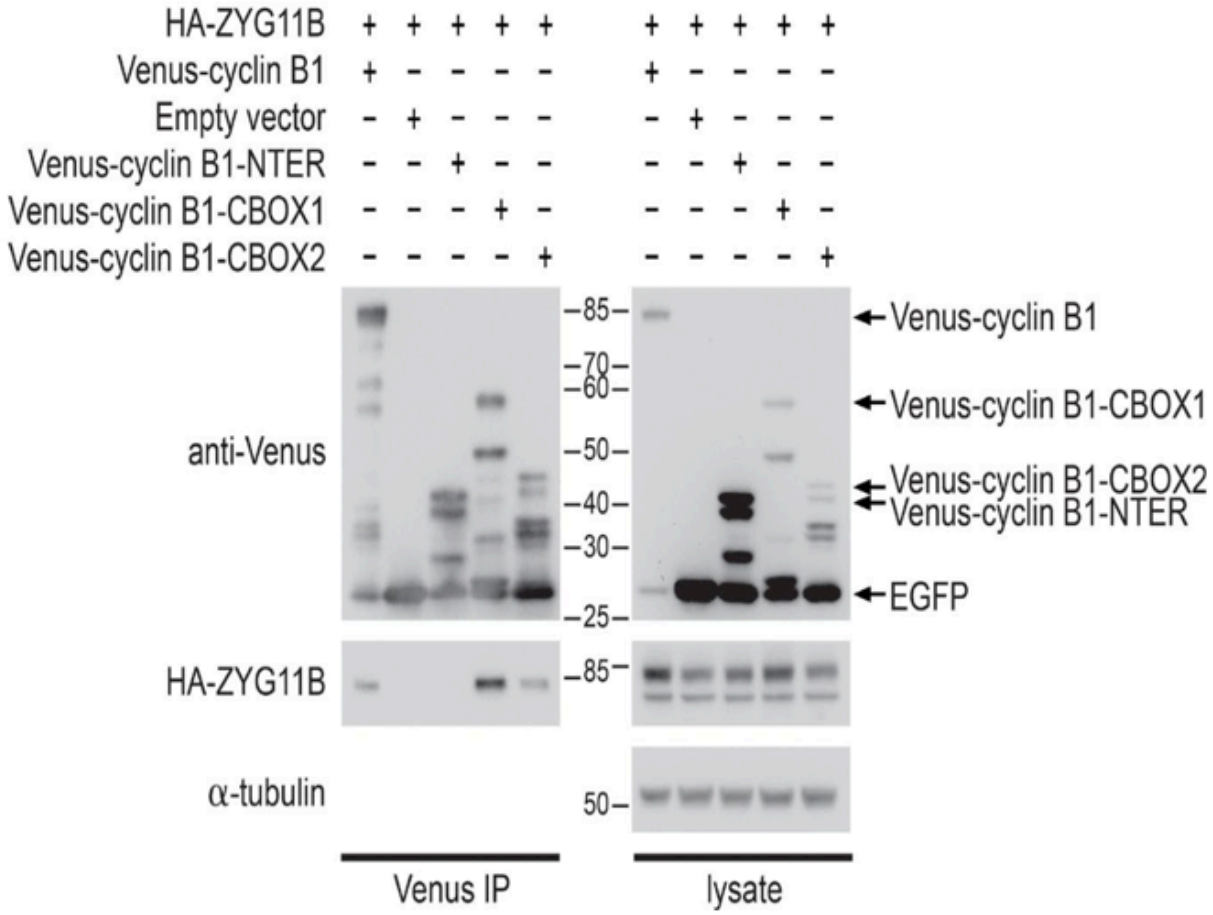

Figure 2.5. ZYG11B binds to CBOX1nl and CBOX2nl, but ZYG11B binds stronger to CBOX1nl. HEK 293T cells were co-transfected with HA-ZYG11B and Venus-tagged CBOX no linker constructs. After cells were lysed, Venus-tagged proteins were pulled down and probed for HA-ZYG11B via western blot. CBOX1nl and CBOX2nl interact with ZYG11B, however CBOX1nl interacts more strongly with ZYG11B. Note the increased HA-ZYG11B present in the fourth lane of the Venus IP relative to the fifth lane.

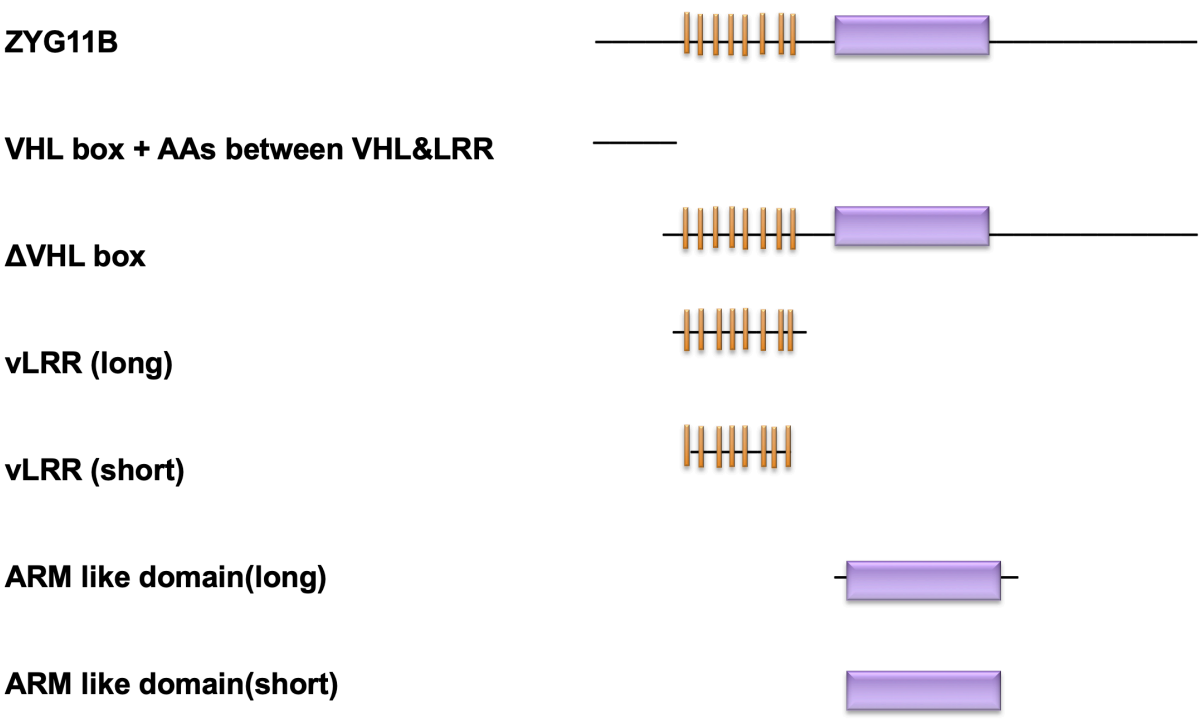

Figure 2.6. HA-tagged truncations of ZYG11B. Full-length HA-ZYG11B and six HA-tagged ZYG11B truncations were generated. The smaller orange rectangles represent each vLRR region, while the larger purple rectangle represents the ARM-like domain.

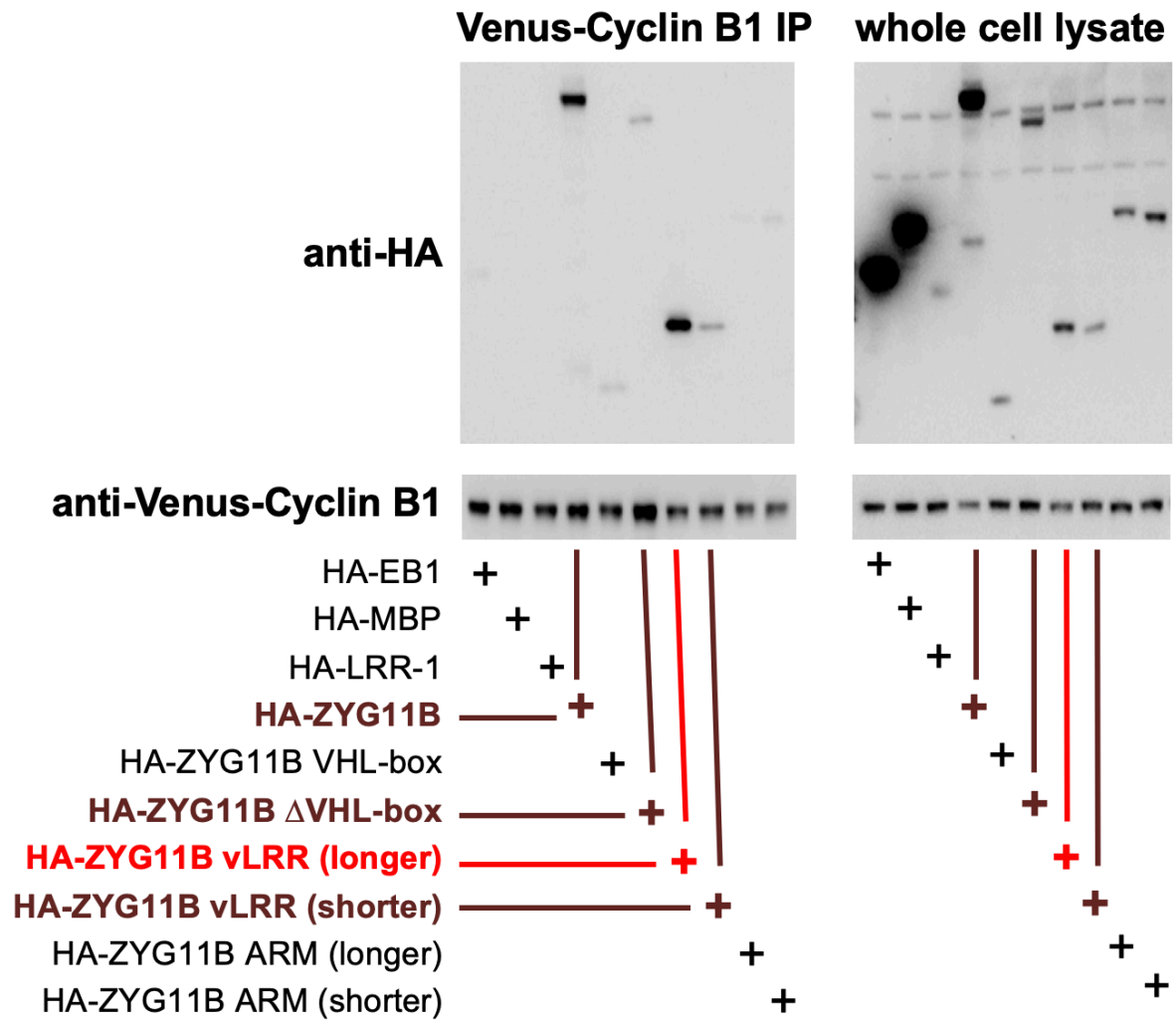

Figure 2.7. The vLRR regions of ZYG11B interact with cyclin B1. HA-tagged truncations of ZYG11B were co-expressed with cyclin B1-Venus in HEK 293T cells. Cyclin B1-Venus was pulled down and probed for the various HA-tagged constructs in the western blot. The vLRR region of ZYG11B interacts strongly with cyclin B1. HA-vLRR(long) interacts more strongly than HA-vLRR (short) protein. HA-EB1, HA-MBP, and HA-LRR-1 were negative controls.

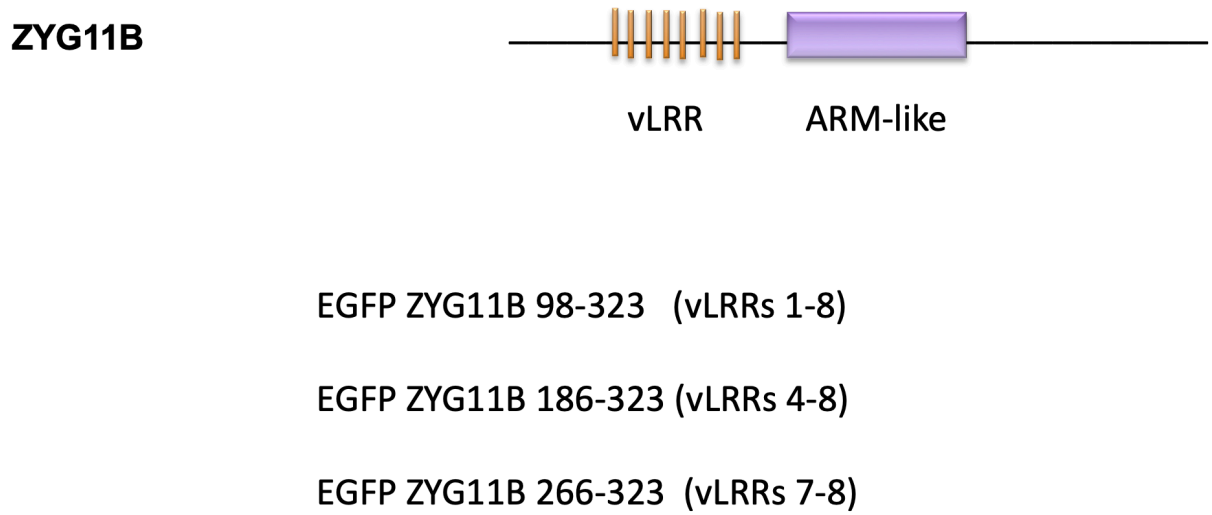

Figure 2.8. Truncations of vLRR region of ZYG11B. Three EGFP-tagged vLRR truncations of ZYG11B were created. EGFP-ZYG11B 98-323 consists of vLRR repeats 1 to 8. EGFP-ZYG11B 186-323 has vLRRs 4 to 8. EGFP-ZYG11B 266-323 contains vLRRs 7 to 8. Each smaller orange rectangle represents a vLRR repeat, while the larger purple rectangle represents the ARM-like domain.

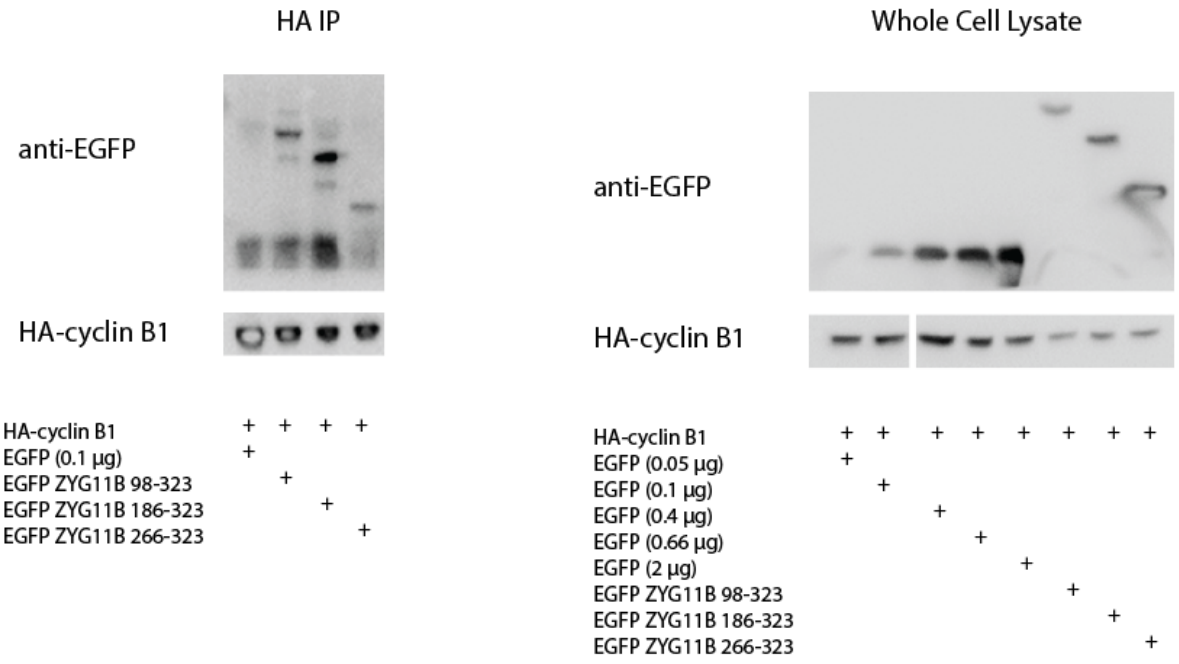

Figure 2.9. ZYG11B 186-323 interacts strongest with cyclin B1. EGFP vLRR truncations were co-expressed with HA-cyclin B1 in HEK 293T cells. We performed an HA IP and probed for the EGFP-tagged vLRR truncations via western blot. EGFP empty vector was used as a negative control, and we tested different DNA transfection conditions for the EGFP empty vector to optimize expression. The 0.1 μg DNA transfection condition for EGFP has the closest level of expression relative to the test proteins. EGFP-ZYG11B 186-323 interacts the strongest with cyclin B1. Since EGFP-ZYG11B 266-323 interacts significantly less with cyclin B1 than does EGFP-ZYG11B 186-323, this suggests that vLRR repeats 4, 5, and/or 6 are significant for interacting with cyclin B1.

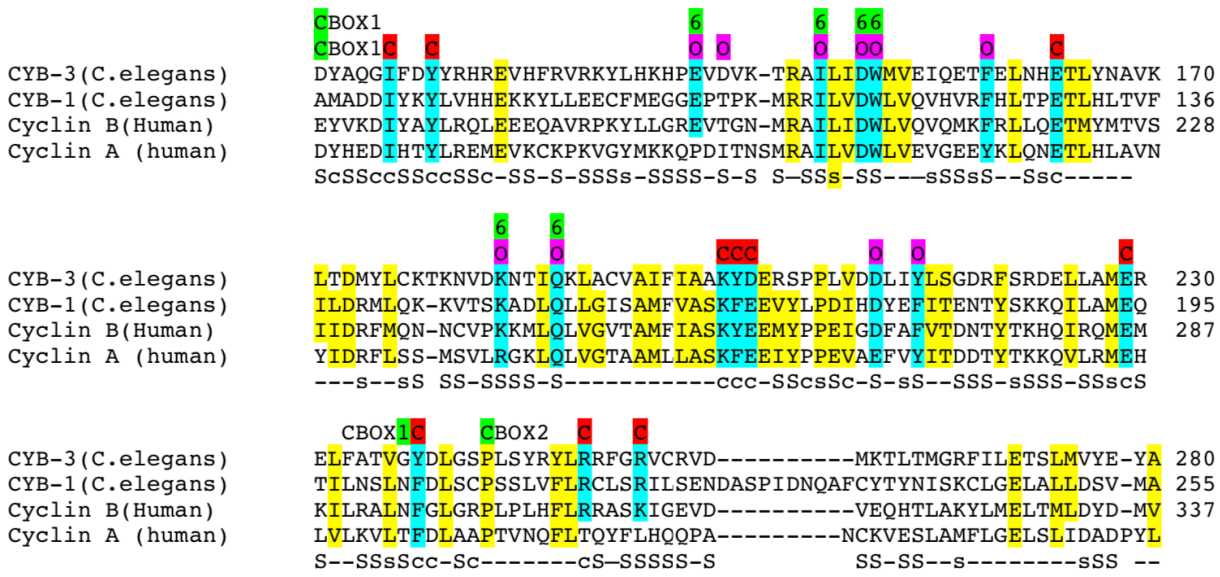

Figure 2.10. Sequence alignment representing cyclin B1 mutant residues. This sequence alignment highlights conserved residues in cyclin B3 (CYB-3; *C. elegans*), cyclin B1 (CYB-1; *C. elegans*), cyclin B1 (*H. sapiens*), and cyclin A (*H. sapiens*). Vertical highlights in cyan identify the human cyclin B1 residue that was mutated. All mutant residues were changed to serine. The magenta highlighted “O’s” represent residues opposite the cyclin B1/CDK binding interface. The red highlighted “C’s represent residues that are on the same side as the cyclin B/CDK binding interface. The green highlighted “6’s” represent residues that were mutated in our first cyclin B1 6-O mutant. Sequence alignment provided by Edward Kipreos.

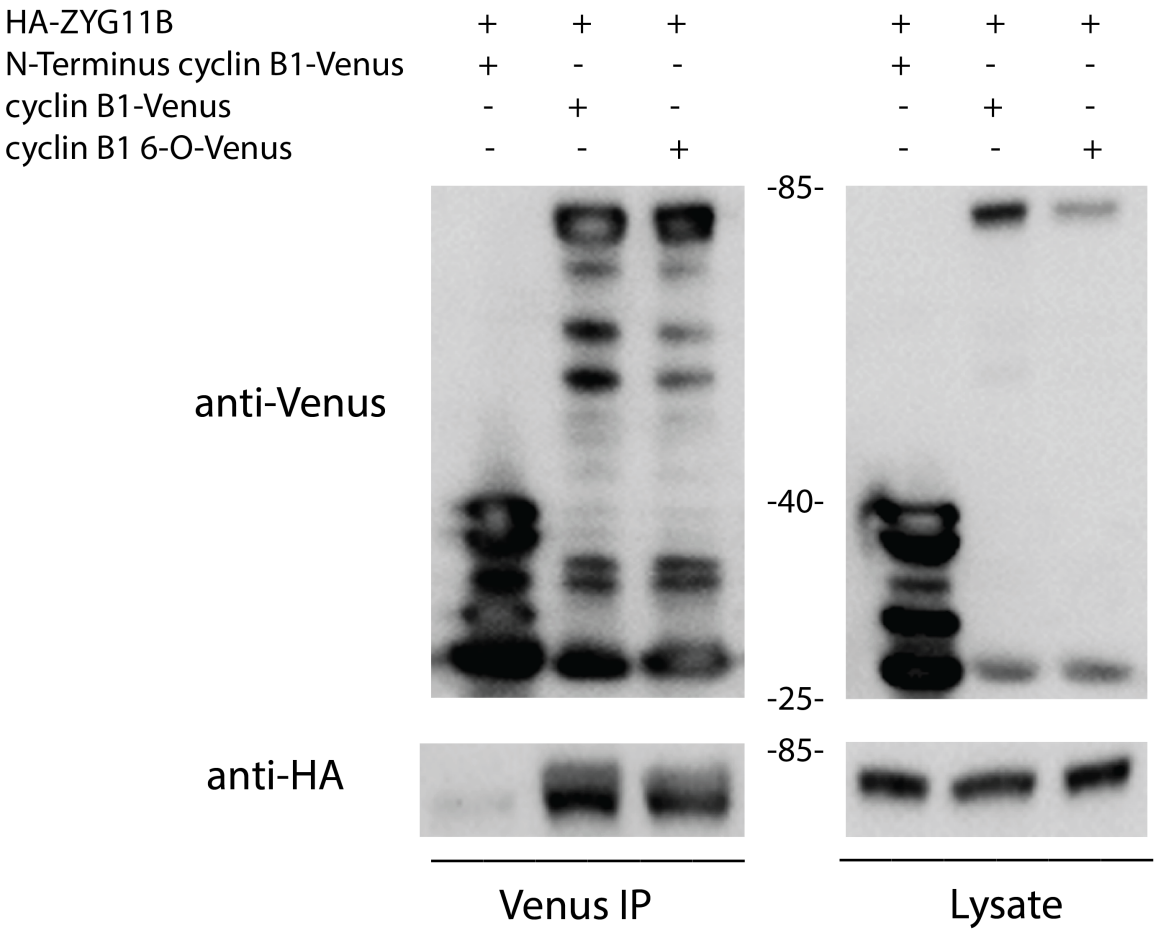

Figure 2.11. HA-ZYG11B interacts with cyclin B1 6-O mutant-Venus. HA-ZYG11B and cyclin B1 6-O mutant-Venus were co-expressed in HEK 293T cells. Subsequently a Venus IP of the lysate was performed followed by probing for HA via western blot. HA-ZYG11B binds to cyclin B1 6-O mutant-Venus.

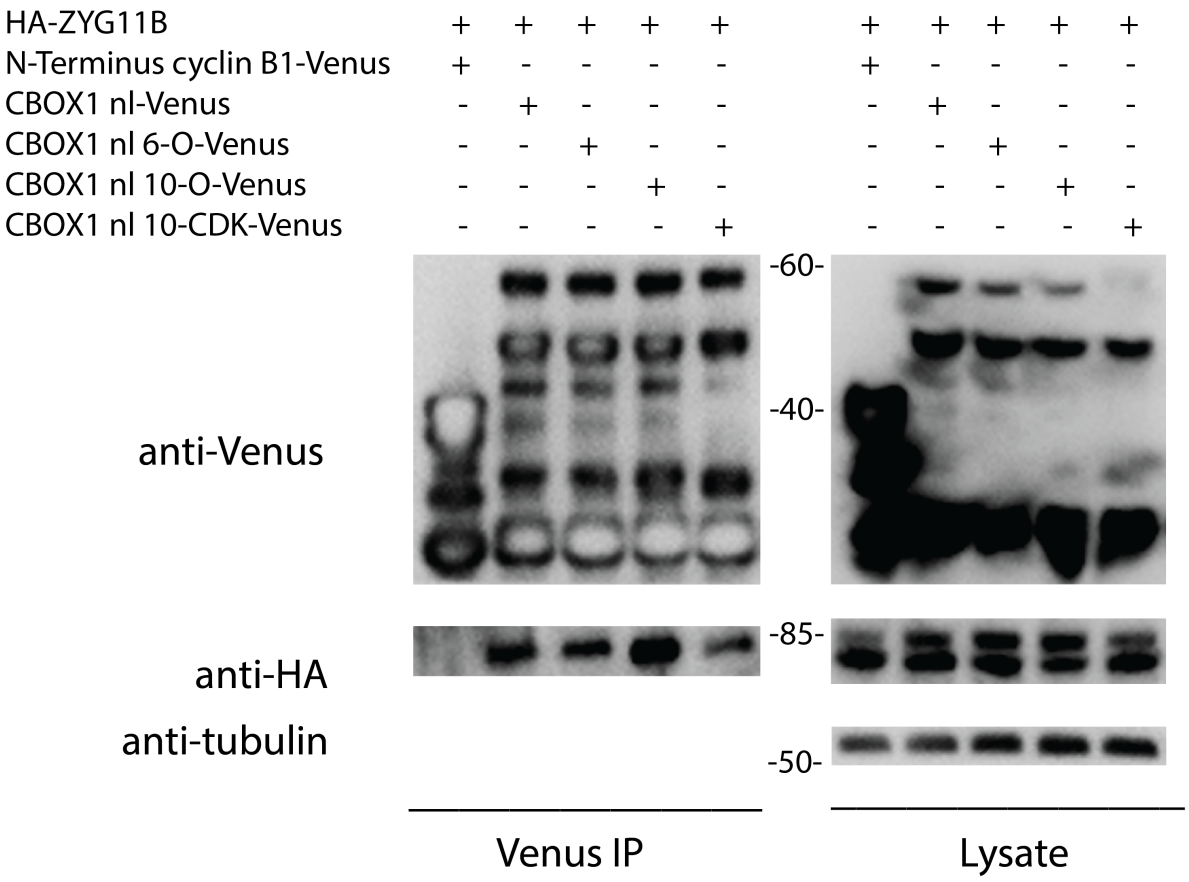

Figure 2.12. HA-ZYG11B has a moderate decrease in interaction with CBOX1nl 6-O and CBOX1nl 10-CDK. CBOX1nl cyclin B1-Venus mutations were co-expressed in HEK 293T cells with HA-ZYG11B. Venus IPs were performed on the lysates, and we probed for HA-ZYG11B via western blot. ZYG11B has a mild reduction in binding to CBOX1nl 6-O and CBOX1nl 10-CDK.

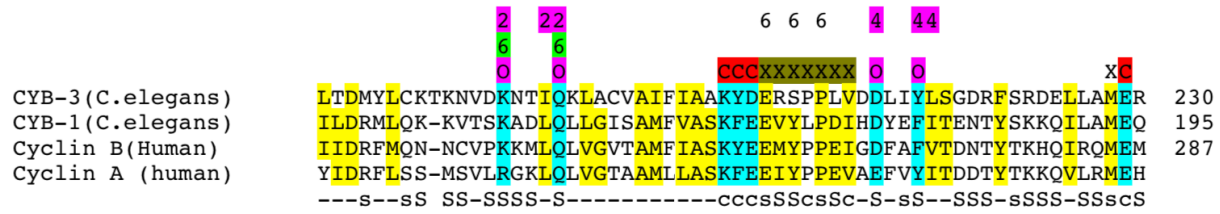

Figure 2.13. Sequence Alignment of CBOX1nl PEI mutations. CBOX1nl PEI mutant consists of mutations in residues EMYPPEI. This series of mutations are indicated by the 7 “X’s” highlighted in dark green on the alignment. Two CBOX1nL PEI mutants were generated. The first mutant has mutated EMYPPEI residues while the rest of cyclin B1 has wildtype residues. This mutant is called CBOX1nl PEI WT-WT. The second mutant has mutated EMYPPEI residues, and the downstream “O” residues highlighted in magenta in the alignment above are mutated. This mutant is call CBOX1nl PEI WT-O. (Sequence alignment provided by Dr. Edward Kipreos).

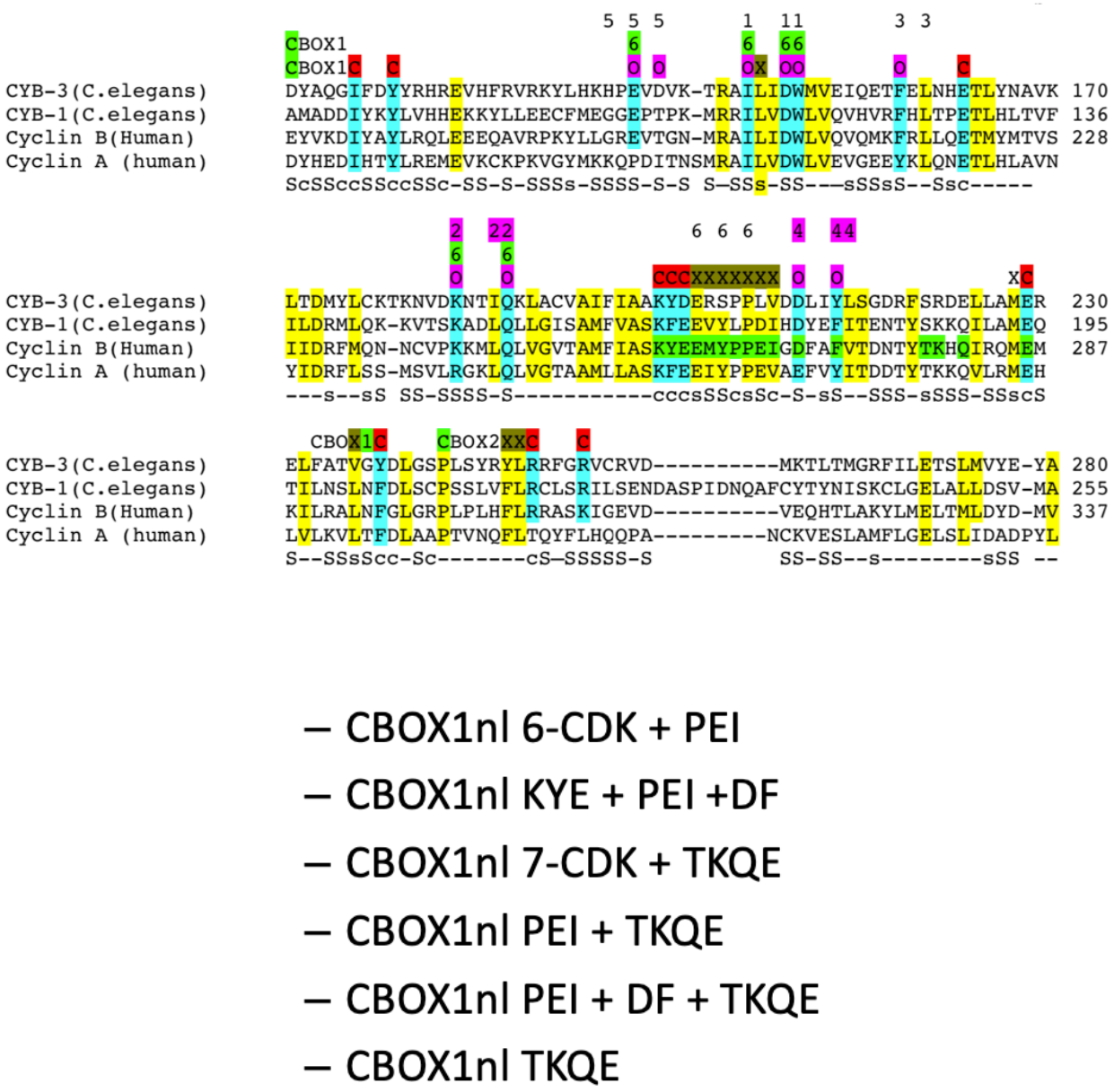

Figure 2.14. Sequence alignment of CBOX1nl combined mutants. CBOX1nl mutants that previously showed a mild reduction in interaction with ZYG11B were combined. The sequence alignment and the list of mutants above give representations of which residues were mutated. "KYE", "DF", and "TKQE" are residues that are mutated and are highlight neon green in the alignment. The EMYPPEI mutant residues

highlighted in neon green are called “PEI” in the mutant protein name. The phrase “CDK” mentioned in the mutant name represents various residues that are opposite the cyclin B1/CDK binding interface. A number of these residues are indicated by a red highlighted “C” in the sequence alignment. Sequence alignment provided by Edward Kipreos.

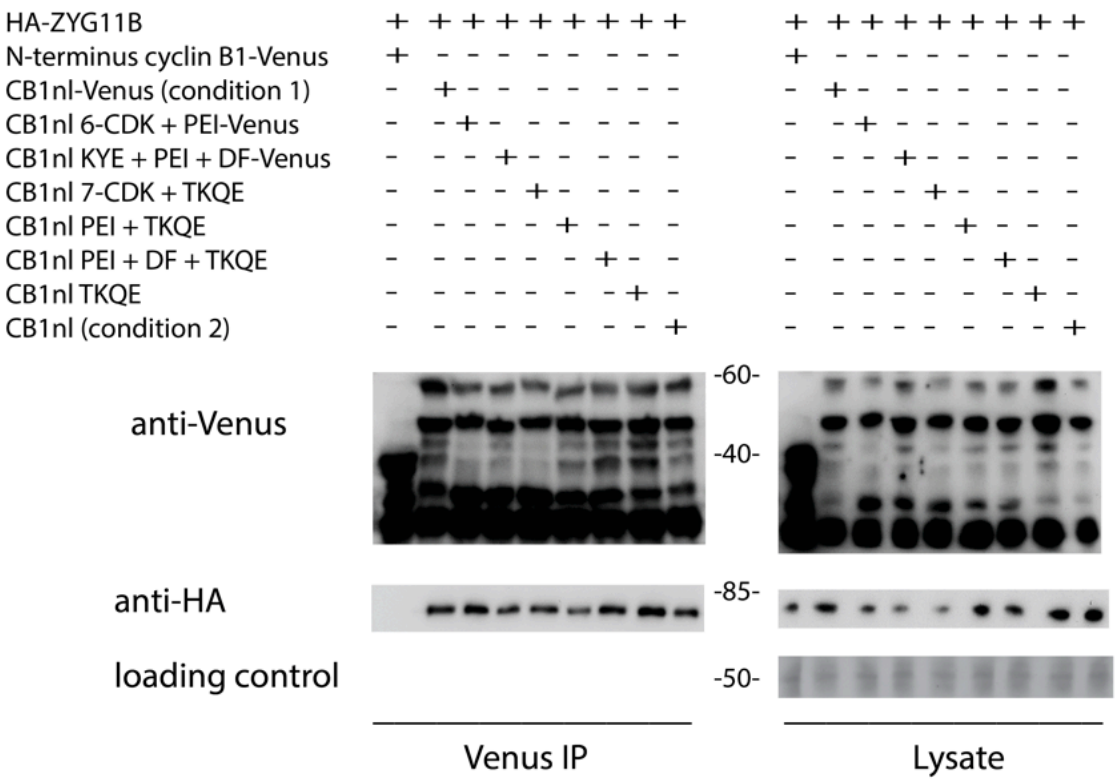

Figure 2.15. ZYG11B interacts with the CBOX1nl combined mutants. HA-ZYG11B and Venus-tagged CBOX1nl combined mutants were co-expressed in 293T cells. Lysates were subject to Venus IPs and HA-ZYG11B was probed via western blot. ZYG11B interacts with all the CBOX1nl combined mutants.

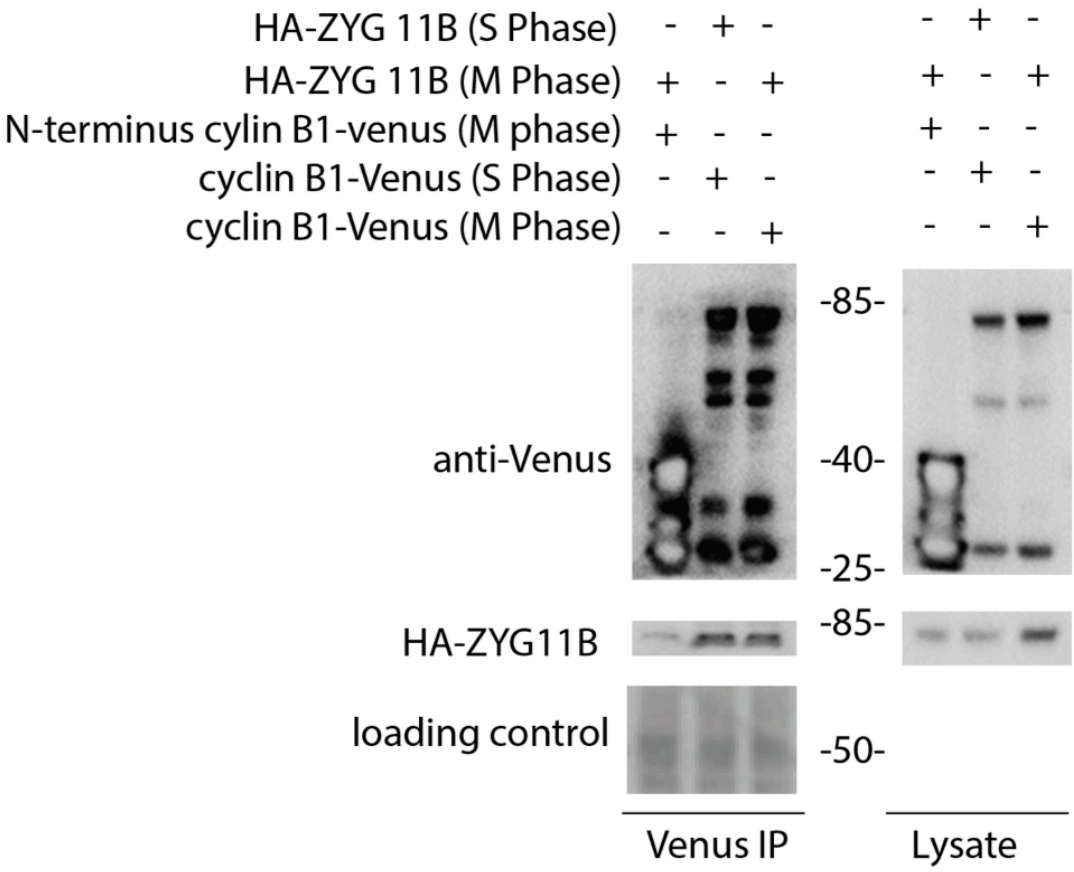

Figure 2.16. ZYG11B interacts with cyclin B1 slightly more in S phase than in M phase. HEK 293T cells were co-transfected with HA-ZYG11B and cyclin B1-Venus. The cells were then arrested in S phase or M phase. Venus IPs were performed on lysates followed by probing for HA via western blot. ZYG11B interacts with cyclin B1 slightly more during S phase than in M phase. Even though the HA-ZYG11B signal in the Venus IP is roughly equal for S phase and M phase samples, we conclude that the interaction in S phase actually is greater than the interaction in M phase because the amount of HA-ZYG11B expressed in the S phase whole cell lysate is significantly less than that expressed in the M phase whole cell lysate.

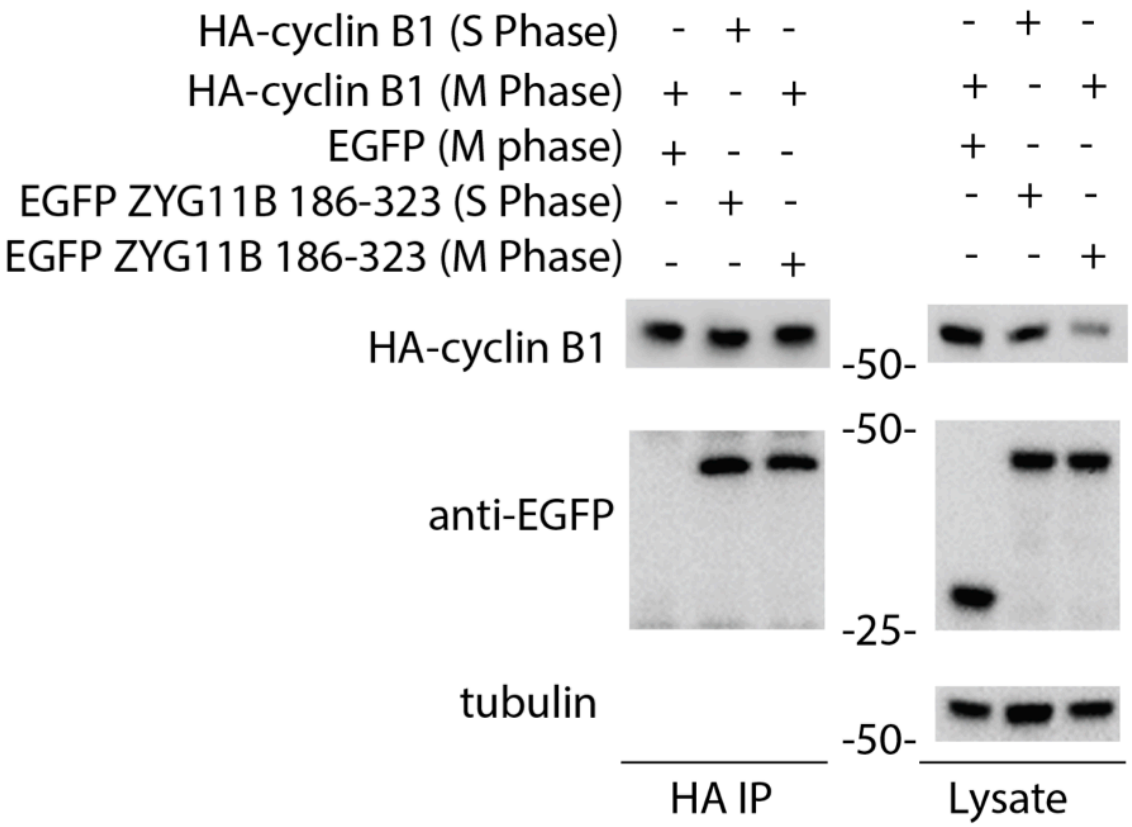

Figure 2.17. The interaction between ZYG11B 186-323 and cyclin B1 is not cell cycle regulated. HEK 293T cells were co-transfected with EGFP-ZYG11B 186-323 and HA-cyclin B1. EGFP alone is used as a negative control. HA-cyclin B1 was pulled down in the lysates followed by probing for EGFP via western blot. Relatively equal amounts of HA-cyclin B1 were pulled down in each sample. Upon probing the HA IPs for EGFP, the results show that there no significant difference in interaction between ZYG11B 186-323 and cyclin B1 in S phase or M phase.

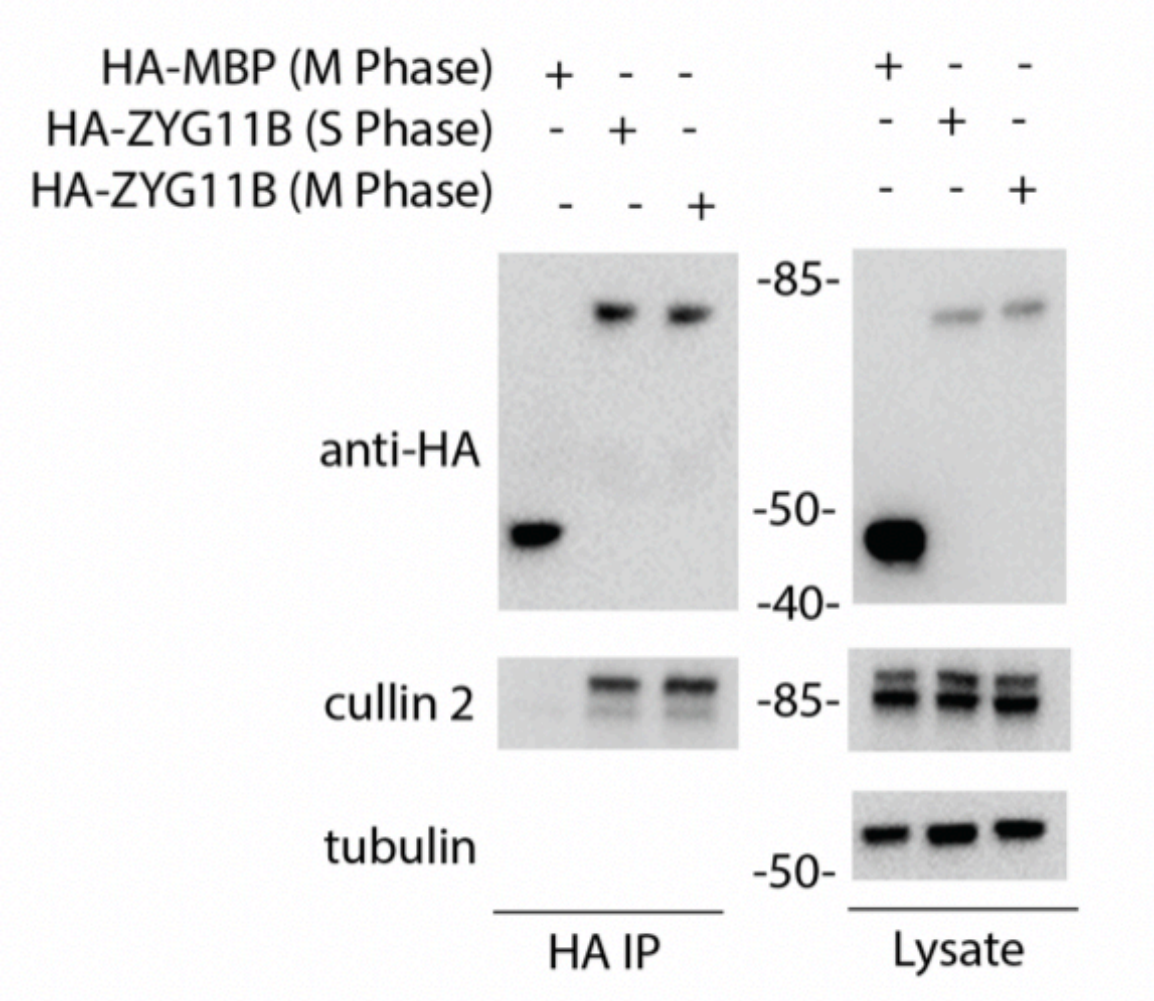

Figure 2.18. The interaction between ZYG11B and CUL2 is not cell cycle regulated. HEK 293T cells were transfected with HA-ZYG11B or HA-MBP. We used HA-MBP as a negative control. Cells were lysed, and the lysates were subject to HA IPs. We probed the HA IPs for CUL2 via western blot. There is no difference in the degree of interaction between ZYG11B and CUL2 in S phase or M phase

A

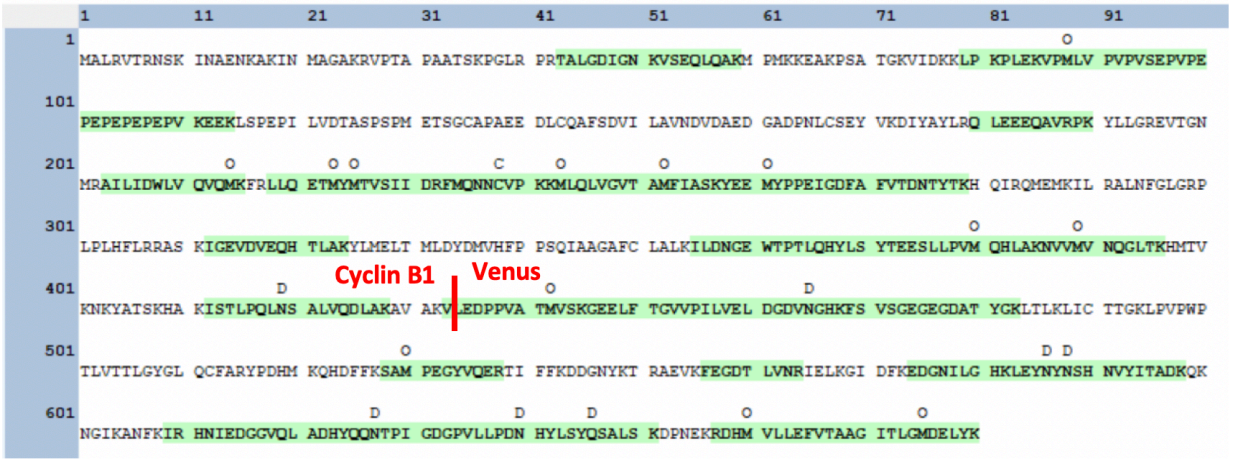

B

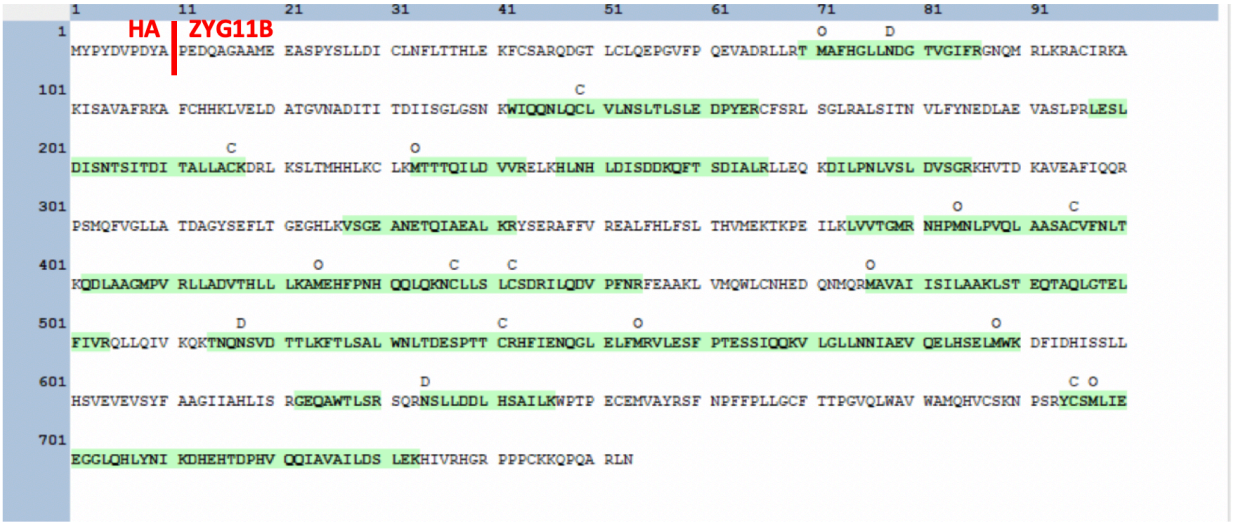

Figure 2.19. Protein coverage of HA-ZYG11B and cyclin B1-Veus in mass spectrometry experiment. (A) This is the sequence of cyclin B1-Venus. The green highlighted peptides are the peptides covered in the mass spectrometry experiment. This is the cyclin B1 sub-pool that was pulled down by HA-ZYG11B. The red line separates the cyclin B1 residues from the Venus residues. There is 48.49% coverage for cyclin B1. (B) This is the sequence of HA-ZYG11B. The green highlighted peptides are the peptides covered in the mass spectrometry experiment. This is the ZYG11B

sub-pool that was pulled down by cyclin B1-Venus The red line separates the ZYG11B residues from the HA residues. There is 49.86% coverage for ZYG11B.

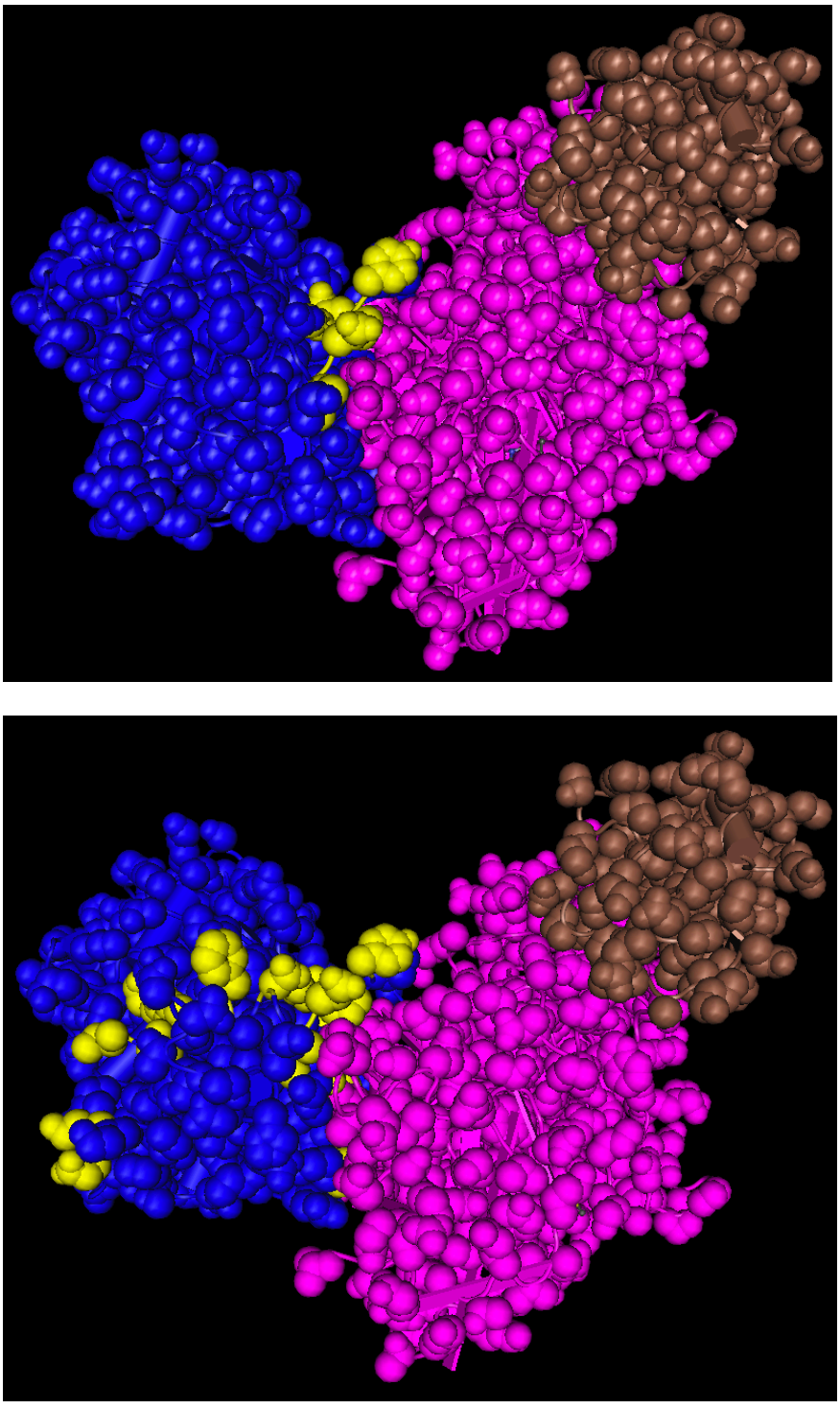

Figure 2.20. Highlighted CBOX1nl decreased binding mutants in crystal structure of cyclin B1 bound to CDK1. These are crystal structures of cyclin B1 bound to CDK1. Cn3D was used to obtain these structures. The blue structure is cyclin B1, the

magenta structure is CDK1, and the brown structure is CKS2 (CKS2 is not relevant for this figure and can be ignored). The image on the top has the CBOX1nl PEI mutations highlighted in yellow. The image on the bottom has all the mutations highlight in yellow from CBOX1nl 6-O, CBOX1nl 10-CDK, CBOX1nl PEI WT-WT, and CBOX1nl PEI WT-O mutants. These are all the mutants that had moderate reduction in interaction with ZYG11B. The PEI mutants are not in an optimal position for ZYG11B binding when CDK1 is bound. The CBOX1nl 10-CDK residues are between cyclin B1 and CDK1 and are difficult to view in the images above. The accessible mutant residues can be seen in the bottom image. (Wood et al., 2019)

A.) PTMs on cyclin B1 in cyclin B1-Venus IP

Modification	Peptide	PTM Peptide	Total Peptide	% PTM
phosphorylation (Y7)	LLQETMyMTVSIIDR	2	174	1.15%
phosphorylation (T5)	LLQEtMYMTVSIIDR	1	174	0.57%
phosphorylation (T3)	IStLPQLNSALVQDLAK	3	32	9.37%
acetylation (S2)	IsTLPQLNSALVQDLAK	7	40	17.5 %

B.) PTMs on cyclin B1 in HA-ZYG11B IP

Modification	Peptide	PTM Peptide	Total Peptide	% PTM
phosphorylation (Y7)	LLQETMyMTVSIIDR	0	10	0% (< 10%)
phosphorylation (T5)	LLQEtMYMTVSIIDR	0	10	0% (< 10%)
phosphorylation (T3)	IStLPQLNSALVQDLAK	0	5	0% (< 20%
acetylation (S2)	IsTLPQLNSALVQDLAK	0	5	0% (< 20%)

Table 2.1. Cyclin-B1-Venus does not contain PTMs when it interacts with HA-ZYG11B in mitosis. We performed a HA-ZYG11B IP and pulled down cyclin B1-Venus from mitotic cells. This sample was sent for mass spectrometry analysis to find PTMs. No relevant PTMs were found on the sub-pool of cyclin B1-Venus that was pulled down with HA-ZYG11B. Table A identifies PTMs found on peptide sequences in cyclin B1 from the cyclin B1-Venus IP. Table B shows the same peptide sequences from table A that lack PTMs. Table B are the peptide sequences on cyclin B1 from the HA-ZYG11B IP

A.) PTMs on ZYG11B in HA-ZYG11B IP

Modification	Peptide	PTM Peptide	Total Peptide	% PTM
acetylation (S2)	LsTEQTAQLGTELFIVR	4	23	17.4%

B.) PTMs on ZYG11B in cyclin B1-Venus IP

Modification	Peptide	PTM Peptide	Total Peptide	% PTM
acetylation (S2)	LsTEQTAQLGTELFIVR	0	2	0% (< 50%)

Table 2.2. HA-ZYG11B does not contain PTMs when it interacts with cyclin B1-Venus in mitosis. We performed a cyclin B1-Venus IP and pulled down HA-ZYG11B from mitotic cells. This sample was sent for mass spectrometry analysis to find PTMs. No relevant PTMs were found in sub-pool of HA-ZYG11B that was pulled down with cyclin B1-Venus . Table A identifies PTMs found on peptide sequences in ZYG11B from the HA-ZYG11B IP. Table B shows the same peptide sequences from table A that lack PTMs. Table B are the peptide sequences on ZYG11B from the cyclin B1-Venus IP

CHAPTER III

IDENTIFYING A NOVEL QUIESCENCE PATHWAY

Anderson J.W. and Kipreos E.T. to be submitted to *Journal of Molecular Biology*

Abstract

The leading cause of death from cancer in the United states is from lung cancer, and the most prevalent form of lung cancer is non-small cell lung cancer (NSCLC) (Ettinger et al., 2010; Siegel et al., 2016). ZYG11A is overexpressed in NSCLC tissue, and ZYG11A expression is positively correlated with progression of NSCLC and poor patient prognosis (Wang et al., 2016). We have identified a quiescence pathway in H1299 NSCLC cells that ZYG11A and ZYG11B are involved in. ZYG11A and ZYG11B are important to mediate the levels of MCM7, CSE1L/CAS, and CCT as cells enter quiescence. We also present evidence that ZYG11A and ZYGB interact directly with a subset of these proteins, suggesting direct regulation.

Introduction

Cancer is the second leading cause of death in the United States, and lung cancer is the number one cause of death from cancers in the United States (Ettinger et al., 2010; Siegel et al., 2016). Most forms of lung cancer reported are non-small cell lung cancer (NSCLC) (Ettinger et al., 2010). ZYG11A is overexpressed in tissue samples from NSCLC patients (Wang et al., 2016). Knocking down ZYG11A in NSCLC cells leads to a G0/G1 arrest, and inhibits the invasion, proliferation, and migration of NSCLC cells (Wang et al., 2016). When ZYG11A is knocked down, cyclin E1 expression and cyclin E1 protein levels decline (Wang et al., 2016). However, if ZYG11A is knocked down in NSCLC cells, followed by overexpression of cyclin E1, the migration and proliferation of the cells is no longer inhibited (Wang et al., 2016). This data suggests that ZYG11A contributes to the cell cycle progression of NSCLC (Wang et al., 2016).

In this chapter, we explore ZYG11A and ZYG11B's roles in a quiescence pathway in H1299 NSCLC cells. Cells enter quiescence when they exit the cell cycle due to nonoptimal conditions (Cheung and Rando, 2013). Nonoptimal conditions that would lead to quiescence are: DNA damage, confluent cell population, or serum starvation (Cheung and Rando, 2013; Heldt et al., 2018). We identified three proteins that are regulated by ZYG11A and ZYG11B in quiescent H1299 cells: MCM7; CCT3; and CSE1L/CAS.

Mini chromosome maintenance complex 7 (MCM7) is a component of the MCM2-7 complex (Snyder et al., 2009). MCM2-7 is a complex that is a helicase and unwinds the DNA in preparation for DNA replication (Snyder et al., 2009). MCM2-7 is loaded on DNA during G1 (Evrin et al., 2014). The origin of replication is bound by the origin recognition complex (ORC), and MCM2-7 is loaded on the ORC by the replication-licensing factors cdc6 and cdt1 (Evrin et al., 2014). Once loaded onto DNA, MCM2-7 dissociates from the ORC complex to unwind DNA to initiate DNA replication (Evrin et al., 2014). MCM2-7 is restricted from being loaded onto DNA during S phase to ensure that DNA replication origins cannot be used more than once. The restriction of the replication licensing system (which loads MCM2-7 onto origins) occurs via various mechanisms (Truong and Wu, 2011). For example, the protein geminin binds to cdt1 and inhibits cdt1 during S phase (Truong and Wu, 2011). Also during S phase, cdt1 is targeted for proteasomal degradation by SCF^{Skp2} and $CRL4^{Cdt2}$, and cdc6 is exported out of the nucleus (Truong and Wu, 2011). These mechanisms prevent MCM2-7 from being loaded on the ORC after S phase is initiated (Truong and Wu, 2011). During

quiescence, MCM2-7 is not present on genomic DNA, and a number of the components of the MCM2-7 complex also have low levels in the nucleus (Kingsbury et al., 2005).

CSE1L/CAS is a nuclear export receptor that is important for exporting importin α out of the nucleus (Kutay et al., 1997). Importin α binds to the nuclear localization signal on cargo proteins and interacts with importin β in order to import the cargo into the nucleus from the cytoplasm (Kutay et al., 1997). Once this complex is in the nucleus, Ran-GTP interacts with the complex, dissociating the complex and releasing the cargo into the nucleus (Kutay et al., 1997). In order for nuclear import to be efficient, importin α must be exported out the nucleus by CSE1L/CAS because importin α needs to be reused for subsequent rounds of nuclear import (Kutay et al., 1997). Inside the nucleus, importin α, CSE1L/CAS, and Ran-GTP form a complex that is exported out the nucleus (Kutay et al., 1997). This complex is then broken apart in the cytoplasm by RanGAP, in turn allowing Importin α to bind to another cargo protein (Kutay et al., 1997).

Chaperonin-containing TCP-1 subunit 3 (CCT3) is a subunit of the chaperonin-containing TCP-1 complex (CCT) (Xu et al., 2020). CCT is a chaperone that forms a barrel structure for folding proteins , and this chaperone floats freely in the cytosol (Vallin and Grantham, 2019). A number of proteins such as actin, α-tubulin, and β-tubulin are folded by CCT (Llorca et al., 2000; Vallin and Grantham, 2019).

In this chapter we show that ZYG11A and ZYG11B play important parts in regulating the levels of MCM7, CSE1L/CAS, and CCT as cells enter quiescence. We also explore ZYG11A and ZYGB's roles in either directly or indirectly targeting MCM7, CSE1L/CAS, and CCT as substrates.

Results

Mass spectrometry analysis shows that ZYG11A interacts with MCM7, CSE1L, and CCT3 in H1299 cells

Since ZYG11A overexpression is associated with progression of NSCLC, we wanted to identify potential ZYG11A substrates in NSCLC cells (Wang et al., 2016). We transfected H1299 cells, a NSCLC cell line, with FLAG-ZYG11A. We also had control cells that were not transfected. After harvesting the cells, we lysed the cells and performed FLAG immunoprecipitations of control lysate and the lysate containing FLAG-ZYG11A proteins. These samples were sent for mass spectrometry analysis at the University of Georgia Proteomics and Mass Spectrometry Facility. Once we received the results of potential ZYG11A interacting proteins, we identified which proteins were present in the ZYG11A sample that were not present in the negative control sample (Table 3.1). Proteins that were present only in the ZYG11A sample most likely were pulled down with ZYG11A instead of non-specifically interacting with the FLAG agarose beads used for the IPs. We identified a number of potential ZYG11A substrates from this mass spectrometry screen.

MCM7, CCT3, and CSE1L are stabilized in H1299 cells upon ZYG11 siRNA treatments

We tested potential substrates from the ZYG11A mass spectrometry screen, as well as other candidate proteins, for stabilization after ZYG11A, ZYG11B, or ZYG11A/B siRNA treatments. We tested proteins such as: dynein heavy chain; 14-3-3; AHNAK; DNA-dependent protein kinase catalytic subunit, PP2A; CCT3; MCM7; and CSE1L. Some

antibodies never detected protein bands, other antibodies detected the wrong sized bands, and some proteins just were not stabilized after ZYG11 siRNA treatments. Of all the proteins tested, MCM7, CSE1L, and CCT3 had stabilized protein levels upon ZYG11 siRNA treatments for some experiments, but other experiments did not show stabilization of these proteins (data not shown). We considered whether the inconsistencies in results reflected differences in cell confluencies. We knew that the components of the MCM2-7 complex decrease during the quiescence, and we knew that highly confluent cells tend to enter quiescence (Cheung and Rando, 2013; Heldt et al., 2018; Kingsbury et al., 2005). Therefore, we hypothesized that quiescence may play a role in determining whether MCM7, CSE1L, and CCT3 are stabilized after ZYG11 siRNA treatments (Kingsbury et al., 2005).

MCM7 is stabilized in the nucleus of serum starved H1299 cells upon ZYG11B and ZYG11A/B siRNA treatment

We tested our quiescence theory by knocking down ZYG11A, ZYG11B, or ZYG11A/B in serum starved H1299 cells. Cells were serum starved by incubation in tissue culture medium with 0% FBS. Serum starvation is known to drive cells into quiescence (Cheung and Rando, 2013; Heldt et al., 2018). One set of cells was grown in 10% FBS media while the other set of cells was grown in 0% FBS media. The serum starvation occurred for one day. MCM7 is stabilized in the nucleus of serum starved cells that were treated with ZYG11B siRNA or ZYG11A/B siRNA (Fig. 3.1). Serum starved cells treated with ZYG11B siRNA alone show greater MCM7 nuclear stabilization than in

serum starved cells treated with ZYG11A/B siRNA. MCM7 levels were quantified using immunofluorescence with anti-MCM7 antibodies.

MCM7, CCT3, and CSE1L are stabilized in quiescent H1299 cells upon ZYG11B or ZYG11A/B siRNA treatments

We wanted to determine to what degree knocking down ZYG11 stabilizes the potential ZYG11A and ZYG11B substrates. To study this, we treated cells with ZYG11A siRNA, ZYG11B siRNA , or ZYG11A/B siRNA. We serum starved H1299 cells for 0, 1, 2, and 3 days. We performed western blots of the samples and probed for various potential substrates. Protein levels of each potential substrate was quantified relative to actin. Our results show that ZYG11B and ZYG11A/B siRNA stabilize MCM7, CCT3, and CSE1L relative to control siRNA or ZYG11A siRNA treat cells (Fig. 3.2). ZYG11A/B siRNA stabilizes the proteins more than does ZYG11B siRNA. This suggests that ZYG11A plays a redundant role with ZYG11B in destabilizing these three proteins under normal conditions. We also show that $p27^{Kip1}$ is increased during quiescence entry in all cells. Since $p27^{Kip1}$ is a marker for quiescence (Andreu et al., 2015; Besson et al., 2006), the increase in $p27^{Kip1}$ after one day of starvation suggests that these cells are entering quiescence normally. Because $p27^{Kip1}$ increases even after ZYG11 siRNA treatments, this suggests that ZYG11A and ZYG11B are not needed for entry into quiescence.

ZYG11A physically interacts with MCM7 and CCT3 but does not interact with CSE1L

Since MCM7, CCT3, and CSE1L are stabilized during quiescence after ZYG11B and ZYG11A/B knockdowns, this suggests that these proteins may be ZYG11A and ZYG11B substrates. We tested this by doing IP western experiments to determine whether ZYG11A interacts with these potential substrates. H1299 cells were transfected with FLAG-ZYG11A. We also transfected cells without DNA to use as a negative control. Cells were either asynchronous or were arrested in quiescence for 24 hours. Additionally, cells were treated with MLN4924 or ALLnL. MLN4924 is an inhibitor of the NEDD8-activating enzyme (NAE) (Swords et al., 2015). Since NAE is needed for the neddylation and activation of cullins, MLN4924 inhibits all CRL E3 complexes (Lan et al., 2016). ALLnL is a proteasome inhibitor (Hughes et al., 1996). Both of these treatments would be expected to stabilize the interaction of substrates with E3 complexes, as the substrates could not be degraded. After both sets of cells were lysed, we pulled down FLAG-ZYG11A and probed for MCM7, CCT3, CSE1L, and PP2A. We found that ZYG11A physically interacts with MCM7 and CCT3; however, ZYG11A does not appear to physically interact with CSE1L or PP2A (Fig. 3.3). ZYG11A interacts with MCM7 in asynchronous cells as well as in quiescent cells. ZYG11A also interacts with CCT3 in asynchronous and quiescent cells that were treated with ALLnL. ZYG11A does not interact with CSE1L or PP2A. PP2A was tested since it was a ZYG11A-interacting protein in our initial mass spectrometry screen. This data suggests that MCM7 and CCT3 may be substrates of ZYG11A and bind directly to ZYG11A. Because ZYG11A does not interact with CSE1L, but ZYG11A/B knockdown

stabilizes CSE1L in quiescent cells, it is possible that the regulation of CSE1L levels is indirect.

ZYG11B physically interacts with MCM7 but lacks interaction with CSE1L

We repeated the previous IP western experiment except we transfected HEK 293T cells with HA-ZYG11B (rather than FLAG-ZYG11A) to determine whether ZYG11B interacts with the potential ZYG11B substrates. We used HEK 293T cells in this experiment because at the time our H1299 cells were not culturing properly. The results suggest that ZYG11B strongly interacts with MCM7 in asynchronous cells treated with MLN4924, but ZYG11B does not interact with MCM7 during quiescence (Fig. 3.4). However, when cells are treated with ALLnL, ZYG11B interacts with MCM7 in asynchronous cells and in quiescent cells, but the interaction is weaker than with MLN4924 treatment. ZYG11B does not stably interact with CSE1L or PP2A. We are not able to determine the degree of interaction of ZYG11B with CCT3 because the secondary antibody nonspecifically recognizes the BSA that was used to block the protein G Sepharose beads in the IP. We did not encounter this problem in the previous FLAG-ZYG11A IP experiment (Fig. 3.3) because the FLAG agarose beads did not need to be pre-blocked with BSA This data suggests that ZYG11B directly interacts with MCM7 in asynchronous cells and potentially in quiescent cells. The results also suggest that ZYG11B must indirectly regulate the level of CSE1L in quiescent cells since ZYG11B does not physically interact with CSE1L.

Discussion

We show that ZYG11A and ZYG11B regulate the levels of MCM7, CSE1L, and CCT3 in H1299 cells. MCM7, CSE1L, and CCT3 are stabilized during quiescence when ZYG11B or ZYG11A/B are knocked down. ZYG11A directly interacts with MCM7 and CCT3 in asynchronous and in quiescent H1299 cells. ZYG11A does not detectably interact with CSE1L in the co-IP assay. ZYG11B interacts strongly with MCM7 in MLN4924 treated asynchronous HEK 293T cells, but ZYG11B does not interact with MCM7 in quiescent cells under the same conditions. However, ZYG11B interacts weakly with MCM7 in ALLnL treated asynchronous and quiescent cells.

Our data suggests that MCM7 may be a ZYG11A and ZYG11B substrate that interacts with ZYG11A and ZYG11B during quiescence and in asynchronous cells. MCM7 interacts with ZYG11A and ZYG11B more in asynchronous cells than in quiescent cells despite ZYG11B and ZYG11A/B siRNA stabilizing MCM7 during quiescence. A possible explanation for this disparity is that other E3 ubiquitin ligases that target MCM7 for degradation may be active in asynchronous cells but may not be active in quiescent cells. Therefore, MCM7 would not be stabilized in asynchronous cells even though ZYG11B or ZYG11A/B are knocked down. This would allow MCM7 to be stabilized in quiescent cells treated with ZYG11B or ZYG11A/B siRNA even though ZYG11A and ZYG11B interact more strongly with MCM7 in asynchronous cells. This indicates that the interaction between ZYG11A or ZYG11B with MCM7 is not quiescence specific. Nevertheless, the interaction still occurs during quiescence. Our data also suggests that CCT3 may be a ZYG11A substrate during quiescence and in asynchronous cells. The fact that MCM7 and CCT3 are stabilized in quiescent cells

after ZYG11B and ZYG11A/B are knocked down suggests that ZYG11B and ZYG11A (to a lesser extent) directly target MCM7 and CCT3 for degradation via the proteasome during quiescence. Also, even though the substrate interaction data for ZYG11A and ZYG11B was collected in two different cells types, the results were very similar. It would be useful to repeat the ZYG11B substrate interaction experiment in H1299 cells and the ZYG11A interaction experiment in HEK 293T cells. Doing these experiments would give us more insight into how the interactions are conserved among different cell types.

CSE1L does not interact with ZYG11A or ZYG11B directly, but CSE1L levels are stabilized when ZYG11B or ZYG11A/B are knocked down during quiescence. This suggests that ZYG11A and ZYG11B indirectly regulate CSE1L during quiescence. One possibility is that ZYG11A and ZYG11B could facilitate the degradation of an inhibitor of the ubiquitin ligase that targets CSE1L for destruction. For example, when ZYG11B or ZYG11A/B are knocked down during quiescence, this could stabilize the inhibitor of the ubiquitin ligase that degrades CSE1L. This in turn would inhibit the degradation of CSE1L, stabilizing its levels during quiescence. Similar type mechanisms for regulating the inhibition of a ubiquitin ligase exist (Fuchs et al., 2004; Margottin-Goguet et al., 2003). For example, the ubiquitin ligase, $SCF^{\beta TrCP}$ targets Emi1 for degradation during early mitosis (Fuchs et al., 2004; Margottin-Goguet et al., 2003). Emi1 is an inhibitor of APC/C, therefore Emi1's degradation allows APC/C to be active and degrade APC/C's substrates (Fuchs et al., 2004; Margottin-Goguet et al., 2003). Another potential mechanism is that a transcriptional activator of CSE1 could be targeted for degradation by ZYG11A or ZYG11B. Therefore, when ZYG11A/B or ZYG11B is knocked down,

CSE1L levels could be stabilized due to a CSE1L transcriptional activator being stabilized and facilitating the expression of CSE1L.

This chapter shows that ZYG11A and ZYG11B play a role in regulating MCM7, CSE1L, and CCT3 levels as cells enter quiescence. This chapter sets the foundation for further studying how ZYG11A and ZYG11B regulate these proteins not only during quiescence but also during other phases of the cell cycle.

Materials and Methods

Expression Constructs

In order to generate the human FLAG-ZYG11A plasmid, ZYG11A was cloned into the pCMV-Tag2B expression vector (Stratagene). The HA-ZYG11B construct was generated by subcloning ZYG11B into an HA-tagged pEGFP-N1 ΔEGFP plasmid. This plasmid contains the same backbone as the pEGFP plasmid (Clontech) except the EGFP gene is cleaved out and replaced with ZYG11B.

Cell Culture and DNA transfections

H1299 cells were maintained in RPMI medium (Hyclone) containing 10% FBS (Sigma-Aldrich) and 100 μg/ml Penicillin/Streptomycin (HyClone). Plasmids were transfected into H1299 cells with Polyethylenimine (PEI). Cells were collected around 48 after transfection. HEK 293T cells were cultured in DMEM medium (HyClone) containing 10% FBS (Sigma-Aldrich) and 100 μg/ml Penicillin/Streptomycin (HyClone). Polyethylenimine (PEI) was used as the transfection reagent for HEK 293T cells when plasmids were transfected. Cells were collected around 48 hours post transfection.

siRNA knockdowns and serum starvation conditions

siRNA transfections were done using pools of four different siRNA sequences for ZYG11A and ZYG11B each. The ZYG11A and ZYG11B siRNA came from Thermo Fisher Scientific. Control siRNA was purchased from Invitrogen. RNAiMAX was used as the transfection reagent for all siRNA transfections. Cells were transfected with siRNA twice, with the second siRNA transfection occurring 24 hours after the first siRNA transfection. For the serum starvation experiments, cells were first treated with ZYG11A, ZYG11B, or ZYG11A/B siRNA twice. Cells were then split and serum starved for the various lengths of time indicated in a given experiment (e.g., 0, 1, 2, and 3 days of serum starvation). For serum starvation experiments of H1299 cells, the cells were serum starved in RPMI (Hyclone) with 0% FBS (Sigma-Aldrich) and 100 μg/ml Penicillin/Streptomycin (Hyclone). For serum starvation experiments of HEK 293T cells, the cells were serum starved in DMEM (Hyclone) with 0% FBS (Sigma-Aldrich) and 100 μg/ml Penicillin/Streptomycin (Hyclone).

Immunoprecipitations

The immunoprecipitation (IP) protocol performed in this chapter is the same as the IP protocol described in the Materials and Methods section of Chapter 2 of this dissertation. One difference is that for the FLAG IPs, we used FLAG agarose beads (Sigma). FLAG IPs were performed overnight at 4°C. Besides the FLAG agarose beads and the incubation time, the FLAG IP protocol uses the same reagents and lysis

conditions as the IPs in Chapter 2. The HA IPs also followed the same HA IP protocol described in Chapter 2.

Antibodies

We used the following mouse primary antibodies: anti-FLAG (Sigma-Aldrich), anti-HA (Thermo Fisher Scientific), anti-CSE1L (Santa Cruz), anti-PP2A (Santa Cruz), anti-AHNAK (Santa Cruz), anti-dynein heavy chain (Santa Cruz), anti-DNA-PK_{cs} (Santa Cruz), anti 14-3-3 (Developmental Studies Hybridoma), and anti-alpha tubulin (Proteintech). We used the following rabbit primary antibodies: anti-HA (Thermo Fisher Scientific), anti-MCM7 (Boster Biological Technology), and anti-CCT3 (Boster Biological Technology). Secondary antibodies used were: goat anti-mouse HRP (Proteintech) and goat anti-rabbit HRP (Proteintech).

Acknowledgements

I would like to thank the University of Georgia Department of Cellular Biology for providing me with a teaching assistantship. The research in this dissertation chapter was supported by grant R01 GM074212 from the National Institute of General Medical Sciences.

References

Andreu, Z., Khan, M.A., González-Gómez, P., Negueruela, S., Hortigüela, R., San Emeterio, J., Ferrón, S.R., Martínez, G., Vidal, A., Fariñas, I.*, et al.* (2015). The cyclin-dependent kinase inhibitor p27 kip1 regulates radial stem cell quiescence and neurogenesis in the adult hippocampus. Stem cells (Dayton, Ohio) *33*, 219-229.

Besson, A., Gurian-West, M., Chen, X., Kelly-Spratt, K.S., Kemp, C.J., and Roberts, J.M. (2006). A pathway in quiescent cells that controls p27Kip1 stability, subcellular localization, and tumor suppression. Genes & development *20*, 47-64.

Cheung, T.H., and Rando, T.A. (2013). Molecular regulation of stem cell quiescence. Nature reviews Molecular cell biology *14*, 329-340.

Ettinger, D.S., Akerley, W., Bepler, G., Blum, M.G., Chang, A., Cheney, R.T., Chirieac, L.R., D'Amico, T.A., Demmy, T.L., Ganti, A.K.*, et al.* (2010). Non-small cell lung cancer. Journal of the National Comprehensive Cancer Network : JNCCN *8*, 740-801.

Evrin, C., Fernández-Cid, A., Riera, A., Zech, J., Clarke, P., Herrera, M.C., Tognetti, S., Lurz, R., and Speck, C. (2014). The ORC/Cdc6/MCM2-7 complex facilitates MCM2-7 dimerization during prereplicative complex formation. Nucleic acids research *42*, 2257-2269.

Fuchs, S.Y., Spiegelman, V.S., and Kumar, K.G. (2004). The many faces of beta-TrCP E3 ubiquitin ligases: reflections in the magic mirror of cancer. Oncogene *23*, 2028-2036.

Heldt, F.S., Barr, A.R., Cooper, S., Bakal, C., and Novák, B. (2018). A comprehensive model for the proliferation–quiescence decision in response to endogenous DNA damage in human cells. Proceedings of the National Academy of Sciences *115*, 2532.

Hughes, E.A., Ortmann, B., Surman, M., and Cresswell, P. (1996). The protease inhibitor, N-acetyl-L-leucyl-L-leucyl-leucyl-L-norleucinal, decreases the pool of major histocompatibility complex class I-binding peptides and inhibits peptide trimming in the endoplasmic reticulum. The Journal of experimental medicine *183*, 1569-1578.

Kingsbury, S.R., Loddo, M., Fanshawe, T., Obermann, E.C., Prevost, A.T., Stoeber, K., and Williams, G.H. (2005). Repression of DNA replication licensing in quiescence is independent of geminin and may define the cell cycle state of progenitor cells. Experimental cell research *309*, 56-67.

Kutay, U., Bischoff, F.R., Kostka, S., Kraft, R., and Görlich, D. (1997). Export of importin alpha from the nucleus is mediated by a specific nuclear transport factor. Cell *90*, 1061-1071.

Lan, H., Tang, Z., Jin, H., and Sun, Y. (2016). Neddylation inhibitor MLN4924 suppresses growth and migration of human gastric cancer cells. Scientific reports *6*, 24218.

Llorca, O., Martín-Benito, J., Ritco-Vonsovici, M., Grantham, J., Hynes, G.M., Willison, K.R., Carrascosa, J.L., and Valpuesta, J.M. (2000). Eukaryotic chaperonin CCT stabilizes actin and tubulin folding intermediates in open quasi-native conformations. The EMBO journal *19*, 5971-5979.

Margottin-Goguet, F., Hsu, J.Y., Loktev, A., Hsieh, H.M., Reimann, J.D., and Jackson, P.K. (2003). Prophase destruction of Emi1 by the SCF(betaTrCP/Slimb) ubiquitin ligase activates the anaphase promoting complex to allow progression beyond prometaphase. Dev Cell *4*, 813-826.

Siegel, R.L., Miller, K.D., and Jemal, A. (2016). Cancer statistics, 2016. CA: a cancer journal for clinicians *66*, 7-30.

Snyder, M., Huang, X.-Y., and Zhang, J.J. (2009). The minichromosome maintenance proteins 2-7 (MCM2-7) are necessary for RNA polymerase II (Pol II)-mediated transcription. The Journal of biological chemistry *284*, 13466-13472.

Swords, R.T., Erba, H.P., DeAngelo, D.J., Bixby, D.L., Altman, J.K., Maris, M., Hua, Z., Blakemore, S.J., Faessel, H., Sedarati, F.*, et al.* (2015). Pevonedistat (MLN4924), a First-in-Class NEDD8-activating enzyme inhibitor, in patients with acute myeloid leukaemia and myelodysplastic syndromes: a phase 1 study. British journal of haematology *169*, 534-543.

Truong, L.N., and Wu, X. (2011). Prevention of DNA re-replication in eukaryotic cells. J Mol Cell Biol *3*, 13-22.

Vallin, J., and Grantham, J. (2019). The role of the molecular chaperone CCT in protein folding and mediation of cytoskeleton-associated processes: implications for cancer cell biology. Cell Stress and Chaperones *24*, 17-27.

Wang, X., Sun, Q., Chen, C., Yin, R., Huang, X., Wang, X., Shi, R., Xu, L., and Ren, B. (2016). ZYG11A serves as an oncogene in non-small cell lung cancer and influences CCNE1 expression. Oncotarget *7*, 8029-8042.

Xu, G., Bu, S., Wang, X., Zhang, H., and Ge, H. (2020). Suppression of CCT3 inhibits the proliferation and migration in breast cancer cells. Cancer Cell Int *20*, 218-218.

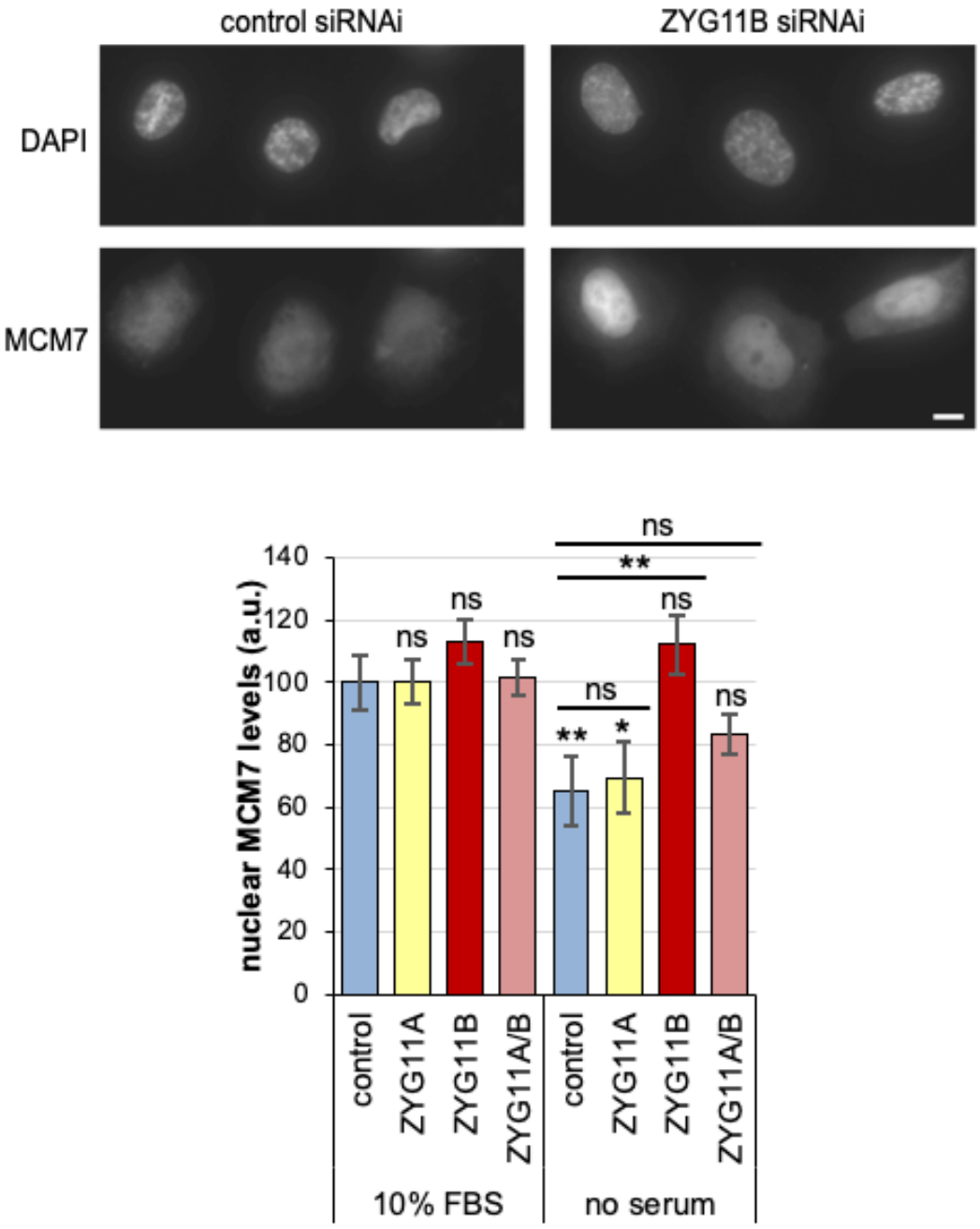

Figure 3.1. MCM7 is stabilized in the nucleus of serum starved H1299 cells upon ZYG11B and ZYG11A/B siRNA treatment. In the top panel is an immunofluorescence image of MCM7 or an image of DAPI stained DNA in control siRNA-treated cells versus ZYG11B siRNA-treated cells after one day of serum starvation. MCM7 levels are increased in the nucleus of the ZYG11B siRNA-treated cells. The scale bar is equal to

20 μm. The bottom panel is quantification of the MCM7 levels in the nucleus. ZYG11B siRNA stabilizes nuclear MCM7 levels more than does ZYG11A/B or ZYG11A siRNA (graph and images provided by Edward Kipreos).

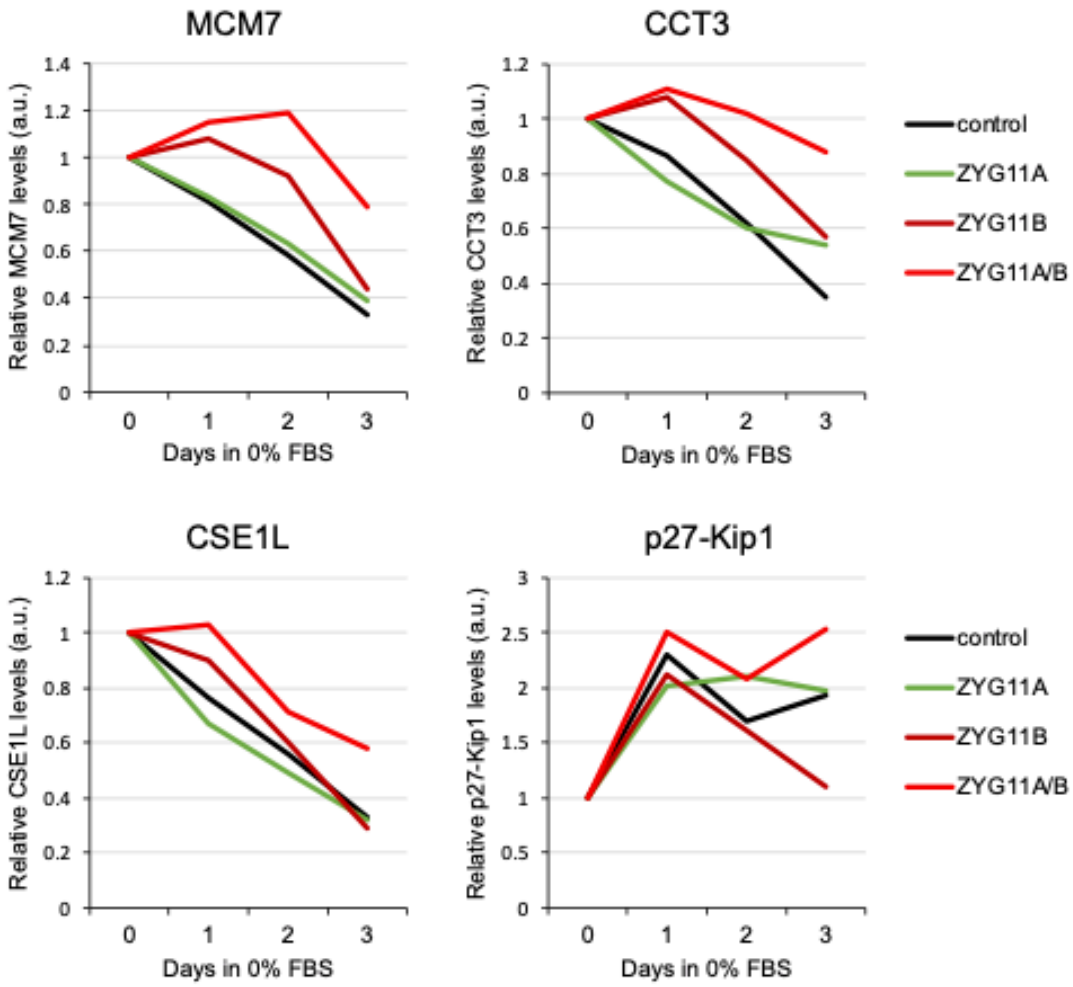

Figure 3.2. MCM7, CCT3, and CSE1L are stabilized in quiescent H1299 cells upon ZYG11B or ZYG11A/B siRNA treatments. H1299 cells were treated with siRNA for ZYG11A, ZYG11B, or ZYG11A/B. The siRNA-treated cells were serum starved for 0, 1, 2, and 3 days. ZYG11B and ZYG11A/B siRNA stabilize MCM7, CCT3, and CSE1L in quiescent cells. The initial increase of $p27^{Kip1}$ in all conditions suggests that the cells are entering quiescence (graphs provided by Edward Kipreos).

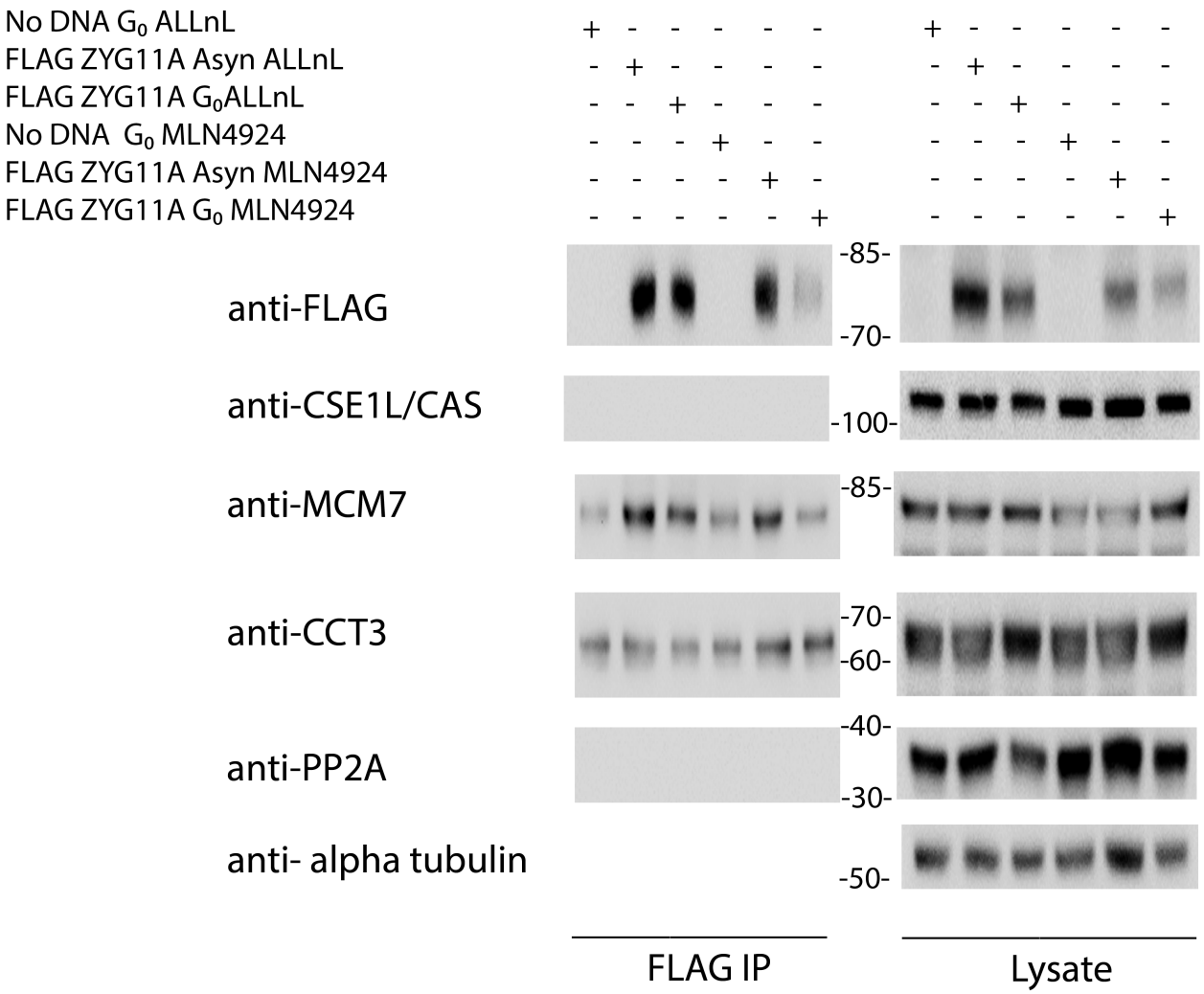

Figure 3.3. ZYG11A physically interacts with MCM7 and CCT3 but does not interact with CSE1L. H1299 cells were transfected with FLAG-ZYG11A or no DNA. Cells were either asynchronous or arrested in quiescence. Cells were also either treated with MLN4924 or ALLnL. IPs were performed on the lysates, and the potential ZYG11A substrates were probed for via western blot. ZYG11A interacts with MCM7 in asynchronous cells and in quiescent cells. ZYG11A interacts with CCT3 in asynchronous cells and quiescent cells upon ALLnL treatment. ZYG11A does not stably interact with CSE1L or PP2A

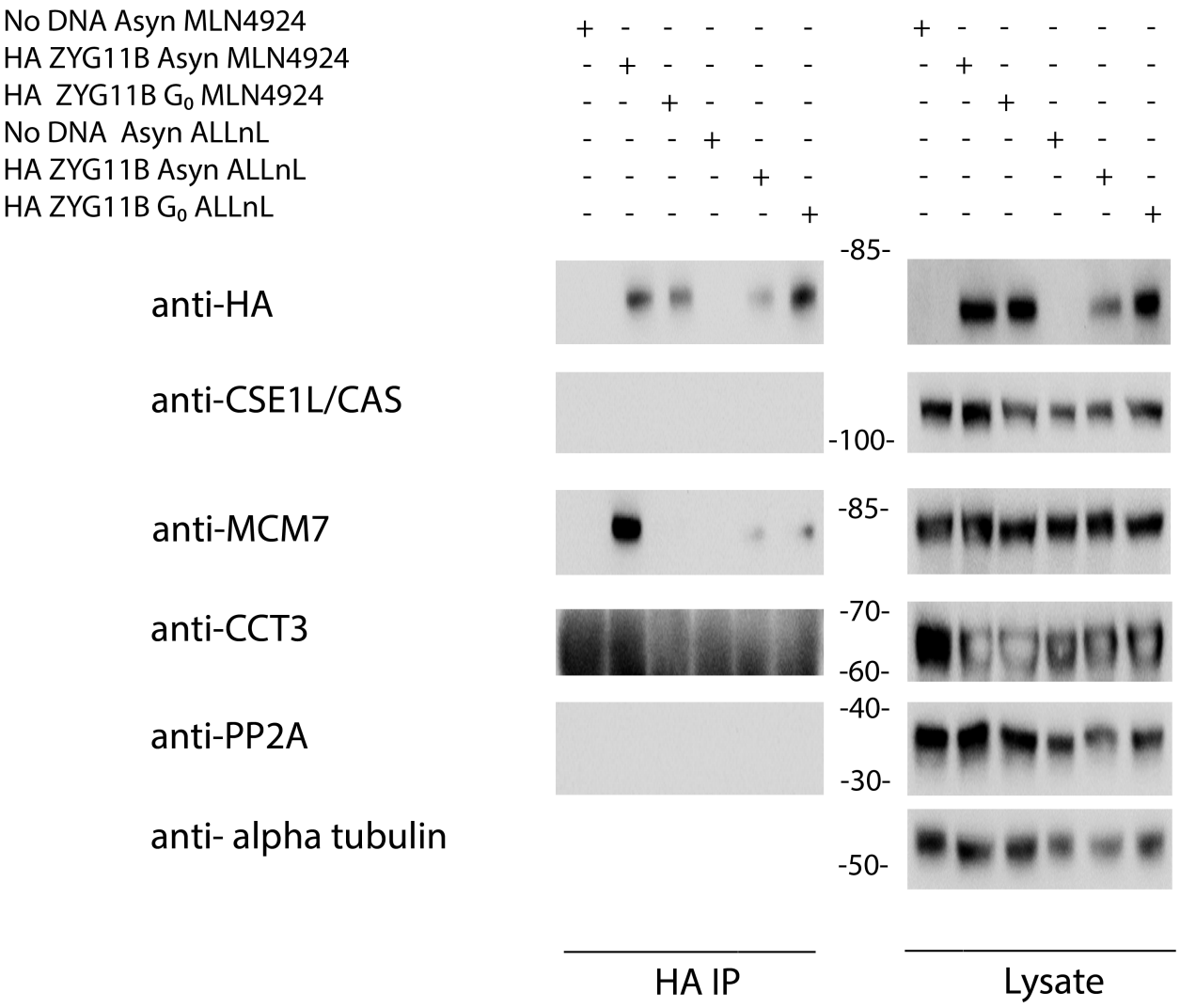

Figure 3.4. ZYG11B physically interacts with MCM7 but lacks interaction with CSE1L. HEK 293T cells were transfected with HA-ZYG11B or no DNA. These cells were either asynchronous or quiescent. Additionally, the cells were treated with MLN4924 or ALLnL. HA IPs were performed on the lysates, and we probed for the potential ZYG11B substrates. ZYG11B strongly interacts with MCM7 in asynchronous cells but does not interact with them in quiescent cells when treated with MLN4924. However, ZYG11B binds to MCM7 in asynchronous and quiescent cells after ALLnL

treatment, but this interaction is weak. ZYG11B does not appear to interact with CSE1L or PP2A in asynchronous or quiescent cells.

Table 3.1. Proteins that interact with ZYG11A in H1299 cells identified by co-IP coupled to tandem mass spectrometry

Protein Description	Score	Coverage	# Proteins	# Unique Peptides	# Peptides
Tubulin alpha-4A chain OS=Homo sapiens GN=TUBA4A PE=1 SV=1 - [TBA4A_HUMAN]	796.13	32.59	4	1	13
DNA replication licensing factor MCM7 OS=Homo sapiens GN=MCM7 PE=1 SV=4 - [MCM7_HUMAN]	510.39	34.91	1	23	23
Cytoplasmic dynein 1 heavy chain 1 OS=Homo sapiens GN=DYNC1H1 PE=1 SV=5 - [DYHC1_HUMAN]	481.25	7.34	1	30	30
Plectin OS=Homo sapiens GN=PLEC PE=1 SV=3 - [PLEC_HUMAN]	472.18	4.08	1	15	15
BAG family molecular chaperone regulator 2 OS=Homo sapiens GN=BAG2 PE=1 SV=1 - [BAG2_HUMAN]	428.98	49.76	1	16	16
ADP/ATP translocase 2 OS=Homo sapiens GN=SLC25A5 PE=1 SV=7 - [ADT2_HUMAN]	296.87	35.91	1	11	11
ATP synthase subunit beta, mitochondrial OS=Homo sapiens GN=ATP5B PE=1 SV=3 - [ATPB_HUMAN]	291.05	26.28	1	9	9
DNA-dependent protein kinase catalytic subunit OS=Homo sapiens GN=PRKDC PE=1 SV=3 - [PRKDC_HUMAN]	250.15	3.44	1	13	13
Peroxiredoxin-4 OS=Homo sapiens GN=PRDX4 PE=1 SV=1 - [PRDX4_HUMAN]	237.48	19.19	1	3	6
Sodium/potassium-transporting ATPase subunit alpha-1 OS=Homo sapiens GN=ATP1A1 PE=1 SV=1 - [AT1A1_HUMAN]	223.18	5.77	1	5	5
Calcium-binding mitochondrial carrier protein Aralar2 OS=Homo sapiens GN=SLC25A13 PE=1 SV=2 - [CMC2_HUMAN]	217.08	9.48	1	5	5
RuvB-like 2 OS=Homo sapiens GN=RUVBL2 PE=1 SV=3 - [RUVB2_HUMAN]	214.76	16.41	1	6	6
Transferrin receptor protein 1 OS=Homo sapiens GN=TFRC PE=1 SV=2 - [TFR1_HUMAN]	207.71	10.92	1	7	7
RuvB-like 1 OS=Homo sapiens GN=RUVBL1 PE=1 SV=1 - [RUVB1_HUMAN]	203.52	16.23	1	6	6
BAG family molecular chaperone regulator 5 OS=Homo sapiens GN=BAG5 PE=1 SV=1 - [BAG5_HUMAN]	194.39	22.60	1	8	8
Heterogeneous nuclear ribonucleoprotein M OS=Homo sapiens GN=HNRNPM PE=1 SV=3 - [HNRPM_HUMAN]	193.10	15.89	1	10	10
Translocon-associated protein subunit delta OS=Homo sapiens GN=SSR4 PE=1 SV=1 - [SSRD_HUMAN]	176.02	30.64	1	4	4

Keratin, type I cytoskeletal 15 OS=Homo sapiens GN=KRT15 PE=1 SV=3 - [K1C15_HUMAN]	175.72	10.09	6	1	5
Keratin, type II cytoskeletal 72 OS=Homo sapiens GN=KRT72 PE=1 SV=2 - [K2C72_HUMAN]	174.51	5.68	4	1	4
Emerin OS=Homo sapiens GN=EMD PE=1 SV=1 - [EMD_HUMAN]	164.09	24.41	1	5	5
Mitochondrial import inner membrane translocase subunit TIM50 OS=Homo sapiens GN=TIMM50 PE=1 SV=2 - [TIM50_HUMAN]	157.81	22.10	1	6	6
Large proline-rich protein BAG6 OS=Homo sapiens GN=BAG6 PE=1 SV=2 - [BAG6_HUMAN]	155.02	4.86	1	5	5
Sarcoplasmic/endoplasmic reticulum calcium ATPase 2 OS=Homo sapiens GN=ATP2A2 PE=1 SV=1 - [AT2A2_HUMAN]	151.42	8.25	1	7	7
E3 ubiquitin-protein ligase CHIP OS=Homo sapiens GN=STUB1 PE=1 SV=2 - [CHIP_HUMAN]	148.87	19.80	1	6	6
Plakophilin-1 OS=Homo sapiens GN=PKP1 PE=1 SV=2 - [PKP1_HUMAN]	145.53	5.09	1	3	3
Galectin-7 OS=Homo sapiens OX=9606 GN=LGALS7 PE=1 SV=2 - [LEG7_HUMAN]	139.43	34.56	1	4	4
Nucleolin OS=Homo sapiens GN=NCL PE=1 SV=3 - [NUCL_HUMAN]	135.85	7.04	1	4	4
Phenylalanine--tRNA ligase alpha subunit OS=Homo sapiens GN=FARSA PE=1 SV=3 - [SYFA_HUMAN]	130.07	6.69	1	3	3
Pyruvate dehydrogenase E1 component subunit beta, mitochondrial OS=Homo sapiens GN=PDHB PE=1 SV=3 - [ODPB_HUMAN]	129.81	4.46	1	1	1
Heterogeneous nuclear ribonucleoprotein F OS=Homo sapiens GN=HNRNPF PE=1 SV=3 - [HNRPF_HUMAN]	129.71	10.60	1	1	3
Phosphate carrier protein, mitochondrial OS=Homo sapiens GN=SLC25A3 PE=1 SV=2 - [MPCP_HUMAN]	126.72	21.82	1	9	9
Lamin-B1 OS=Homo sapiens GN=LMNB1 PE=1 SV=2 - [LMNB1_HUMAN]	118.25	9.39	1	5	6
Heat shock 70 kDa protein 4L OS=Homo sapiens GN=HSPA4L PE=1 SV=3 - [HS74L_HUMAN]	115.29	2.98	1	1	2
Nuclear pore complex protein Nup93 OS=Homo sapiens GN=NUP93 PE=1 SV=2 - [NUP93_HUMAN]	113.62	2.81	1	2	2
CTP synthase 1 OS=Homo sapiens GN=CTPS1 PE=1 SV=2 - [PYRG1_HUMAN]	102.56	6.09	1	4	4
60S acidic ribosomal protein P1 OS=Homo sapiens GN=RPLP1 PE=1 SV=1 - [RLA1_HUMAN]	87.03	28.95	1	2	2
Translocon-associated protein subunit gamma OS=Homo sapiens GN=SSR3 PE=1 SV=1 - [SSRG_HUMAN]	87.00	11.89	1	2	2
Polyubiquitin-C OS=Homo sapiens GN=UBC PE=1 SV=3 - [UBC_HUMAN]	86.61	72.26	4	5	5

ATP synthase subunit O, mitochondrial OS=Homo sapiens GN=ATP5O PE=1 SV=1 - [ATPO_HUMAN]	84.88	14.55	1	2	2
ATP-dependent RNA helicase DDX39A OS=Homo sapiens GN=DDX39A PE=1 SV=2 - [DX39A_HUMAN]	83.52	4.92	1	2	2
Puromycin-sensitive aminopeptidase OS=Homo sapiens GN=NPEPPS PE=1 SV=2 - [PSA_HUMAN]	83.02	4.03	1	3	3
Dolichyl-diphosphooligosaccharide--protein glycosyltransferase subunit 1 OS=Homo sapiens GN=RPN1 PE=1 SV=1 - [RPN1_HUMAN]	81.64	7.41	1	5	5
60S ribosomal protein L12 OS=Homo sapiens GN=RPL12 PE=1 SV=1 - [RL12_HUMAN]	81.61	29.09	1	4	4
Proteasome subunit alpha type-6 OS=Homo sapiens GN=PSMA6 PE=1 SV=1 - [PSA6_HUMAN]	80.41	5.28	1	1	1
Importin subunit beta-1 OS=Homo sapiens GN=KPNB1 PE=1 SV=2 - [IMB1_HUMAN]	78.22	1.71	1	1	1
Eukaryotic initiation factor 4A-I OS=Homo sapiens GN=EIF4A1 PE=1 SV=1 - [IF4A1_HUMAN]	78.15	3.45	2	1	1
Mitochondrial import inner membrane translocase subunit Tim23 OS=Homo sapiens OX=9606 GN=TIMM23 PE=1 SV=1 - [TIM23_HUMAN]	76.75	12.92	2	2	2
Serine/threonine-protein phosphatase 2A catalytic subunit beta isoform OS=Homo sapiens GN=PPP2CB PE=1 SV=1 - [PP2AB_HUMAN]	76.36	15.53	2	3	3
40S ribosomal protein S10 OS=Homo sapiens GN=RPS10 PE=1 SV=1 - [RS10_HUMAN]	75.79	8.48	2	1	1
Keratin, type I cuticular Ha3-I OS=Homo sapiens GN=KRT33A PE=2 SV=2 - [KT33A_HUMAN]	70.27	2.97	6	1	1
Transmembrane protein 33 OS=Homo sapiens GN=TMEM33 PE=1 SV=2 - [TMM33_HUMAN]	70.09	4.86	1	1	1
ATP synthase subunit gamma, mitochondrial OS=Homo sapiens GN=ATP5C1 PE=1 SV=1 - [ATPG_HUMAN]	68.96	4.03	1	1	1
Small nuclear ribonucleoprotein F OS=Homo sapiens GN=SNRPF PE=1 SV=1 - [RUXF_HUMAN]	68.25	15.12	1	1	1
T-complex protein 1 subunit gamma OS=Homo sapiens GN=CCT3 PE=1 SV=4 - [TCPG_HUMAN]	67.77	2.02	1	1	1
Transmembrane emp24 domain-containing protein 10 OS=Homo sapiens GN=TMED10 PE=1 SV=2 - [TMEDA_HUMAN]	63.60	5.02	1	1	1
Apoptosis-inducing factor 1, mitochondrial OS=Homo sapiens GN=AIFM1 PE=1 SV=1 - [AIFM1_HUMAN]	62.67	3.75	1	2	2
NADH dehydrogenase [ubiquinone] iron-sulfur protein 7, mitochondrial OS=Homo sapiens OX=9606 GN=NDUFS7 PE=1 SV=3 - [NDUS7_HUMAN]	62.03	6.57	1	1	1

Intercellular adhesion molecule 1 OS=Homo sapiens OX=9606 GN=ICAM1 PE=1 SV=2 - [ICAM1_HUMAN]	61.50	2.63	1	1	1
Peroxiredoxin-2 OS=Homo sapiens GN=PRDX2 PE=1 SV=5 - [PRDX2_HUMAN]	60.93	14.14	1	1	2
Eukaryotic translation initiation factor 3 subunit I OS=Homo sapiens GN=EIF3I PE=1 SV=1 - [EIF3I_HUMAN]	60.05	3.69	1	1	1
E3 ubiquitin-protein ligase HUWE1 OS=Homo sapiens GN=HUWE1 PE=1 SV=3 - [HUWE1_HUMAN]	59.51	1.69	1	5	5
Cathepsin B OS=Homo sapiens GN=CTSB PE=1 SV=3 - [CATB_HUMAN]	52.52	2.36	1	1	1
Serine/threonine-protein phosphatase PGAM5, mitochondrial OS=Homo sapiens GN=PGAM5 PE=1 SV=2 - [PGAM5_HUMAN]	51.60	3.46	1	1	1
60S ribosomal protein L31 OS=Homo sapiens GN=RPL31 PE=1 SV=1 - [RL31_HUMAN]	51.27	7.20	1	1	1
Succinyl-CoA ligase [ADP-forming] subunit beta, mitochondrial OS=Homo sapiens GN=SUCLA2 PE=1 SV=3 - [SUCB1_HUMAN]	50.43	2.16	1	1	1
Coatomer subunit gamma-2 OS=Homo sapiens GN=COPG2 PE=1 SV=1 - [COPG2_HUMAN]	50.40	1.38	2	1	1
Secretory carrier-associated membrane protein 3 OS=Homo sapiens GN=SCAMP3 PE=1 SV=3 - [SCAM3_HUMAN]	49.90	5.19	1	1	1
Dynein light chain roadblock-type 2 OS=Homo sapiens OX=9606 GN=DYNLRB2 PE=1 SV=1 - [DLRB2_HUMAN]	49.25	12.50	2	1	1
Phospholipase D3 OS=Homo sapiens OX=9606 GN=PLD3 PE=1 SV=1 - [PLD3_HUMAN]	49.16	2.04	1	1	1
ATP synthase subunit f, mitochondrial OS=Homo sapiens GN=ATP5J2 PE=1 SV=3 - [ATPK_HUMAN]	48.87	13.83	1	1	1
Katanin p60 ATPase-containing subunit A-like 2 OS=Homo sapiens GN=KATNAL2 PE=2 SV=3 - [KATL2_HUMAN]	48.74	2.23	2	1	1
Dolichyl-diphosphooligosaccharide--protein glycosyltransferase subunit DAD1 OS=Homo sapiens OX=9606 GN=DAD1 PE=1 SV=3 - [DAD1_HUMAN]	47.68	10.62	1	1	1
MICOS complex subunit MIC19 OS=Homo sapiens GN=CHCHD3 PE=1 SV=1 - [MIC19_HUMAN]	47.36	7.49	1	2	2
Translocon-associated protein subunit alpha OS=Homo sapiens GN=SSR1 PE=1 SV=3 - [SSRA_HUMAN]	47.27	2.80	1	1	1
Lamin-B2 OS=Homo sapiens GN=LMNB2 PE=1 SV=4 - [LMNB2_HUMAN]	47.06	3.55	1	1	2
Insulin-like growth factor 2 mRNA-binding protein 2 OS=Homo sapiens GN=IGF2BP2 PE=1 SV=2 - [IF2B2_HUMAN]	46.69	4.17	1	1	2

Fructose-bisphosphate aldolase A OS=Homo sapiens GN=ALDOA PE=1 SV=2 - [ALDOA_HUMAN]	46.06	3.85	1	1	1
40S ribosomal protein S15a OS=Homo sapiens GN=RPS15A PE=1 SV=2 - [RS15A_HUMAN]	45.40	6.15	1	1	1
Voltage-dependent anion-selective channel protein 2 OS=Homo sapiens GN=VDAC2 PE=1 SV=2 - [VDAC2_HUMAN]	45.36	2.72	1	1	1
UDP-glucose 6-dehydrogenase OS=Homo sapiens GN=UGDH PE=1 SV=1 - [UGDH_HUMAN]	45.21	2.63	1	1	1
PDZ and LIM domain protein 7 OS=Homo sapiens OX=9606 GN=PDLIM7 PE=1 SV=1 - [PDLI7_HUMAN]	44.41	2.41	1	1	1
Destrin OS=Homo sapiens GN=DSTN PE=1 SV=3 - [DEST_HUMAN]	43.95	6.67	1	1	1
Nucleosome assembly protein 1-like 4 OS=Homo sapiens GN=NAP1L4 PE=1 SV=1 - [NP1L4_HUMAN]	43.37	2.67	2	1	1
60S ribosomal protein L23 OS=Homo sapiens GN=RPL23 PE=1 SV=1 - [RL23_HUMAN]	43.31	10.71	1	1	1
Coatomer subunit beta OS=Homo sapiens GN=COPB1 PE=1 SV=3 - [COPB_HUMAN]	42.70	1.15	1	1	1
Endoplasmin OS=Homo sapiens GN=HSP90B1 PE=1 SV=1 - [ENPL_HUMAN]	42.44	1.74	1	1	1
Methionine--tRNA ligase, cytoplasmic OS=Homo sapiens GN=MARS PE=1 SV=2 - [SYMC_HUMAN]	41.83	1.11	1	1	1
DnaJ homolog subfamily B member 4 OS=Homo sapiens GN=DNAJB4 PE=1 SV=1 - [DNJB4_HUMAN]	41.77	2.97	1	1	1
Insulin-like growth factor 2 mRNA-binding protein 1 OS=Homo sapiens GN=IGF2BP1 PE=1 SV=2 - [IF2B1_HUMAN]	41.58	5.55	1	2	3
Proteasome subunit alpha type-5 OS=Homo sapiens GN=PSMA5 PE=1 SV=3 - [PSA5_HUMAN]	41.37	4.15	1	1	1
Cytochrome b-c1 complex subunit Rieske, mitochondrial OS=Homo sapiens GN=UQCRFS1 PE=1 SV=2 - [UCRI_HUMAN]	41.34	3.28	2	1	1
ATP-binding cassette sub-family F member 2 OS=Homo sapiens GN=ABCF2 PE=1 SV=2 - [ABCF2_HUMAN]	40.86	1.77	1	1	1
Elongation of very long chain fatty acids protein 1 OS=Homo sapiens OX=9606 GN=ELOVL1 PE=1 SV=1 - [ELOV1_HUMAN]	38.97	4.30	1	1	1
60S ribosomal protein L27 OS=Homo sapiens GN=RPL27 PE=1 SV=2 - [RL27_HUMAN]	38.73	6.62	1	1	1
Pachytene checkpoint protein 2 homolog OS=Homo sapiens GN=TRIP13 PE=1 SV=2 - [PCH2_HUMAN]	38.06	2.31	1	1	1

Proteasome subunit beta type-4 OS=Homo sapiens GN=PSMB4 PE=1 SV=4 - [PSB4_HUMAN]	36.76	3.79	1	1	1
Cytoplasmic dynein 1 light intermediate chain 1 OS=Homo sapiens GN=DYNC1LI1 PE=1 SV=3 - [DC1L1_HUMAN]	35.36	3.25	1	1	1
NADH dehydrogenase [ubiquinone] iron-sulfur protein 3, mitochondrial OS=Homo sapiens GN=NDUFS3 PE=1 SV=1 - [NDUS3_HUMAN]	34.32	4.92	1	1	1
Protein transport protein Sec16A OS=Homo sapiens GN=SEC16A PE=1 SV=3 - [SC16A_HUMAN]	34.18	0.50	1	1	1
Proteasome subunit beta type-3 OS=Homo sapiens GN=PSMB3 PE=1 SV=2 - [PSB3_HUMAN]	33.67	7.80	1	1	1
DNA-directed RNA polymerase II subunit RPB1 OS=Homo sapiens GN=POLR2A PE=1 SV=2 - [RPB1_HUMAN]	32.78	0.46	1	1	1
Ancient ubiquitous protein 1 OS=Homo sapiens GN=AUP1 PE=1 SV=1 - [AUP1_HUMAN]	32.48	2.52	1	1	1
Tetratricopeptide repeat protein 37 OS=Homo sapiens GN=TTC37 PE=1 SV=1 - [TTC37_HUMAN]	32.20	0.51	1	1	1
Gamma-glutamyl hydrolase OS=Homo sapiens GN=GGH PE=1 SV=2 - [GGH_HUMAN]	31.32	2.52	1	1	1
Synaptophysin-like protein 1 OS=Homo sapiens GN=SYPL1 PE=1 SV=1 - [SYPL1_HUMAN]	31.05	4.25	1	1	1
Lysosomal protective protein OS=Homo sapiens OX=9606 GN=CTSA PE=1 SV=2 - [PPGB_HUMAN]	30.95	1.46	1	1	1
Cytochrome c1, heme protein, mitochondrial OS=Homo sapiens GN=CYC1 PE=1 SV=3 - [CY1_HUMAN]	30.53	4.92	1	1	1
Ras-related protein Rab-10 OS=Homo sapiens GN=RAB10 PE=1 SV=1 - [RAB10_HUMAN]	30.24	5.50	24	1	1
Peptidyl-prolyl cis-trans isomerase FKBP8 OS=Homo sapiens GN=FKBP8 PE=1 SV=2 - [FKBP8_HUMAN]	29.86	1.70	1	1	1
L-lactate dehydrogenase B chain OS=Homo sapiens GN=LDHB PE=1 SV=2 - [LDHB_HUMAN]	29.36	3.29	1	1	1
Peroxiredoxin-5, mitochondrial OS=Homo sapiens GN=PRDX5 PE=1 SV=4 - [PRDX5_HUMAN]	28.99	5.14	1	1	1
Dual specificity mitogen-activated protein kinase kinase 2 OS=Homo sapiens OX=9606 GN=MAP2K2 PE=1 SV=1 - [MP2K2_HUMAN]	28.66	2.25	1	1	1
GTP-binding nuclear protein Ran OS=Homo sapiens GN=RAN PE=1 SV=3 - [RAN_HUMAN]	28.63	5.09	1	1	1
14-3-3 protein sigma OS=Homo sapiens GN=SFN PE=1 SV=1 - [1433S_HUMAN]	28.58	5.65	1	1	1
Protein phosphatase 1F OS=Homo sapiens OX=9606 GN=PPM1F PE=1 SV=3 - [PPM1F_HUMAN]	28.43	4.41	1	1	1
DNA-directed RNA polymerase II subunit RPB2 OS=Homo sapiens	28.26	0.60	1	1	1

GN=POLR2B PE=1 SV=1 - [RPB2_HUMAN]					
Tyrosine-protein kinase receptor UFO OS=Homo sapiens OX=9606 GN=AXL PE=1 SV=4 - [UFO_HUMAN]	27.97	1.34	1	1	1
CD44 antigen OS=Homo sapiens GN=CD44 PE=1 SV=3 - [CD44_HUMAN]	27.41	1.08	1	1	1
Cytochrome c oxidase subunit NDUFA4 OS=Homo sapiens GN=NDUFA4 PE=1 SV=1 - [NDUA4_HUMAN]	27.17	9.88	1	1	1
YTH domain-containing family protein 2 OS=Homo sapiens GN=YTHDF2 PE=1 SV=2 - [YTHD2_HUMAN]	27.06	2.07	1	1	1
ATP-dependent RNA helicase DDX55 OS=Homo sapiens OX=9606 GN=DDX55 PE=1 SV=3 - [DDX55_HUMAN]	26.09	1.33	1	1	1
T-box brain protein 1 OS=Homo sapiens GN=TBR1 PE=1 SV=1 - [TBR1_HUMAN]	26.01	1.76	1	1	1
Paxillin OS=Homo sapiens GN=PXN PE=1 SV=3 - [PAXI_HUMAN]	25.55	3.05	1	1	1
Proteasomal ubiquitin receptor ADRM1 OS=Homo sapiens GN=ADRM1 PE=1 SV=2 - [ADRM1_HUMAN]	25.40	3.93	1	1	1
NADH dehydrogenase [ubiquinone] 1 alpha subcomplex subunit 11 OS=Homo sapiens OX=9606 GN=NDUFA11 PE=1 SV=3 - [NDUAB_HUMAN]	25.17	10.64	1	1	1
NADH dehydrogenase [ubiquinone] 1 alpha subcomplex subunit 13 OS=Homo sapiens OX=9606 GN=NDUFA13 PE=1 SV=3 - [NDUAD_HUMAN]	25.02	6.94	1	1	1
SUMO-activating enzyme subunit 1 OS=Homo sapiens GN=SAE1 PE=1 SV=1 - [SAE1_HUMAN]	24.71	2.60	1	1	1
Cytochrome c oxidase subunit 2 OS=Homo sapiens GN=MT-CO2 PE=1 SV=1 - [COX2_HUMAN]	24.67	3.08	1	1	1
Arginine and glutamate-rich protein 1 OS=Homo sapiens GN=ARGLU1 PE=1 SV=1 - [ARGL1_HUMAN]	24.63	2.93	1	1	1
Sn1-specific diacylglycerol lipase alpha OS=Homo sapiens GN=DAGLA PE=1 SV=3 - [DGLA_HUMAN]	24.56	0.67	1	1	1
Keratin, type I cuticular Ha6 OS=Homo sapiens GN=KRT36 PE=1 SV=1 - [KRT36_HUMAN]	24.31	1.71	1	1	1
L-lactate dehydrogenase A chain OS=Homo sapiens GN=LDHA PE=1 SV=2 - [LDHA_HUMAN]	23.76	2.41	1	1	1
Dynein heavy chain 3, axonemal OS=Homo sapiens GN=DNAH3 PE=2 SV=1 - [DYH3_HUMAN]	23.49	0.24	1	1	1
D-3-phosphoglycerate dehydrogenase OS=Homo sapiens GN=PHGDH PE=1 SV=4 - [SERA_HUMAN]	23.45	1.50	1	1	1
4F2 cell-surface antigen heavy chain OS=Homo sapiens GN=SLC3A2 PE=1 SV=3 - [4F2_HUMAN]	23.31	1.90	1	1	1
Succinyl-CoA ligase [ADP/GDP-forming] subunit alpha, mitochondrial OS=Homo sapiens GN=SUCLG1 PE=1 SV=4 - [SUCA_HUMAN]	23.14	2.60	1	1	1

Keratinocyte proline-rich protein OS=Homo sapiens GN=KPRP PE=1 SV=1 - [KPRP_HUMAN]	23.09	1.38	1	1	1
1-acyl-sn-glycerol-3-phosphate acyltransferase alpha OS=Homo sapiens GN=AGPAT1 PE=1 SV=2 - [PLCA_HUMAN]	22.84	3.53	1	1	1
Neuroblast differentiation-associated protein AHNAK OS=Homo sapiens GN=AHNAK PE=1 SV=2 - [AHNK_HUMAN]	22.55	0.46	1	1	1
40S ribosomal protein S20 OS=Homo sapiens GN=RPS20 PE=1 SV=1 - [RS20_HUMAN]	22.47	10.08	1	1	1
Fumarate hydratase, mitochondrial OS=Homo sapiens GN=FH PE=1 SV=3 - [FUMH_HUMAN]	21.98	1.37	1	1	1
Exportin-2 OS=Homo sapiens GN=CSE1L PE=1 SV=3 - [XPO2_HUMAN]	21.80	0.82	1	1	1
Putative small nuclear ribonucleoprotein G-like protein 15 OS=Homo sapiens GN=SNRPGP15 PE=5 SV=2 - [RUXGL_HUMAN]	21.27	9.21	2	1	1
Centriolin OS=Homo sapiens GN=CNTRL PE=1 SV=2 - [CNTRL_HUMAN]	21.25	0.30	1	1	1
60S ribosomal protein L38 OS=Homo sapiens GN=RPL38 PE=1 SV=2 - [RL38_HUMAN]	21.23	18.57	1	1	1
PDZ and LIM domain protein 5 OS=Homo sapiens GN=PDLIM5 PE=1 SV=5 - [PDLI5_HUMAN]	21.04	1.17	1	1	1
5-oxoprolinase OS=Homo sapiens GN=OPLAH PE=1 SV=3 - [OPLA_HUMAN]	18.57	0.54	1	1	1

Table 3.1. Proteins that interact with ZYG11A in H1299 cells identified by co-IP coupled to tandem mass spectrometry. H1299 cells were transfected with FLAG-ZYG11A or no DNA (negative control). Once cells were lysed, IPs were performed on both samples, and the IP samples were sent for mass spectrometry analysis to identify proteins that were specific for the ZYG11A IP. Above is the mass spectrometry data of proteins specific for interacting with FLAG-ZYG11A. MCM7, CSE1L, and CCT3 are highlighted in yellow.

CHAPTER 4

DISCUSSION AND CONCLUSION

Elucidating the protein interactions controlling mitotic slippage

$CRL2^{ZYG11A/B}$ contributes to mitotic slippage by targeting cyclin B1 for degradation by the proteasome when APC/C is inactive (Balachandran et al., 2016). Chapter 2 explores which protein regions are involved in the interaction between ZYG11B and cyclin B1, and we also carry out experiments to assess how the interaction is regulated.

We showed that ZYG11B interacts with CBOX1 and CBOX2 domains of cyclin B1. The interaction between ZYG11B and CBOX1 is significantly stronger than the interaction between ZYG11B and CBOX2. When ZYG11B interacts with cyclin B1 via CBOX1, it's possible that CDK1 cannot be bound to cyclin B1 at the same time. Our CBOX1nl PEI WT-WT, CBOX1nl PEI WT-O, and CBOX1nl 10-CDK mutants show reduced interaction with ZYG11B, and they contain a number of amino acids that are inaccessible when CDK1 is bound to cyclin B1 (Fig. 2.21). If we confirm that these residues are actually part of the cyclin B1 degron, this would suggest that ZYG11B would interact with cyclin B1 via CBOX2 whenever CDK1 is bound to cyclin B1 because CDK1 would be blocking access to CBOX1. Despite this, CBOX1nl 6-O and CBOX1nl PEI WT-O contain a number of residues that are not at the cyclin B1/ CDK1 interface

and are accessible. These two mutants also showed reduced interaction with ZYG11B. CBOX1nl PEI WT-O is unique in that it has mutant residues that are accessible and are not accessible to ZYG11B when CDK1 is bound to cyclin B1. If we determine that the accessible mutant residues on these two proteins are part of the cyclin B1 degron, then that would suggest that ZYG11B can interact with CBOX1 when CDK1 is bound. Another possibility is that the cyclin B1 degron consists of residues that are accessible and inaccessible when CDK1 is bound. In this case, ZYG11B would need to interact with CBOX2 when CDK1 is bound to cyclin B1. We have shown that ZYG11B can physically interact with cyclin B1 that is not bound to CDK, and ZYG11B can interact with cyclin B1 that is bound to CDK (Balachandran et al., 2016). When cyclin B1 is degraded by ZYG11B during mitotic slippage, ZYG11B potentially recognizes both CDK1 bound and CDK1 unbound cyclin B1. Even though the interaction between cyclin B1 and CDK1 can be strong, the strength of this interaction can vary depending on intrinsic thermal stability and environmental salt concentrations (Brown et al., 2015). Nevertheless, most of the cyclin B1 recognized by ZYG11B in the cell probably is in the CDK1 bound form since there is a significant excess of CDK in the cell in comparison to cyclin B1 (Arooz et al., 2000). there are a number of cases in which the. We previously showed that ZYG11B plays a significant role in degrading cyclin B1 when cyclin B1 is over expressed (Balachandran et al., 2016). If cyclin B1 is overexpressed, that could potentially increase the chances of more free cyclin B1 being present that is not bound to CDK1.

Cyclin B1 interacts with the vLRR repeats of ZYG11B. Specifically, vLRR repeats 4, 5, and 6 seem to be most important in the interaction. In the future, it would

be useful to mutate various residues within these vLRR regions to determine which residues are involved in the interaction. However, generating a crystal structure or NMR structure of ZYG11B alone, and ZYG11B bound to cyclin B1 would be the best method to understand what amino acids residues are involved in the interaction between ZYG11B and cyclin B1. We previously attempted to generate full length ZYG11B purified proteins using the Baculovirus expression system, however we were not able to generate enough protein needed to crystalize the proteins. We also generated purified vLRR truncations of ZYG11B in bacteria, however we had issues with protein solubility. We were going to use the vLRR truncation to make an NMR structure of vLRR alone and of vLRR bound to a cyclin B1 truncation (this truncation contained CBOX1 and CBOX2). We should re-explore purifying soluble ZYG11B proteins in the future. Resolving the structure of ZYG11B bound to cyclin B1 not only would allow us to determine the residues involved in the interaction, but the structures would also allow us to determine how ZYG11B interacts with cyclin B1 when CDK1 is bound. Lastly, generating a structure of ZYG11B bound to cyclin B1 could be used as a platform to identify anti-cancer drugs that may disrupt the interaction (Arkin et al., 2014; Sliwoski et al., 2014). ZYG11A/B allows cells to be resistant to anti-microtubule drugs, such as nocodazole, by enabling the cells to slip out of mitosis despite the spindle assembly checkpoint being active (Balachandran et al., 2016). Drugs that disrupt the interaction between ZYG11B and cyclin B1could be administered in combination with anti-microtubule drugs in order to increase the effectiveness of cancer treatment.

We determined that ZYG11B interacts with cyclin B1 during S phase and M phase, but ZYG11B interacts slightly more with cyclin B1 during S phase. We expected

that ZYG11B would interact with cyclin B1 during M phase because ZYG11B contributes to mitotic slippage by degrading cyclin B1 when APC/C is inactive (Balachandran et al., 2016). However, we did not expect that ZYG11B would interact moderately more with cyclin B1 during S phase than in M phase. ZYG11B may help regulate cyclin B1 levels during S phase as an additional check to prevent premature entry into mitosis. A number of other redundant mechanism exists to prevent premature mitotic entry such as: inhibitory phosphorylations on CDK1, activating phosphorylations on CDK1, transcriptional regulation of cyclin B1,cyclin B1 localization, and cyclin B1 degradation (Li et al., 2015; Soni et al., 2008; Toyoshima et al., 1998; Trunnell et al., 2011). To further investigate the role of ZYG11B in regulating cyclin B1 during S phase, we would use mass spectrometry to look for PTMs on ZYG11B and cyclin B1 when they are bound during S phase. If PTMs are identified, then the modifying enzymes can be analyzed to obtain insights into the regulation. Our previous mass spectrometry data did not find PTMs on ZYG11B or cyclin B1 when they interact in M phase. However, we did not have complete peptide coverage in the mass spectrometry analysis. The use of different proteases to generate peptides would be necessary to obtain further peptide coverage due to the placement of lysine and arginine residues that leads trypsin to generate many peptides that are either too small or too large for mass spectrometry analysis. By increasing the amount of protein and the peptide coverage, we should be able to identify PTMs if they exist. If PTMs are still not identified under these circumstances, then that would suggest that PTMs do not regulate the interaction between ZYG11B and cyclin B1 in mitosis. It's also possible that PTMs could inhibit the interaction between ZYG11B and cyclin B1. In order to identify these negative PTMs,

we would need to have increased total peptides and peptide coverage to confidently conclude that specific PTMs are excluded from the interaction.

ZYG11B has a redundant role with APC/C, and we believe that ZYG11B's main job in the cell is to degrade cyclin B1 under abnormal circumstances such as APC/C being inhibited or cyclin B1 being overexpressed. Cyclin B1 plays a significant role in the cell cycle, and if there is a breakdown in its regulation, this could lead to cancer. (Song et al., 2008). The cell has a number of redundant mechanisms to ensure that processes are tightly controlled (Yasunaga et al., 2016; Yasunaga et al., 2013). For example, APC/C and Scmh1 both have ubiquitin ligase activity for geminin (Yasunaga et al., 2016; Yasunaga et al., 2013). ZYG11B provides redundancy to ensure that cyclin B1 levels are regulated regardless of the circumstances in the cell.

Identifying a Novel Quiescence Pathway

Non-small cell lung cancer (NSCLC) is the most common form of lung cancer in the United States (Ettinger et al., 2010; Siegel et al., 2016). Lung cancer is the number one cause of death from cancer in the U.S. (Ettinger et al., 2010; Siegel et al., 2016). ZYG11A is overexpressed in NSCLC patient tissues, and the overexpression of ZYG11A supports the migration, proliferation and invasion of NSCLC cells (Wang et al., 2016).

In chapter 3 of this dissertation, we described a novel quiescence pathway in which ZYGA and ZYG11B regulate the levels of MCM7, CCT3, and CSE1L in H1299 NSCLC cells. When ZYG11B or ZYG11A/B are knocked down in quiescent cells, the

levels of MCM7, CCT3, and CSE1L are stabilized as cells enter quiescence. We also showed that ZYG11A directly interacts with MCM7 and CCT3 but does not interact appreciably with CSE1L. Additionally, ZYG11B directly interacts with MCM7 but does not interact with CSE1L.

ZYG11A potentially recognizes MCM7 and CCT3 directly as substrates, and ZYG11B potentially recognizes MCM7 directly as a substrate. The interactions of ZYG11A and ZYG11B with these potential substrates occurs in asynchronous cells and quiescent cells. Because the interaction also occurs in asynchronous cells, it would be useful to determine whether the interaction occurs in G1, S, G2, and/or M phases. It's possible that the interactions between ZYG11A/B and MCM7 or CCT3 occurs in all cell cycle stages, or the interaction may be specific to a cell cycle stage.

ZYG11A and ZYG11B do not recognize CSE1L directly as a substrate, however when ZYG11B and ZYG11A/B are knocked down in quiescent cells, CSE1L levels are stabilized. This suggests that ZYG11A and ZYG11B may regulate CSE1L indirectly. A possible mechanism for this indirect interaction is that ZYG11A and ZYG11B facilitate the proteasomal degradation of an inhibitor protein that inhibits the ubiquitin ligase that targets CSE1L for degradation. This mechanism could explain why ZYG11B and ZYG11A/B siRNA stabilizes CSE1L levels, but neither ZYG11A nor ZYG11B interact with CSE1L. An example of such a mechanism in the cell is when the ubiquitin ligase, $SCF^{\beta TrCP}$, targets the APC/C inhibitor, Emi1, for degradation during early mitosis (Fuchs et al., 2004; Margottin-Goguet et al., 2003). Once APC/C no longer is inhibited by Emi1, APC/C can subsequently target other substrates for degradation (Fuchs et al., 2004; Margottin-Goguet et al., 2003). An approach to investigate this potential

mechanism would be by carrying out a mass spectrometry analysis of ZYG11A IP samples derived from quiescent cells. This data could give us insights into whether ZYG11A is interacting with a protein that inhibits a ubiquitin ligase involved in degrading CSE1L. Such a mass spectrometry experiment could also help us identify other proteins that ZYG11A regulates in the quiescence pathway.

MCM7, CSE1L, and CCT3 are stabilized as cells enter quiescence after ZYG11B and ZYG11A/B siRNA treatment. Despite this stabilization, MCM7, CSE1L, and CCT3 levels continue to decline especially after two days of serum starvation. This suggests that other proteins may function redundantly with ZYG11A and ZYG11B in mediating quiescence degradation. ZER1 is a potential candidate that has a redundant function with ZYG11 in this pathway. ZER1 is a ZYG11-related protein that is present in vertebrates (Vasudevan et al., 2007). We knocked out ZER1 in H1299 cells, and performed serum starvation experiments similar to those described in Chapter 3, except H1299 WT cells were compared to H1299 ZER1 KO cells. We treated cells with ZYG11A, ZYG11B, and ZYG11A/B siRNA before serum starvation. Once the data from this experiment is obtained and analyzed, we will be able to determine whether the ZER1 knockout further stabilizes MCM7, CSE1L, and CCT3 when ZYG11A, ZYG11B, or ZYG11A/B are knocked down in quiescent cells. If the ZER1 knockout further stabilizes these proteins, that would suggest that ZER functions redundantly with ZYG11A and ZYG11B in this quiescence pathway.

We believe that the regulating of MCM7, CSE1L, and CCT3 levels by ZYG11A and ZYG11B may be important for regulating quiescence. In future research, the

importance of the ZYG11 quiescence pathway for the maintenance of quiescence could be assessed.

References

Arkin, M.R., Tang, Y., and Wells, J.A. (2014). Small-molecule inhibitors of protein-protein interactions: progressing toward the reality. Chemistry & biology *21*, 1102-1114.

Arooz, T., Yam, C.H., Siu, W.Y., Lau, A., Li, K.K., and Poon, R.Y. (2000). On the concentrations of cyclins and cyclin-dependent kinases in extracts of cultured human cells. Biochemistry *39*, 9494-9501.

Balachandran, R.S., Heighington, C.S., Starostina, N.G., Anderson, J.W., Owen, D.L., Vasudevan, S., and Kipreos, E.T. (2016). The ubiquitin ligase CRL2ZYG11 targets cyclin B1 for degradation in a conserved pathway that facilitates mitotic slippage. J Cell Biol *215*, 151-166.

Brown, N.R., Korolchuk, S., Martin, M.P., Stanley, W.A., Moukhametzianov, R., Noble, M.E.M., and Endicott, J.A. (2015). CDK1 structures reveal conserved and unique features of the essential cell cycle CDK. Nature communications *6*, 6769-6769.

Ettinger, D.S., Akerley, W., Bepler, G., Blum, M.G., Chang, A., Cheney, R.T., Chirieac, L.R., D'Amico, T.A., Demmy, T.L., Ganti, A.K.*, et al.* (2010). Non-small cell lung cancer. Journal of the National Comprehensive Cancer Network : JNCCN *8*, 740-801.

Fuchs, S.Y., Spiegelman, V.S., and Kumar, K.G. (2004). The many faces of beta-TrCP E3 ubiquitin ligases: reflections in the magic mirror of cancer. Oncogene *23*, 2028-2036.

Li, Y., Zhang, J., Gao, W., Zhang, L., Pan, Y., Zhang, S., and Wang, Y. (2015). Insights on Structural Characteristics and Ligand Binding Mechanisms of CDK2. International journal of molecular sciences *16*, 9314-9340.

Margottin-Goguet, F., Hsu, J.Y., Loktev, A., Hsieh, H.M., Reimann, J.D., and Jackson, P.K. (2003). Prophase destruction of Emi1 by the SCF(betaTrCP/Slimb) ubiquitin ligase activates the anaphase promoting complex to allow progression beyond prometaphase. Dev Cell *4*, 813-826.

Siegel, R.L., Miller, K.D., and Jemal, A. (2016). Cancer statistics, 2016. CA: a cancer journal for clinicians *66*, 7-30.

Sliwoski, G., Kothiwale, S., Meiler, J., and Lowe, E.W. (2014). Computational Methods in Drug Discovery. Pharmacological Reviews *66*, 334-395.

Song, Y., Zhao, C., Dong, L., Fu, M., Xue, L., Huang, Z., Tong, T., Zhou, Z., Chen, A., Yang, Z*., et al.* (2008). Overexpression of cyclin B1 in human esophageal squamous cell carcinoma cells induces tumor cell invasive growth and metastasis. Carcinogenesis *29*, 307-315.

Soni, D.V., Sramkoski, R.M., Lam, M., Stefan, T., and Jacobberger, J.W. (2008). Cyclin B1 is rate limiting but not essential for mitotic entry and progression in mammalian somatic cells. Cell Cycle *7*, 1285-1300.

Toyoshima, F., Moriguchi, T., Wada, A., Fukuda, M., and Nishida, E. (1998). Nuclear export of cyclin B1 and its possible role in the DNA damage-induced G2 checkpoint. Embo j *17*, 2728-2735.

Trunnell, N.B., Poon, A.C., Kim, S.Y., and Ferrell, J.E., Jr. (2011). Ultrasensitivity in the Regulation of Cdc25C by Cdk1. Mol Cell *41*, 263-274.

Vasudevan, S., Starostina, N.G., and Kipreos, E.T. (2007). The Caenorhabditis elegans cell-cycle regulator ZYG-11 defines a conserved family of CUL-2 complex components. EMBO Rep *8*, 279-286.

Wang, X., Sun, Q., Chen, C., Yin, R., Huang, X., Wang, X., Shi, R., Xu, L., and Ren, B. (2016). ZYG11A serves as an oncogene in non-small cell lung cancer and influences CCNE1 expression. Oncotarget *7*, 8029-8042.

Yasunaga, S., Ohno, Y., Shirasu, N., Zhang, B., Suzuki-Takedachi, K., Ohtsubo, M., and Takihara, Y. (2016). Role of Geminin in cell fate determination of hematopoietic stem cells (HSCs). International journal of hematology *104*, 324-329.

Yasunaga, S.i., Ohtsubo, M., Ohno, Y., Saeki, K., Kurogi, T., Tanaka-Okamoto, M., Ishizaki, H., Shirai, M., Mihara, K., Brock, H.W*., et al.* (2013). Scmh1 has E3 ubiquitin ligase activity for geminin and histone H2A and regulates geminin stability directly or indirectly via transcriptional repression of Hoxa9 and Hoxb4. Molecular and cellular biology *33*, 644-660.